1-1-1990

Mobility of poly(amidoamine) dendrimers :: a study of NMR relaxation times/

A. Donald Meltzer
University of Massachusetts Amherst

MOBILITY OF POLY(AMIDOAMINE) DENDRIMERS; A STUDY OF NMR RELAXATION TIMES

A Dissertation Presented

by

A. DONALD MELTZER

Submitted to the Graduate School of the
University of Massachusetts in partial fulfillment
of the requirements for the degree of

DOCTOR OF PHILOSOPHY

February 1990

Polymer Science and Engineering Department

MOBILITY OF POLY(AMIDOAMINE) DENDRIMERS; A STUDY OF NMR RELAXATION TIMES

A Dissertation Presented

by

A. DONALD MELTZER

Approved as to style and content by:

David A. Tirrell, Chairperson of Committee

Murugappan Muthukumar, Member

Paul Lahti, Member

William J. MacKnight, Department Head
Polymer Science and Engineering Department

ACKNOWLEDGMENTS

I would like to take this opportunity to thank those who gave me the support and guidance that I needed to accomplish this work.

First I would like to thank Drs. David A. Tirrell and Alan A. Jones for the guidance I received while under their supervision. I would also like to express my gratitude to Drs. Paul Lahti and Murugappan Muthukumar for sitting on my committee, as well as for their helpful advice. I would like to recognize Drs. Larry Wilson, Pat Smith and Donald Tomalia, with whom I had many helpful discussions concerning the chemistry of dendritic polymer sytems, and of course their employer, the Dow Chemical Company, who funded the research discussed herein.

I am especially grateful to Douglas Wicks, who was particularly helpful when I was first getting started, and who, along with Dr. Daniel Kost, spurred my interest in NMR.

Finally, I wish to thank Ben, Shirley, Michael and James, without whose support I might not have persisted in my efforts to obtain a Ph.D..

ABSTRACT

MOBILITY OF POLY(AMIDOAMINE) DENDRIMERS;
A STUDY OF NMR RELAXATION TIMES

FEBRUARY 1990

A. DONALD MELTZER, B.Sc., MCGILL UNIVERSITY
Ph.D., UNIVERSITY OF MASSACHUSETTS

Directed by: Professor David A. Tirrell

The steric nature of the new topology created by the starburst polymer has been studied by ^{13}C and ^{2}H dynamic nuclear magnetic resonance (NMR) relaxation measurements. For two series of poly(amidoamines), PAMAM, (one OH terminated, the other NH_2 terminated), ^{13}C correlation times (τ) of the terminal carbons were found to be almost independent of the number of end groups; τ varied from 1.0×10^{-11} to 6.3×10^{-11}, and no evidence of dense-packing of the end groups was observed. The τ's of the methylene carbons on the interior of the dendrimers were found to increase with molecular weight,

indicative of a progressive increase in local monomer density within the polymer.

No significant differences in relaxation parameters of the internal carbons were observed for the NH_2 terminated PAMAM compared to the OH terminated analogues, in either D_2O of DMSO-d_6. Thus, the results reflect topological effects, and are not due to specific solvent or end group behavior. Larger relaxation times were observed for both series when measured in D_2O. While the differences in polymer behavior in the two solvents indicate that the polymer chains are more flexible in D_2O than in DMSO-d_6, intrinsic viscosities were determined to be comparable in the two solvents (0.04 - 0.10 dl/g). The difference in the NMR behavior is thus attributed to strong H-bonding between the polymer and DMSO, resulting in an increase in the hydrodynamic volume of the mobile unit. The relaxation behavior of the terminal carbon, in D_2O, differed upon changing the end group. The terminal carbon of the OH terminated PAMAM was observed to be less mobile than the corresponding carbon atom in the NH_2 terminated PAMAM.

^2H NMR relaxation measurements were used in a more extensive study of the mobility of amine terminated PAMAM chains as a function of molecular weight and position. The τ's were found to increase with molecular weight, irrespective of the location of the labelling. In the last generation the τ's were found to increase as the number of termini increases from 3 ($\tau = 1.7 \times 10^{-12}$s) to 384 ($\tau = 2.2 \times 10^{-11}$s), and were smaller than the τ's observed when the polymers were labelled at interior positions. No significant difference in relaxation parameters was observed when the label was located in the interior repeat units, irrespective of chain length following deuteration. No evidence of radial gradients was observed.

TABLE OF CONTENTS

LIST OF TABLES

LIST OF FIGURES

CHAPTER 1

INTRODUCTION

Starburst polymers, or dendrimers, are a relatively new class of highly branched polymers. The class of polymers to which the dendrimers belong is unique in that the symmetric branching creates an architecture that is dominated by a large, well defined number of branch points. The concept of starburst branching is general in scope, and utilizes multifunctional repeating units in order to generate the highly branched systems. The topology is initiated from a central point and proceeds by linear growth to a predetermined length. Subsequent introduction of a branch point followed by a repetition of the linear growth, possibly but not necessarily identical with the chain structure prior to the branch point, permits the desired increase in molecular weight. Precise repetition of the branching process, and of the overall growth reaction, results in the formation of dendritic macromolecules (refer to Figure 1.1). The methodology involved in the synthesis of the starburst topology permits precise control of chemical structure, has important ramifications in the area of polydispersity, and allows for the formation of dense polymer networks, without the formation of gelatinous networks.

It is believed that a polymer that meets the constraints described above could exhibit certain unique behavior. Specifically, de Gennes (8) has illustrated that "ideal starburst growth" is restricted to a limiting size. The perfect cascade branching process is only possible up to a real limiting value of the packing density. Above this limit, the branching pattern will be

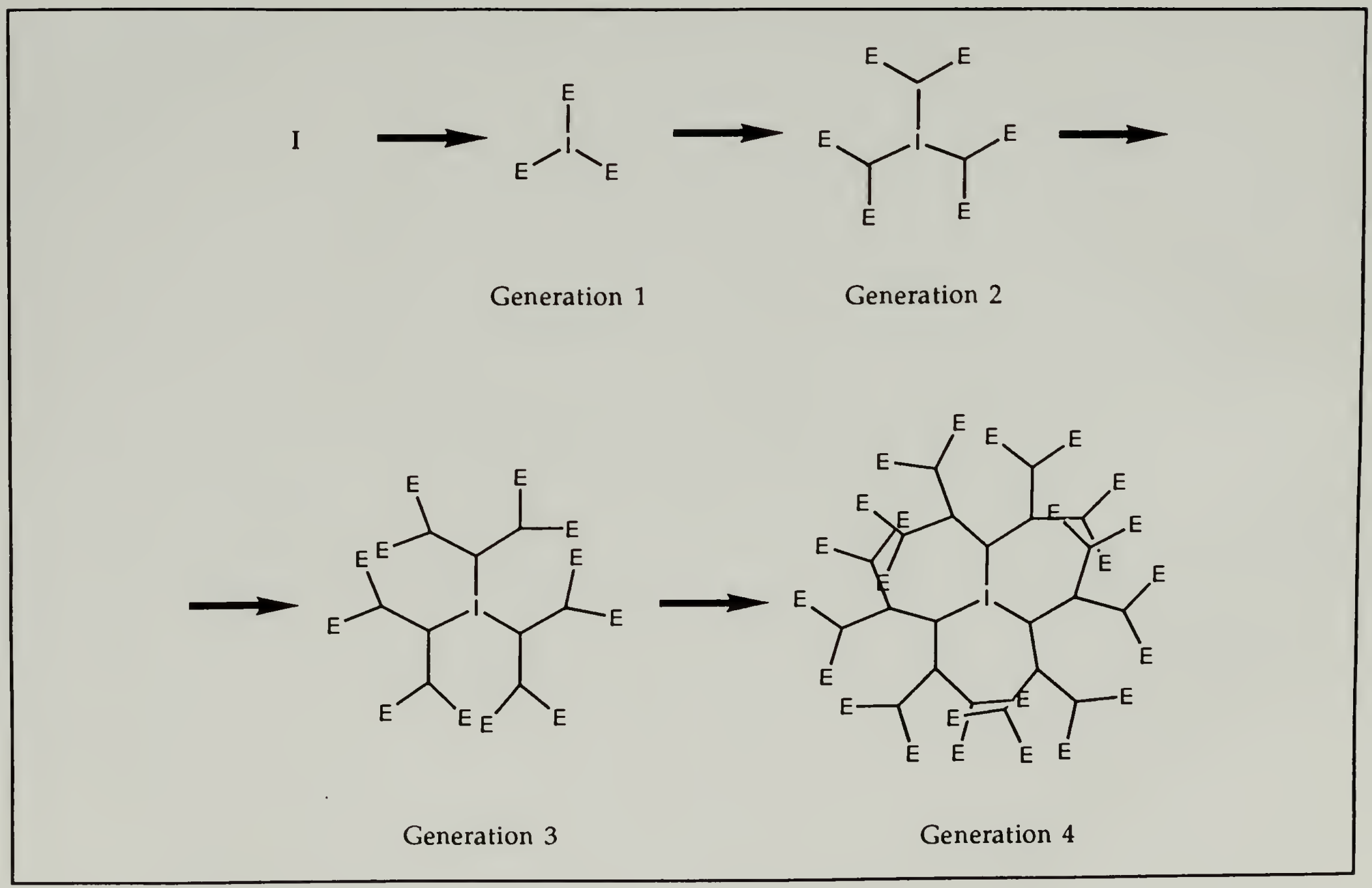

Figure 1.1. The development of the starburst topology. I denotes the initiator core and E denotes the end groups of the dendrimers.

interrupted by overcrowding of the end groups. Exactly where this limit is reached will depend on the rate at which the local monomer density increases with molecular weight, and as such, ought to depend on the functionality of the core and repeating units involved in the polymerization. The length of the spacer groups between branch points should affect the rate at which local monomer density builds up so that the size of the polymer necessary for the formation of a region of dense packing is also dependent on this parameter.

The topology created in the advent of starburst polymers has been described in a theoretical paper by Maciejewski (36). Maciejewski proposed that large molecules, possessing a certain type of topology, might be capable of forming an outer barrier, or shell, which could restrict access to the interior of the molecule. When the barrier is supported by a structure onto which the polymer has been moulded or cast, Maciejewski adopted the term "cast shell". The formation of a cast shell is actually an extreme case of the dense packing described by de Gennes. Should a barrier to the interior of the polymer form during the preparation of the dendritic topology, the dendrimers could have several obvious applications, e.g., as sequestering agents and controlled delivery systems. Even in the absence of a shell, the dendrimers could serve as gelation agents.

Molecular dynamic simulations of the starburst dendrimers have been performed by Naylor and Goddard (40-42). The simulations indicate that the overall shape of β-alanine dendrimers changes as the polymer is grown from generation 1 to 7. Internal cavities and channels in the polymer matrix were observed once the transition from an open, extended structure to a spherical moiety occurred in the simulated dendrimers. The simulations indicate that approximately 50% of the internal volume is a "solvent-filled void", from

which Goddard concluded that the internal regions could be used for sequestering small molecules.

By simulating the growth pattern of dendrimers, Lescanec and Muthukumar (26) have also made certain predictions with regard to the behavior of the new topology. Their model does not predict the existence of the radial gradients that the other theories suggest, nor does it predict that the end groups are located on the surface of the polymer. Instead the model suggests that there is an increase in the local monomer density as the molecular weight (MW) of the system increases, and this is interpreted in terms of the chains folding back into the interior of the polymer.

These contradictory predictions demonstrate the need of fundamental, experimental exploration of the new topology. A good understanding of the local properties of the dendritic system must be obtained prior to the design of dendrimers with specific applications in mind, and it is with the acquisition of this fundamental understanding that the work presented herein is concerned.

Earlier investigations have already illustrated that the starburst polymers exhibit certain interesting phenomena. Measurements of the intrinsic viscosity, radius of gyration, and density, and calculations of the surface area per unit end-group (S/E) have been performed as a function of generation (58). In all cases nonlinear relationships were noted, and the molecular weight dependences were interpreted in terms of congestion and dense-packing. Calculations of the aspect ratio show that the dendrimer is initially disklike in form, but that the overall shape of the polymer approaches that of a sphere above generation 4 (40-42). The dendrimers are reminiscent of micelles in terms of size and shape; e.g., spherical micelles of sodium dodecyl sulfate (SDS) have been shown to be 17A in diameter (22)

whereas a generation 2 PAMAM is 16A in diameter (55). SDS micelles of aggregation number of 60, with an effective MW of 17,300 are similar in mass to the generation 6 PAMAM with a MW of 21,600. At higher generations the calculated S/E is similar to that observed in the bilayer surfaces of liposomes (39), i.e., 30-50 A^2/head group for generations 7, 8 and 9 (58), while at lower generations the S/E is more typical of micelles (30), i.e., 90-130 A^2/head group for generations 1-5 (58). S/E calculations assume that all the end-groups are located on the surface of the sphere, and that no significant penetration back into the interior of the polymer occurs. While these inferences are speculative, they do suggest some interesting possibilities in terms of the behavior of the polymer. For example it has been suggested that dendrimers, being of colloidal dimensions, could be used much in the same way that micelles have been employed, i.e., in solubilization of organic compounds in aqueous media and in controlled delivery of drugs and agricultural products (30, 42). Other possible applications include gelation agents and carriers for catalytic sites. However, even if the dense packing phenomenon does occur, it is far from certain that the polymer will be capable of entrapping a guest molecule. There must be a sufficient amount of unoccupied volume in the interior of the polymer, the guest molecule must be able to penetrate into the interior of the dendrimer, and the local environment inside the dendrimer must be favourable to the dissolution of the guest molecule. Local congestion can be observed by implementing such techniques as nuclear magnetic resonance spectroscopy (NMR). In the past this method has been applied to the study of segmental mobility in polymeric systems (15, 27), and as such may prove useful in observing the dense-packing that is predicted to build up at higher generations (8, 55, 58). A more complete discussion of the utility of NMR as applied to the study of molecular motion will be deferred until later.

A. The History of the Syntheses of Starburst Polymers

In general, the synthesis of the dendrimers involves a stepwise propagation technique. The synthesis of the desired topology has been accomplished either by employing excesses of multifunctional monomers, or by protection/deprotection methods. The successful generation of the dendritic structure has been reported for a variety of chemical interiors, branch multiplicities and end-group functionalities including the following: amidoalcohols (43-45), poly(ethers) (61), poly(thioethers) (59), poly(ethylenimines) (59), poly(amides) (59), poly(arylamines) (13) and poly(amidoamine) (54-60). While it is only studies of the poly(amidoamine) polymer, or PAMAM, that are reported herein, all of the dendrimers comprise network cells that are introduced in a concentric radial manner around an initiator core, and as such fundamental properties discovered for any particular dendrimer ought to apply to the topology in general.

The PAMAM has been prepared by the method of excess multifunctional reagents. Generally speaking, the method involves the reaction of a nucleophilic initiator core (ammonia) with a multifunctional electrophilic reagent (methyl acrylate) which possesses moieties of significantly different reactivities toward the initiator core. Subsequent reaction of this adduct with a large molar excess of a multifunctional nucleophile (ethylenediamine) produces an adduct with terminal nucleophilic sites that can serve to further expand the system upon repetition of the reaction sequence. In repeating the sequence over and over again, a highly symmetrically branched condensation polymer can be prepared (refer to Figure 1.2). Reaction steps in all cases must be essentially quantitative to

ensure the ideal nature of the dendritic topology. As well, the reactions must be performed under conditions that avoid intermolecular bridging, intramolecular "looping" and any other side reactions that may result in deviations from ideal nature. In designing such a polymer one creates a system where the number of branch points doubles with each successive cycle (with this particular choice of monomers). Table 1.1 illustrates the dependence of the branching and molecular weight on the number of repetative cycles performed in the preparation of a PAMAM dendrimer.

Table 1.1. The number of end-groups, diameter and molecular weight as a function of generation for poly(amidoamine) dendrimers prepared from methyl acrylate and ethylenediamine (ammonia core).

Generation	Number of end-groups	Molecular weight	Diameter* (A)
1	3	360	11
2	6	1040	16
3	12	2070	24
4	24	5150	31
5	48	10600	40
6	96	21600	56
7	192	43500	66
8	384	87300	75
9	768	175000	90
10	1536	350000	104

* as determined by intrinsic viscosity (59).

In order to facilitate further discussion of this new class of polymers some new terminology has been adopted. The term normally used to describe the progress of a polymerization reaction, degree of polymerization, loses significance when applied to the starburst system, and so the term "generation" was adopted (56). In its simplest form, a generation can be regarded as the number of times through which the synthetic sequence has been cycled. More precisely, the term is related to the number of branch points between a specified site in the polymer and the initiator core, along any single chain, in that the generation is equal to one plus the number of branch points between a specified site in the polymer and the initiator core. In the particular example presented in Figure 1.2, the initiator core is surrounded by a shell ('first generation') of three sites (In this context a "site" comprises either an end group or a branch point, depending on whether the generation of interest is a terminal generation or not). In the second shell there are six sites ('second generation') followed by a third generation of twelve sites. Thus a polymer of n generations contains $1+3(1+2+4+...+2^{n-1}) = 3(2^n)-2$ sites of which the last generation of $3(2^{n-1})$ sites are surface sites so that, for large n, half of the sites lie in the terminal generation, the other half being in the internal generations. The exponential increase in the number of sites with increasing generation and the relative numbers of terminal versus internal sites are worth noting for such properties of the dendrimers will be of utmost importance in the interpretation of the results to be presented.

The nature of the stepwise polymerization by which the PAMAM starburst polymer is prepared necessitates the introduction of some additional terminology. The synthesis involves two monomers, and as such, the groups. In order to distinguish between the two, the terms "half generation"

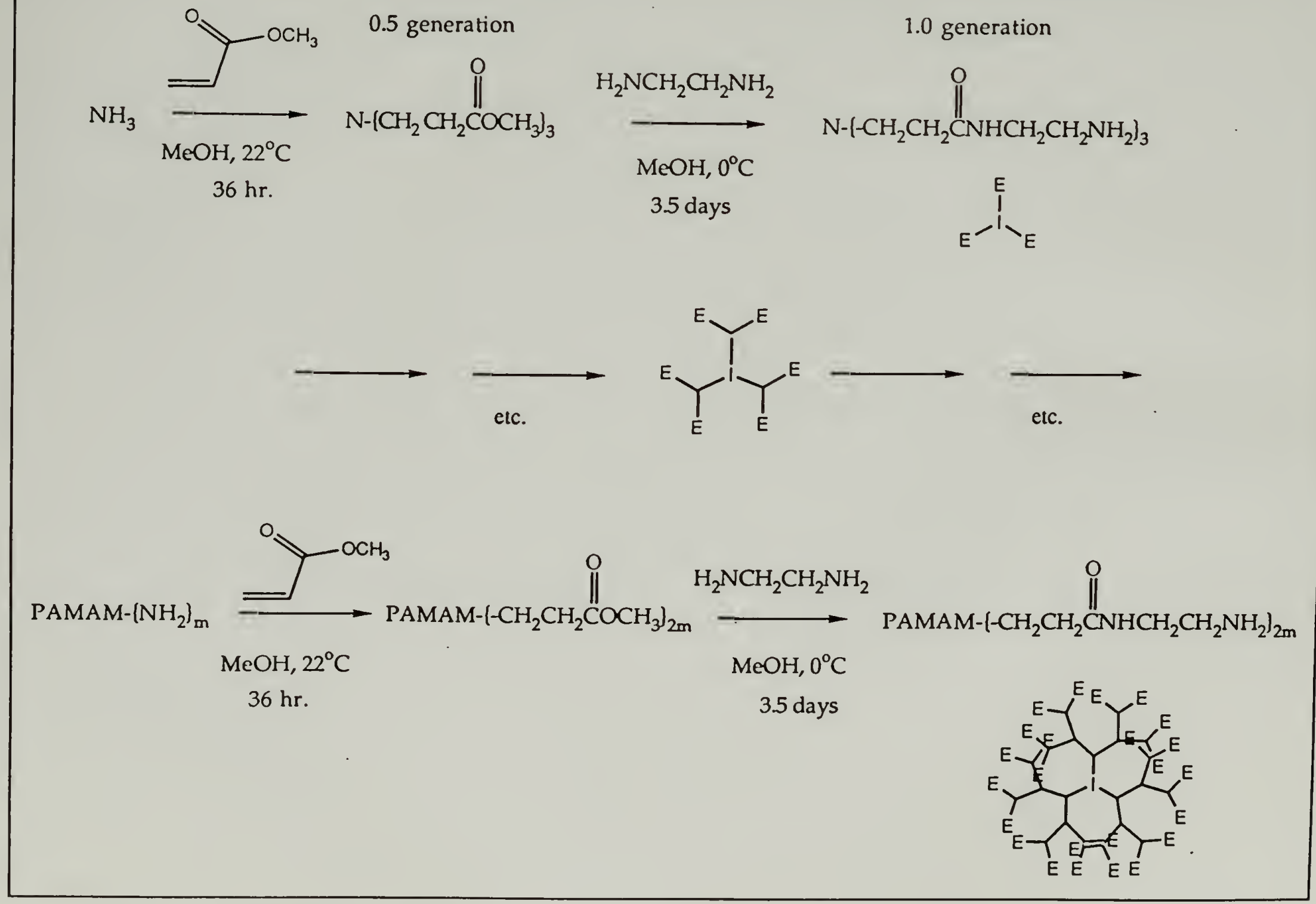

Figure 1.2. The synthesis of the poly(amido amine) starburst polymer.

terminal unit of the polymer alternates between two different functional and "full generation" have been adopted. The latter term indicates that a full cycle has been completed, whereas the former term indicates that only the first step of the sequence has been accomplished. There is believed not to be any ambiguity in attempting to refer to a specific generation within a larger polymer (e.g.: the third generation within an eighth generation PAMAM starburst polymer). In the specific case discussed herein, namely the PAMAM starburst polymer, the half generations are ester terminated, while the full generations are amine terminated. However, these terms are not specific to the PAMAM starburst, and can be applied to other starburst polymers.

Although the synthesis of PAMAM starburst polymers has been developed by Tomalia et al. (54-60), the experimental procedures for the preparation of the PAMAM are still at the stage where significant numbers of defects occur (e.g.,. incomplete alkylation, retro-Michael addition and intramolecular linking via amidation), and efforts to perfect the technique and minimize the number of defects in the structure are reported herein. This is of utmost importance and the greatest of care must be maintained in keeping track of the number of defects at each stage of the stepwise polymerization. It is equally important to obtain an understanding of the nature of the polymer which, as yet, is not well understood. This lack of a fundamental understanding of the nature of the structure can be prohibitive in designing new structures to serve specific purposes, and needs to be addressed. The novel design has created a topology which might form a "cast shell". Should this be the case, the behavior of the polymer chains that form the shell might differ from that of polymers of more classical topology. This suggests a study of flexibility. How does the mobility of the repeat units vary as the molecular weight increases? Or as the distance from the core increases?

How does the steric crowding of the end groups vary as the number of ends per chain increases? We hoped to be able to answer all of these questions with a series of dynamic NMR experiments.

B. Previous Characterization of PAMAM Dendrimers

It is conceivable that the dendrimers may possess some interesting physical properties, and some experiments designed to help characterize the new topology have been reported (56, 59). The polymers have been reported to be amorphous syrups, becoming stiff glasses at higher molecular weights. The ester terminated PAMAM were observed to be of lower viscosity than the amine terminated polymers. The polymers are soluble in many organic solvents (e.g.., chloroform, methanol and dimethylformamide), and the half generation samples were reported to exhibit surface active properties in water, i.e., foamy solutions were obtained. Viscosity studies conducted in a variety of solvents were reported to show that the full generation PAMAM exhibit higher intrinsic viscosities ($[\eta]$) than the corresponding half generation polymers. The hydrodynamic volumes of the dendrimers were also determined from viscosity measurements. Intrinsic viscosity was reported to initially increase with increasing MW, but was observed to reach a maximum value around generation 6, subsequently decreasing. Nonetheless, the radial dimensions of the dendrimers were calculated from the $[\eta]$ data and were reported to increase in a linear fashion with MW. The dependence of the monomer density (ρ) of the dendrimers on MW was also calculated from the hydrodynamic volumes. The ρ was reported to exhibit a minimal value around generation 6. The shape of the curves observed for the $[\eta]$ and ρ on generation are interpreted in terms of an accumulation of monomer density.

Other experiments that have been previously performed on the PAMAM dendrimers include titrations of the amine functionalities, mass spectroscopy (MS), nuclear magnetic resonance spectroscopy (NMR), electron microscopy (EM) and low angle laser light scattering (LALLS). The titrimetry

exhibited two distinctive endpoints, one for the primary amines on the end of the chains and one for the tertiary amines along the polymer backbone. MS was used to identify defect fragments that may occur during the synthesis, and the structure of the defects was confirmed by NMR. LALLS was reported as a means of determining molecular weights of the dendrimers along with size exclusion chromatography and intrinsic viscosity. EM has also been used to monitor the size of the polymers, and the technique was applied to the determination of the shape of the dendrimers.

None of the experiments described above, however, address the existence of a densely packed layer, or of radial gradients within the dendrimers. The experiments reported herein were designed to address these, as yet unresolved, questions.

C. Dynamic NMR Spectroscopy

An important method that has been employed in the study of segmental mobility of polymer chains is dynamic NMR. NMR is a formidable tool that has been applied extensively to the characterization of polymers (15). Not only can NMR be used to determine the molecular weight and structure of the polymer, but the technique also lends itself to the study of segmental mobility and the energy barriers associated therewith (15, 27). This is made possible by the determination of the rates at which the induced magnetization relaxes to its equilibrium value. The relaxation process is governed by fluctuations in the local magnetic field which can be generated by the lattice, or by the loss of phase coherence due to the interaction of different nuclear spins (10).

When the lattice field oscillates at the same frequency as the precessional rate of the nuclei, an exchange of energy from the nuclei to the lattice can occur. The more efficient the relaxation processes, the faster the nuclei will relax. This form of relaxation is referred to as the spin-lattice relaxation (T_1). The value of T_1 is dependent on the type and rate of the molecular motions that are responsible for the fluctuations in the lattice field, i.e., rotational and translational motions (10).

There are several mechanisms that may contribute to the relaxation of a particular nucleus within a molecule (27). One possible mechanism, which is more prominent in the solid state than in solution, is the chemical shift anisotropy (CSA). The magnetic shielding of a nucleus results from the differences in the density of the surrounding electrons. If the chemical shift is anisotropic, then motion of the nucleus will create fluctuations in the local

magnetic field that can induce relaxation (10, 27). Scalar coupling (SC) is another possible mechanism by which relaxation could be induced. When the relaxation of one nucleus is fast, it generates fluctuations in the field, and these fluctuations can affect the relaxation rate of adjacent nuclei (10, 27). Spin rotation (SR) is a result of molecules, or segments thereof, rotating and causing the magnetic vectors of the bonding electron spins to rotate as well. This can contribute to the overall relaxation of the nuclei by inducing fluctuations in the local magnetic field (4). Dipoles of nuclei which are of relatively close proximity can interact and induce relaxation from the excited state. When relaxation is induced by this mechanism it is said to occur by a dipole-dipole interaction (DD), and is typically the predominant means by which many nuclei with spin 1/2 relax (10, 25, 27, 51). Nuclei with spin greater than 1/2 are known to relax via a quadrupolar mechanism (Q). The asymmetry of the charge distribution within these nuclei can give rise to an electric quadrupole moment which can interact with the electric field gradient of the molecule (10, 27). The relative contributions of these mechanisms to the overall relaxation process will depend on the electronic and atomic environment of the nucleus. Due to the variety of relaxation mechanisms, relaxation experiments are dependent on the chemical composition of the polymer, as well as on the flexibility of the system being studied.

Quantitative treatment of relaxation measurements in terms of the molecular correlation time, τ, is possible, but depends on the nature of the system being studied (10, 27). In the majority of cases (very small molecules and rapidly rotating methyl groups being the exceptions) the dominant contribution to ^{13}C magnetic relaxation comes from ^{13}C-^{1}H DD interactions (25, 51). Scalar interactions and chemical shift anisotropy usually do not contribute significantly to the ^{13}C relaxation of protonated carbons. Schaefer

(50) derived a relationship between T_1 and τ for ^{13}C relaxation in the case where only dipolar interactions between carbons and fully decoupled protons were involved. By assuming isotropic motion, and a distribution of τ to describe the segmental motion of long chains, Schaefer showed that:

$$\frac{1}{T_1} = 0.1(h/2\pi)^2 \gamma^2_H \gamma^2_C r^{-6} N\{J(\omega_C-\omega_H) + 3J(\omega_C) + 6J(\omega_C+\omega_H)\} \quad (1)$$

and

$$NOEF = 1+ \frac{-J(\omega_C-\omega_H)+6J(\omega_H)}{J(\omega_C)+4J(\omega_C+\omega_H)} \quad (2)$$

where

$$J(\omega) = \int \frac{\tau F(s)\{b^2-1\}ds}{(b-1)(1 + \omega^2\tau^2[(b^s-1)/(b-1)]^2)} \quad (3)$$

where

$$s = \log b[1+(b-1)\tau_o/\tau)] \quad (4)$$

and

$$F(s) = P\Gamma(P)^{-1}(P^s)^{P-1}\exp(-Ps) \quad (5)$$

Here, $\Gamma(P)$ represents the gamma function, b, P and τ are chosen to fit the data, τ_o is defined to be a correlation time proportional to τ, ω_C and ω_h represent the frequencies at which the ^1H and ^{13}C resonate, respectively; h is Planck's constant, r is the C-H internuclear distance, N is the number of

covalently bonded ^1H, and γ_C and γ_H are the gyromagnetic ratios of the ^{13}C and ^1H, respectively. It is generally agreed that b and P are not totally independent and the model is essentially a pseudo-two-parameter model (15). Although the model is an empirical one, it has found favour within the NMR community as it has been shown to accurately reflect the observed behavior of polymers in solution (15). The reason for Schaefer postulating that a distribution of τ is associated with each relaxation time lies in the fact that, unlike low molecular weight compounds, polymers can exhibit cooperative motions between units. Equally probable, and incorporated into the model via the distribution, are variations in the through space distances within the polymer chain, and such variations can contribute to the overall relaxation of the induced magnetization. In the narrowing limit where $\omega\tau << 1$, Equation 1 reduces to the familiar:

$$\frac{1}{T_1} = (h/2\pi)^2\gamma^2_H\gamma^2_C r^{-6}N \qquad (6)$$

In the case of deuterated carbons the equation would take the form of:

$$\frac{1}{T_1} = \frac{8}{3}(h/2\pi)^2\gamma^2_H\gamma^2_D\ r^{-6}N \qquad (7)$$

where γ_D is the gyromagnetic ratios for deuterium.

Relationships between T_1 and τ have also been developed for quadrupolar nuclei such as deuterium (I=1) (1). The nearly axial symmetry of the C-^{2}H bond vector, along which the field gradient lies, has permitted the development of the relationship between relaxation times and τ listed below:

$$\frac{1}{T_1} = \frac{3(e^2qQ)^2}{20h^2}[J(\omega_o) + 4J(2\omega_o)] \qquad (8)$$

and

$$\frac{1}{T_2} = \frac{3(e^2qQ)^2}{40h^2}[3J(0) + 5J(\omega_o) + 2J(2\omega_o)] \qquad (9)$$

where e^2qQ/h is the quadrupolar coupling constant. Both ^{13}C and ^{2}H relaxation times arise from intramolecular interactions. Consequently, a comparison of the corresponding relaxation times can enable further insight into the nature of relaxation mechanisms involved in a particular system, or can be used to calculate quadrupolar coupling constants. In practice this can be accomplished by taking the ratios of equations 1 and 7 to yield (9, 22):

$$(e^2qQ/h)^2 = 4/3\gamma^2_C\,\gamma^2_H(h/2\pi)^2/r^6_{CH}(T_1{}^{DD}/T_1{}^{Q}) \qquad (10)$$

where $T_1{}^{DD}$ is the T_1 of the ^{13}C relaxing by a DD mechanism, and $T_1{}^{Q}$ is the T_1 of the quadrupolar nucleus bonded to the ^{13}C in a isotopically labelled compound. The angular dependence of the ^{13}C-^{1}H DD relaxation is exactly the same as that of the C-^{2}H so that a comparison of T_1 values for ^{13}C and ^{2}H is reasonable under any kind of anisotropic motion, and if a model describing the motional properties is proven to be appropriate for ^{13}C then it ought to be equally valid for ^{2}H relaxation measurements as well.

Once a suitable model to convert the experimentally determined relaxation parameters to τ has been found, the temperature dependence of τ may be expressed with good accuracy in the usual Arrhenius form:

$$\tau = \tau_o \exp(E_a/kT) \qquad (11)$$

where E_a is the activation energy for the motion responsible for the spin-lattice relaxation, k is the Boltzmann constant, τ_o is a solvent dependent pre-exponential factor and T is the absolute temperature (15). Thus the activation energy associated with the segmental motions responsible for the relaxation process can be determined from NMR experiments as well.

Dynamic NMR studies have already been applied to a wide variety of problems concerning the behavior of polymers. It has been demonstrated that above a fairly low critical MW, T_1 is independent of chains length due to the dominance of segmental motions (37). Below a critical MW T_1 decreases with increasing MW, indicating that the overall rates of tumbling of short polymers are sufficiently rapid to influence the relaxation process. For poly(ethylene oxide) (18), poly(isobutylene) (21) and polystyrene (1) the critical degrees of polymerization above which T_1 is independent of MW have been observed to be 30, 50 and 100, respectively. For these three linear polymers, as well as for other linear systems, it has also been observed that the T_1 of random coils is independent of concentration up to approximately 10-15 monomer mole-% in spite of large changes in macroscopic viscosity (1, 11, 19, 33, 34, 37, 52). Above this critical value of concentration, T_1 was observed to decrease with increasing concentration indicating greater hindrance to segmental motions. The insensitivity to a wide range of concentration is consistent with short-range segmental motions being responsible for

inducing relaxation, irrespective of the mechanism responsible. The motions are controlled by the "microviscosity" of the immediate environment and only intramolecular interactions are responsible for inducing relaxation below the critical concentration. The intramolecular interactions within a polymer chain can be divided into two categories: interactions between nuclei separated by a few bonds, and interactions between nuclei separated by some distance along the backbone but brought close together due to the conformation of the coil. However, the contribution of the second type of interaction has been shown to be negligible (16).

Although the T_1 value is unaffected by large changes in the macroscopic viscosity arising from varying MW or concentration in the same solvent, it does depend on the hydrodynamic or thermodynamic properties of the solvent itself. The reported variations in relaxation behavior have been explained in terms of thermal activation parameters (12, 16, 20, 37). The determination of the activation parameters requires an interpretation of the relaxation times in terms of τ for particular motions. Solvent induced changes in the conformational energies can affect relaxation times in two ways. If the distribution of stable conformations alters, then the average internuclear distances may change and if barrier heights are altered then τ may change. Furthermore, if there is a strong association between the polymer and the solvent, eg.: hydrogen bonding, the effective volume of the mobile unit may increase due to the tightly bound shell of solvent molecules which can lead to an increase in τ. Differences in the average τ have been observed to correlate well with solvent viscosity. For example, in the case of polystyrene, the values of τ decrease in order of decreasing viscosity (11).

As segmental motions control T_1 in reasonably dilute solutions, a comparison of T_1 values provides a measure of the relative barriers to

conformational transitions. Heatley (15) has reviewed the available relaxation data and has found, for example, that separating groups of two carbon atoms by a heteroatom has been shown to have an appreciable liberating influence, whereas inserting a heteroatom between every pair of carbons leads to a greater restriction. If the heteroatom itself carries pendant groups then the segmental motions have been shown to be more strongly hindered. The effect of side groups on the relaxation process, in general, has also been studied, and has been shown to influence the extent of the restriction, and the structure of the group influences the extent of restriction. For example the small nonpolar methyl group is less restrictive than the phenyl or carbazole groups or the polar chlorine and cyano groups.

As such a wide variety of problems that has already been addressed by dynamic NMR, we chose this technique to study the PAMAM dendrimers. We have employed the technique in order to determine how the mobility of the repeating units varies as the molecular weight increases, or as the distance from the core increases. We also address the problems of how the steric crowding of the end groups varies as the number of ends per chain increases and as the nature of the end group is modified.

CHAPTER 2

EXPERIMENTAL SECTION

A. Materials

The following is a list of all reagents and solvents used in the work described herein. Unless otherwise indicated the materials were used as recieved. Letter codes indicate the source of the material.

Calcium hydride (A)

Chloroform-d_1 99.9%d

Deuterium oxide (A)

Dibutylphthalate (A)

Dimethylformamide (A)

Dimethyl sulfoxide (A)

Dimethyl sulfoxide-d_6 99.9% d (A)

Ethanolamine, distilled over CaH_2 bp 42^{o}C/4 Torr (A)

Ethylenediamine, distilled over CaH_2 bp 110^{o}C (A)

Hydroquinone (A)

Methanol (F)

Methanol-d4 99.9% d (A)

Methyl acrylate (A)

Methyl (triphenylphosphoranylidene acetate) (A)

Paraformaldehyde-d_2 99.5% d (CIL)

Toluene (F)

Water deuterium depleted 0.01% natural abundance (A)

Sources

A - Aldrich Chemical Company

CIL - Cambridge Isotope Labs

F - Fisher Scientific Co.

B. Preparations

1. β-d2-Methyl acrylate (d_2-MA)

The synthesis of the β–d_2-methyl acrylate (d_2-MA) used in this work was carried out in a manner similar to that reported by Nugent and McKinney (48). To a 300 mL 3-neck flask were added 104 g (0.032 mol) of methyl (triphenylphosphoranylidene acetate), 50 mg of hydroquinone and 10 g (0.031 mol) of d_2-paraformaldehyde. The reaction vessel was flushed with N_2, and the escaping gas was passed through a dry ice trap. Dibutylphthalate (100 mL) was cannulated into the reaction vessel. The mixture was heated to 80°C for 2 hr before raising the temperature to 110°C for 30 min. The reaction was allowed to cool to room temperature. The reaction vessel was connected to a vacuum pump and the remaining d_2-MA was collected in the dry ice trap. GC-MS indicated the isotopic purity of the acrylate to be > 99%. ^{13}C NMR (75MHz, $CDCl_3$): 51, 128, 131 (quintet) and 167 ppm.

2. Generation 0.5 PAMAM

Into a 250 mL round bottom flask was placed 120 mL of methanol (MeOH). The solvent was deoxgenated by bubbling a steady stream of N_2 through it for no less than 30 min. NH_3 was then bubbled through the MeOH, and the amount added (5.0 g, 0.29 mol) was determined by measuring the increase in mass of the reaction flask. Methyl acrylate (90 g, 1.05 mol) was cannulated into the reaction flask. The reaction vessel was left stirring at room temperature in the dark for 36 hr., at which time all volatile materials

were removed under reduced pressure (15-20 Torr) to provide a quantitative yield (79 g) of generation 0.5 PAMAM. ^{1}H NMR (300 MHz, $CDCl_3$) 3.65 (s, 3H), 2.75 (t, 2H) and 2.43 (t, 3H). ^{13}C NMR (50 MHz, $CDCl_3$): 32.8, 49.4 and 51.6 ppm. IR(liquid): 2950, 2850, 1730, 1440, 1370, 1320, 1180, 1040, 850 cm^{-1}.

3. Generation 1.0 PAMAM

A 10% solution of generation 0.5 PAMAM (2.0 g, 5.6 mmol) in MeOH was deoxgenated by bubbling a steady stream on N_2 through the solution for no less than 30 min. The solution was cannulated into an excess (50 fold by weight, 100 fold on a molar basis) of distilled ethylenediamine (100 g, 1.7 mol) which had been cooled to $0^{o}C$ in an ice bath. The solution was stirred at $0^{o}C$ for 3.5 days, after which time the solvent and EDA were removed under reduced pressure (15-20 Torr). The residual amine was removed by repetitive azeotropic distillations, as follows: the sample was dissolved in 10 mL MeOH and 120 mL of toluene was added to the mixture. The volatile material was then removed on a Buchi rotary evaporator under reduced pressure ($35^{o}C$, 15-20 Torr). Repetition of the procedure twice proved to be sufficient to remove the residual EDA to the point where the EDA was undetectable by GC (residual EDA levels in the polymer were estimated to be < 1% by weight). The reaction provided a quantitative yield of 4.8 g of generation 1.0 PAMAM. ^{1}H NMR (300 MHz, $CDCl_3$): 3.05 (t, 2H), 2.61 (t, 2H), 2.52 (t, 2H), 2.24 (t, 2H). ^{13}C NMR (50 MHz, D_2O): 178.0, 177.4, 50.0, 42.9, 41.0 and 33.8 ppm. IR(liquid): 3300, 3080, 2950, 2850, 1640, 1550, 1470, 1440, 1360, 1290, 1140, 1040, 930 cm^{-1}..

4. Generation 1.5 PAMAM

Generation 1.0 PAMAM (1.0 g , 2.8 mmol or 34 mmol end groups) was dissolved in 10 mL of MeOH in a 20 dram vial fitted with a rubber septum. The solution was deoxgenated as described above. To the solution was added 4.0 mL (44 mmol) of MA. The reaction was stirred for 36 hr at room temperature. Subsequently, the volatile materials were removed under reduced pressure (35^{o}C, 15-20 Torr) to provide a quantitative yield (2.9 g) of generation 1.5 PAMAM. ^{13}C NMR (50 MHz, $CDCl_3$): 53.0, 51.6, 49.3, 37.1, 33.6, 33.3 and 32.7 ppm. IR(liquid): 3300, 2950, 2820, 1740, 1650, 1520, 1440, 1180, 1050, 850 cm^{-1}.

5. Full Generation (Amine Terminated) PAMAM

The procedure followed in the syntheses of these polymers is similar to that of generation 1.0 PAMAM, beginning with the appropriate half generation sample. Larger excesses of EDA were used; the exact weight and molar ratios are listed in Table 2.1. The syntheses of generations 3 and higher required the addition of 10% MeOH to the EDA prior to cooling in order to lower the freezing point of the amine below the reaction temperature. For polymers of sufficient molecular weight (ie.: above generation 3) the residual amine, trapped in the polymer after attempted removal under reduced pressure, was removed via ultrafiltration using the system described in the measurements section. ^{13}C NMR (50 MHz, D_2O): 52.3, 50.1, 49.6, 42.7, 40.9, 37.8, 33.9 and 33.7 ppm. IR(liquid): 3300, 3080, 2950, 2850, 1640, 1550, 1470, 1440, 1360, 1290, 1140, 1040, 930 cm^{-1}.

Table 2.1. The excess of EDA used in the synthesis of amine terminated PAMAM dendrimers.

Generation	Weight ratio*	Molar ratio*
1	50	100
2	60	170
3	100	290
4	200	720
5	370	1400
6	730	2700
7	1440	5400
8	2870	11000
9	5740	22000

* The ratios are of EDA:ester terminated PAMAM

6. Half Generation (Ester Terminated) PAMAM

The procedure used for the synthesis of generation 1.5 PAMAM was followed starting with the appropriate full generation PAMAM.

7. Hydroxyl Terminated PAMAM

Half generation PAMAM starburst polymers (generations 0.5 - 10.5, supplied by The Dow Chemical Company), 0.2 g (1 mmol of end groups) were individually dissolved in 50 mL MeOH. The solutions were deoxygenated by

passing a flow of N_2 through the solution for no less than 30 min. Distilled aminoethanol, 10 mL (170 mmol) was added by syringe. The solutions were stirred at room temperature for 9 days, after which the solvent was removed under reduced pressure. The polymers of fifth and higher generations were purified by dialysis against MeOH using Spectropore cellulose membranes with a molecular weight cutoff of 1000. The excess aminoethanol was removed from the lower molecular weight dendrimers by repeated reduced pressure azeotropic distillations under reduced pressure of a 4:1 mixture of MeOH and toluene. The procedure was repeated until it was not possible to detect the presence of aminoethanol in the distillate by GC. The success of the reactions was determined by ^{13}C NMR, ^{1}H NMR and IR. ^{1}H NMR (200 MHz, D_2O): 3.45, 3.18, 2.67, 2.48, and 2.24 ppm. ^{13}C NMR (50 MHz, D_20): 177.9, 177.4, 61.8, 53.2, 50.7, 43.3, 38.8 and 33.8 ppm. IR(liquid): 3300, 2940, 2870, 1645, 1560, 1070 cm^{-1}.

8. Selectively Deuterated PAMAM

The procedure used for undeuterated samples was followed with the modification of substituting d_2-MA for MA at the desired point during the synthetic sequence. The d_2-MA was added so as to create a single deuterated layer within an otherwise undeuterated dendrimer (ie.: substituted for MA once during the stepwise polymerization). The location of the deuteration was varied so as to create a series of dendrimers selectively deuterated at different locations.

C. Measurements

^{1}H NMR spectra were obtained using Varian XL-200, XL-300 and CFT-20 nuclear magnetic resonance spectrometers at frequencies of 200, 300 and 80 MHz, respectively. ^{13}C NMR spectra were obtained on Varian XL-200 and XL-300 spectrometers operating at 50 and 75 MHz, respectively. ^{2}H NMR spectra were obtained on Varian XL-300 and Bruker AC-200 spectrometers operating at 46.0 and 30.7 MHz respectively. Chemical shifts (δ) are reported in parts per million (ppm) downfield from tetramethylsilane (TMS). For samples that did not contain TMS the chemical shifts were referenced to the published shifts of resonances from the lock solvent. In the case of ^{13}C NMR spectra obtained in water, either dioxane or sodium trimethylsilylpropionate (DSS) was used as an internal references of known chemical shift. All of the spin-lattice relaxation time (T_1) measurements were performed using the standard inversion recovery method with a pulse sequence 180^{o} -variable delay - 90^{o} - acquisition - fixed delay. In the case of ^{13}C, the T_1 measurements were performed with broadband decoupling of the protons. The temperature inside the probe was maintained to within $0.2^{o}C$ by the variable temperature regulator. i.e., by passing a steady flow of air over the sample. The concentration of polymer was approximately 3% in all cases. Choices of delay times and actual T_1 calculations were performed using standard commands (DOT1 and T1(all)) contained within the standard Varian VXR version 4.1 software package. The nuclear Overhauser enhancement factors (NOEF) were determined by comparison of the peak heights from ^{13}C NMR spectra obtained using continuous broadband ^{1}H decoupling with those obtained with gated decoupling in which the decoupler was only on during

acquisition. For all spectra obtained in NOEF measurements, the delay times between the end of acquisition and the next pulse were no less than 5 times T_1 for the peaks of interest.

Infrared spectra were obtained on either a Perkin-Elmer 283 spectrometer or a Perkin Elmer 1320 infrared spectrometer. All spectra were referenced to the 1601 cm^{-1} band of a thin polystyrene (PS) film.

Gel permeation chromatographic measurements were made on a Waters instrument, using dimethylformamide (DMF) as the carrier solvent, a flow rate of 1.0 mL/min, and three μBondagel columns (E-1000, E-500 and E-125) in series. Peak molecular weights were estimated on the basis of a calibration curve derived from 4 narrowly dispersed polyethylene oxide standards obtained from Scientific Polymer Products, Inc.

Single point intrinsic viscosity measurements were performed in both DMSO and H_2O. All measurements were performed with a semimicro-viscometer 50. The temperature was maintained at 35.2°C ± 0.1°C by submersing the viscometer in a water bath whose temperature was controlled by a Lauda mgw circulator. Polymer concentrations were chosen so as to obtain a ratio of solution to solvent flow times between 1.1 and 1.5.

Polymers were purified by ultrafiltration employing a S1Y3 spiral wound membrane cartridge from Amicon (molecular weight cutoff 3000; 1 sq. ft. of membrane area). The aqueous polymer solutions were pumped through the cartridge by a Masterflex peristaltic pump at a rate of approximately 1 L/hr while maintaining a pressure of 20 -25 PSI over the membrane.

Residual ethanolamine (EA) and ethylenediamine (EDA) contents of the polymers were analysed by gas chromatography, performed on a Varian 1400 gas chromatograph (6 ft. 4 in. glass column; 10% SP-100 on 80/100 mesh Supelcoport; column 178°C for EA, 150°C for EDA; injector 200°C, detector

190°C; flame ionization detection). Reaction sequences were only continued when residual EDA levels in the polymer were determined to be < 1% by weight.

CHAPTER 3

RESULTS AND DISCUSSION

A. Goals and Accomplishments

The goal of this work from the outset was to gain some understanding of the microenvironment created by dendritic macromolecules. This was to be accomplished by the synthesis of poly(amidoamines), or PAMAM, and the subsequent application of ^{13}C and ^{2}H nuclear magnetic resonance (NMR) spectroscopy.

The base polymers were prepared from ammonia, ethylenediamine (EDA) and methyl acrylate (MA). The polymers were prepared so as to possess either primary amine or primary hydroxyl end groups. The syntheses were carried out so as to obtain a minimal number of defects present due to incomplete alkylation, retro-Michael additions and intramolecular "linking" between chain ends. The level of defects was monitored by ^{13}C NMR. It was demonstrated that the intensities of small peaks observed in the spectra, which are attributed to retro-Michael additions, are a function of the temperature at which the amidation reaction is performed. The assignment of the "defect peaks" at the half generation level was based on kinetic data obtained by observing changes in the ^{13}C NMR spectrum of a generation 4 PAMAM upon reaction with MA. The assignments of the peaks present due to defects within full generation PAMAM were further accomplished by obtaining ^{13}C NMR spectra of a series of polymers which were intentionally synthesized with defects.

The steric nature of the new topology created by the starburst polymer has been studied by dynamic NMR; measurements of relaxation parameters being a means by which one can address the question of chain mobility of the starburst branches as a function of molecular weight and position within the polymer. For a series of hydroxyl terminated PAMAM in dimethyl sulfoxide-d_6 (DMSO-d_6), spin-lattice relaxation times (T_1) of the terminal carbons were found to decrease as the number of termini increases from 3 (T_1 = 0.54 ± 0.01s, at 75 MHz) to 3072 (T_1 = 0.23 ± 0.01s, at 75 MHz). Decreases in the nuclear Overhauser enhancement factors (NOEF) of these nuclei were also observed; NOEF ranged from 2.9 ± 0.2 to 2.4 ± 0.2. T_1 was found to increase with temperature; sensitivity to temperature decreased with increasing molecular weight (MW). The T_1's of the methylene carbons on the interior of the dendrimers were found to decrease initially with molecular weight, but were independent of molecular weight above third generation. T_1's determined at lower magnetic field strength (50 MHz) were higher than those at higher field strength (75 MHz). Consistent correlation times (τ) were obtained at both frequencies upon the application of Schaefer's Log(χ) distribution function. Similar results were observed in D_2O. In this solvent, the T_1's of the terminal carbons varied from 0.81 ± 0.08 s to 0.32 ± 0.03 s (at 75 MHz). The NOEF of these nuclei were determined to be 2.8 ± 0.2. The T_1's of the methylene carbons on the interior of the dendrimers varied from 0.42 ± 0.04s to 0.11 ± 0.01s (at 75 MHz) and were found to decrease initially with molecular weight, but were independent of molecular weight above third generation. The NOEF of these nuclei ranged from 2.9 ± 0.2 to 1.7 ± 0.2, and were found to decrease initially with molecular weight, but were independent of molecular weight above sixth generation..

A similar set of data was accumulated for the amine terminated PAMAM. When measured in D_2O, under conditions similar to those used for the hydroxyl terminated PAMAM (25°C, 75MHz), the T_1's of the terminal carbons were found to decrease as the number of termini increases from 3 (T_1 = 0.92 ± 0.09s, at 75 MHz) to 384 (T_1 = 0.50 ± 0.05s, at 75 MHz). The NOEF of these nuclei were determined to be 2.8 ± 0.2. The T_1's of the methylene carbons on the interior of the dendrimers were found to decrease initially with molecular weight, but were independent of molecular weight above third generation. No significant differences in relaxation parameters of the internal carbons were observed, as compared to the study of hydroxyl terminated PAMAM in D_2O.

The larger relaxation times obtained for both series of PAMAM (OH and NH_2 terminated) indicate that the polymer chains are more flexible in D_2O than in DMSO-d_6. Intrinsic viscosities were determined to be comparable in the two solvents (0.04 - 0.10 dl/g, at 35.2 °C), thus the difference in the NMR behavior is attributed to strong H-bonding between the polymer and DMSO resulting in an increase in the hydrodynamic volume of the mobile unit. An increase in the volume of the mobile unit could result if hydrogen bonding were sufficiently strong in DMSO so that the solvent shell was tightly bound and was incorporated into the mobile unit. This would result in a slowing of the motion and an increase in τ. Furthermore, the relaxation behavior of the terminal carbon, as observed in D_2O, was different for the two different end groups. The terminal carbon of the hydroxyl terminated PAMAM was observed to be less mobile than the corresponding carbon atom in the amine terminated PAMAM. The relaxation behavior of the other carbons was indistinguishable for the two end group modifications. All of the trends observed in the relaxation data were very similar, irrespective of

solvent or end group functionality. Thus, these trends reflect topological effects, and are not due to specific solvent or end group behavior.

^2H NMR relaxation measurements were used in a more extensive study of the mobility of amine terminated PAMAM chains as a function of molecular weight and position. When the chain was labelled in the last generation T_1 was found to decrease as the number of termini increases from 3 ($T_1 = 30 \pm 3$ ms, at 75 MHz) to 384 ($T_1 = 7.6 \pm 0.7$ ms, at 46 MHz), and was smaller than the T_1's observed when the polymers were labelled in the interior. Decreases in the spin-spin relaxation times (T_2) of these nuclei were also observed; T_2 ranged from 10 ± 1 ms to 2.4 ± 0.2 ms. No significant difference in relaxation parameters was observed when the label was located in the interior repeat units of dendrimers of similar MW, irrespective of chain length following deuteration, and no evidence of radial gradients was found.

B. Monomer and Polymer Preparations

In order to obtain a good understanding of the effects of the starburst topology on chain mobility a well defined series of systematically varied samples must be prepared. As mentioned in the Introduction, the necessary background work on the synthesis of PAMAM was reported by Tomalia et al. (54-60), but the polymers synthesized in that laboratory had defect levels unsuitable for a comprehensive NMR study. Selective labelling of the polymer with an NMR active nucleus (e.g., ^2H) has the potential of being a very powerful tool but only if the samples are of high quality or, at a very minimum, of known quality. As a continuation of the work of Tomalia et al., synthetic techniques were developed to prepare a series of polymers ranging in molecular weight from 350 to 350,000 with defect levels one fifth those of samples prepared according to the previously reported techniques. Furthermore, syntheses of polymers with two different end groups (primary amines and primary hydroxyls) have facilitated a study of the effect of end-group functionality on chain mobility.

1. Monomer Synthesis.

The synthesis of the β-d2-methyl acrylate (d2-MA) used in this work was carried out according to the method reported by Nugent and McKinney (48). The method involved a Wittig reaction between d2-formaldehyde, generated in situ from d2-paraformaldehyde, and methyl (triphenylphosphoranylidene acetate). The monomer was easily purified from the reaction mixture by cryogenic distillation in 72% yield. GC-MS

indicated that the d_2-MA incorporated 99% of the maximum level of deuteration, or better.

2. Poly(amidoamine) Syntheses.

The poly(amidoamine) has been prepared by the method of excess multifunctional reagents. The method involves the reaction of a nucleophilic initiator core (ammonia) with a multifunctional electrophilic reagent (methyl acrylate, MA) which possesses moieties of significantly different reactivities toward the initiator core. Subsequent reaction of this adduct with a large molar excess of a multifunctional nucleophile (ethylenediamine, EDA), produces an adduct of increased terminal multiplicity, and with terminal nucleophilic sites that can serve to further expand the system upon repetition of the reaction sequence. In repeating the sequence over and over again, a highly symmetrically branched condensation polymer can be prepared. In designing a polymer with this particular set of comonomers one can create a system where the number of branch points doubles with each successive cycle. In order to ensure the creation of the ideal dendritic topology, all reaction steps must be essentially quantitative. Furthermore, the reactions must be performed under conditions that avoid intermolecular bridging, intramolecular "looping", retro-Michael additions, incomplete alkylations and any other side reactions that may result in deviations from the desired topology. The effect of defects, due to retro-Michael additions and incomplete alkylations (Figure 3.1) on the actual distribution of chains comprising the dendrimer population, can be calculated according to the equation below:

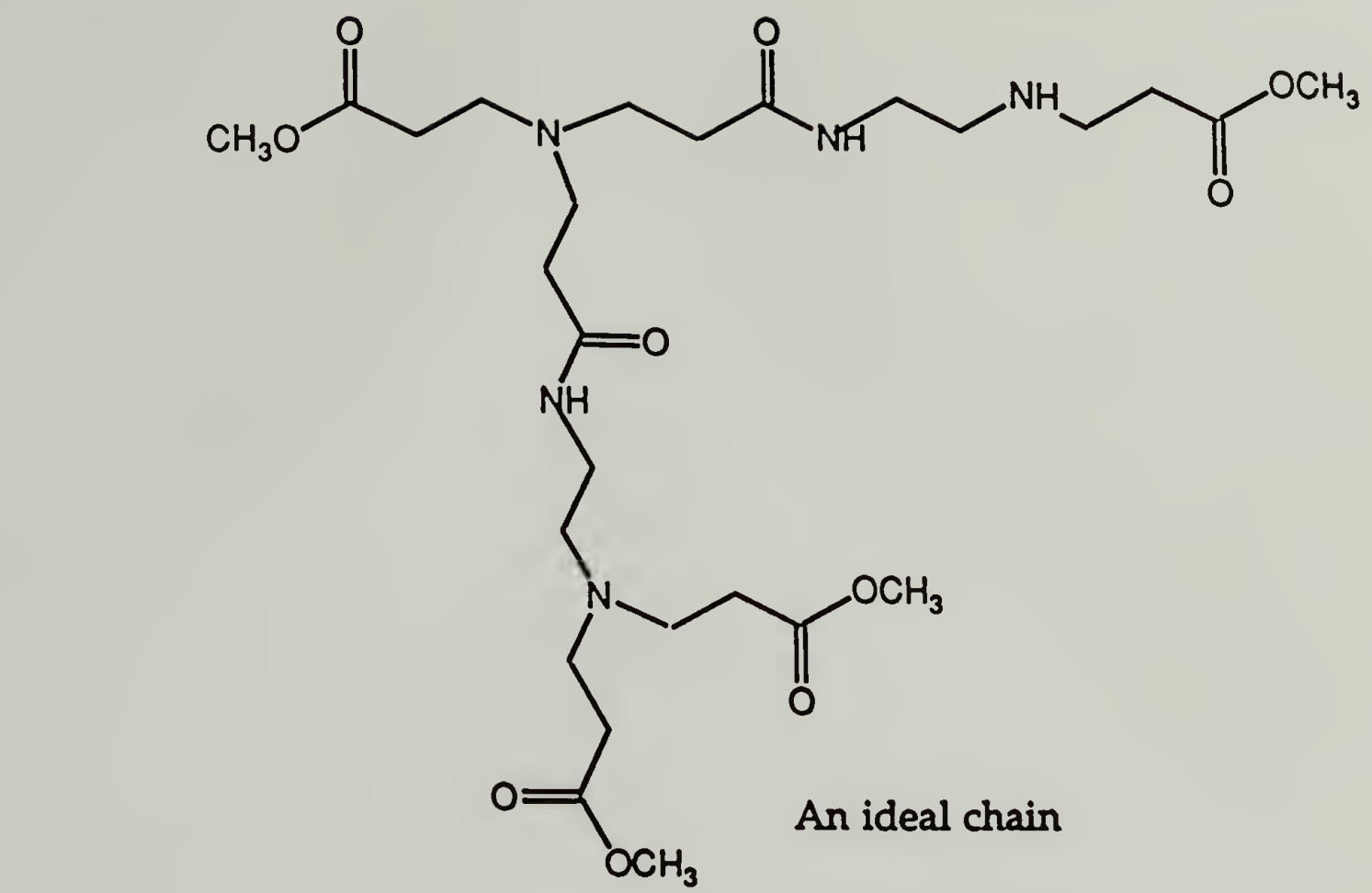

Figure 3.1. An illustration of the defects that can be present in a generation 1.5 PAMAM due to retro-Michael additions and incomplete alkylations, as well as the healing process at earlier generations.

$$F = \binom{G+D}{D} p^{G} (1-p)^{D} \qquad (12)$$

where F is the fraction of direct paths from the topological centre to an end group that has been successfully synthesized to the specified length defined as G and D is the number of times that defects occurred along a specified path from the topological centre of the molecule. Thus, G+D is the number of times that the synthetic sequence has been attempted during a stepwise polymerization and $\binom{G+D}{D}$ is the number of permutations possible for a chosen level of defects or value of D. The parameter p would then correspond

to the probability of successfully adding a particular generation or of increasing the value of G by 1, and 1-p would then correspond to the probability of increasing the value of D by 1, or the probability of a defect occurring. Figure 3.2 illustrates the dependence of the distribution of chain lengths on the value of p. The plots illustrate the necessity to maintain defect levels at as low a level as possible. The distribution of chain lengths, from which a dendrimer is comprised, is strongly dependent on the level of defects incurred at each stage of the stepwise polymerization. The figure also demonstrates the importance of tabulating the level of defects at each stage of the polymerization so as to maintain a fundamental understanding of the nature of the final dendrimer. With defect levels of approximately 1% the total number of defects accumulated during the synthesis of a generation 10 PAMAM is on the same order of magnitude as the experimental errors typically estimated for NMR experiments (10%). As such, synthetic procedures to maintain levels as low as possible (preferably ca. 1%) had to be developed.

In perfecting the synthesis of PAMAM dendrimers, it was first necessary to find an appropriate method with which to monitor the level of defects. The technique had to be sensitive to very small deviations from "ideal" molecular weight. One possible choice is ^{13}C NMR. The determination of the sensitivity of the technique to imperfections was ascertained by two methods. First, defects were intentionally introduced into the system by stopping the alkylation step prior to the completion of the reaction (defect levels are ca. 10%). Defects are plainly evident, and are still observed even after subsequent reactions are performed. This is demonstrated

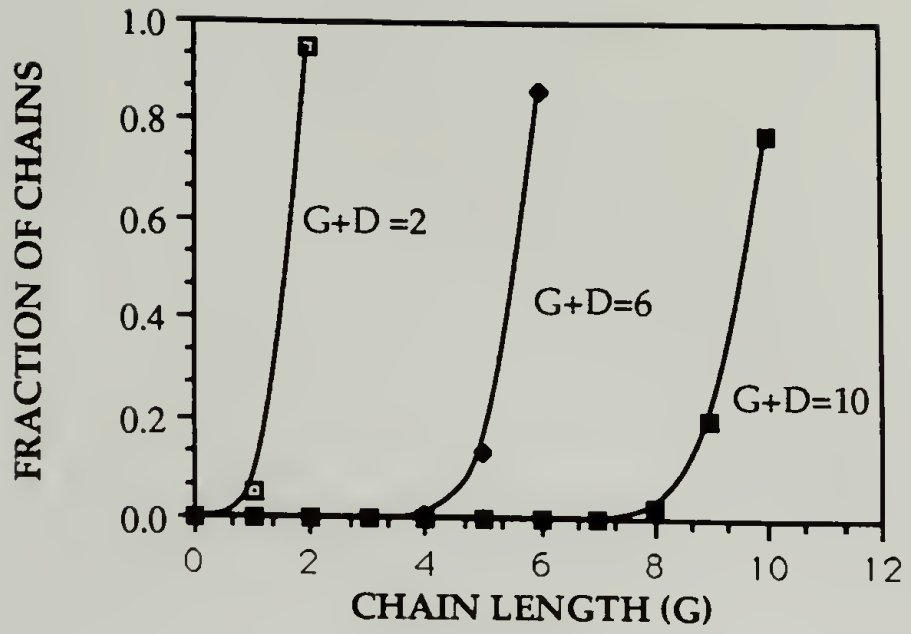

(a)

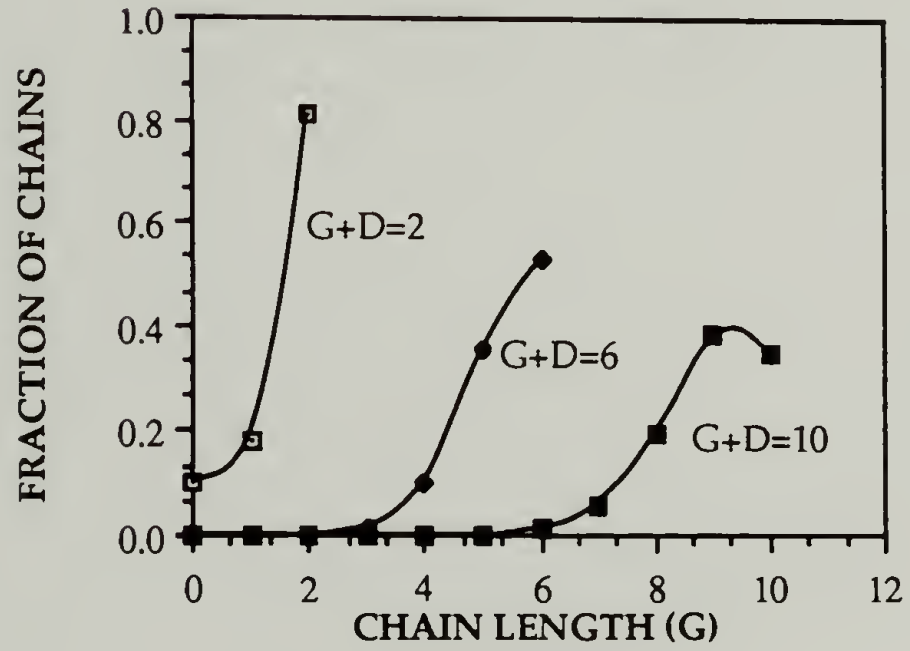

(b)

Figure 3.2. The distribution of chain lengths comprising dendrimers with defect levels due to incomplete alkylation and retro-Michael additions; (a) 1-p = 0.025; (b) 1-p = 0.10.

in Figure 3.3 which contains illustrative spectra of PAMAM of generations 0.5, 1.0 and 1.5, and shows the ^{13}C chemical shift assignments of the defect peaks as well as of the major peaks due to "ideal" structures. The assignments of the peaks were made on the basis of the assignments reported by Tomalia (54, 56) for dendritic oligomers, and from calculations of the theoretical chemical shifts through the use of additive substituent parameters (52). The ^{13}C NMR spectra of PAMAM which have been selectively labelled with ^{2}H at the position β to the carbonyl facilitated the assignment of the resonance frequency of this carbon as the intensity of this peak is significantly diminished as compared to that of the corresponding signal in the spectrum of the undeuterated analogue. The observed spin-lattice (T_1) relaxation times of dendrimers of full generation facilitated the distinction between the terminal and internal carbons as the end groups, whose motions are not as restricted as those of the backbone, have significantly longer relaxation times than any of the internal carbons. The spectra of generations 0.5 and 1.0 clearly show two peaks that are assigned to defects (at 34.3 and 44.8 ppm for generation 0.5; at 36.3 and 45.1 ppm for generation 1.0), while in the spectrum of generation 1.5 there are 6 peaks which are identified in structure 1. It is important to realize the second addition of excess MA permits the alkylation of any unreacted amine at the core. Eventually, the imperfections due to incomplete alkylation at lower generations are obscured such that one can only distinguish defects that occur at the terminal generation from those that occur in the interior of the polymer; the latter having identical chemical shifts. Because of this phenomenon, the system is said to be self-correcting or self-healing. This makes it necessary to determine the degree of incomplete alkylation at every step of the polymerization; mere analysis of the defect

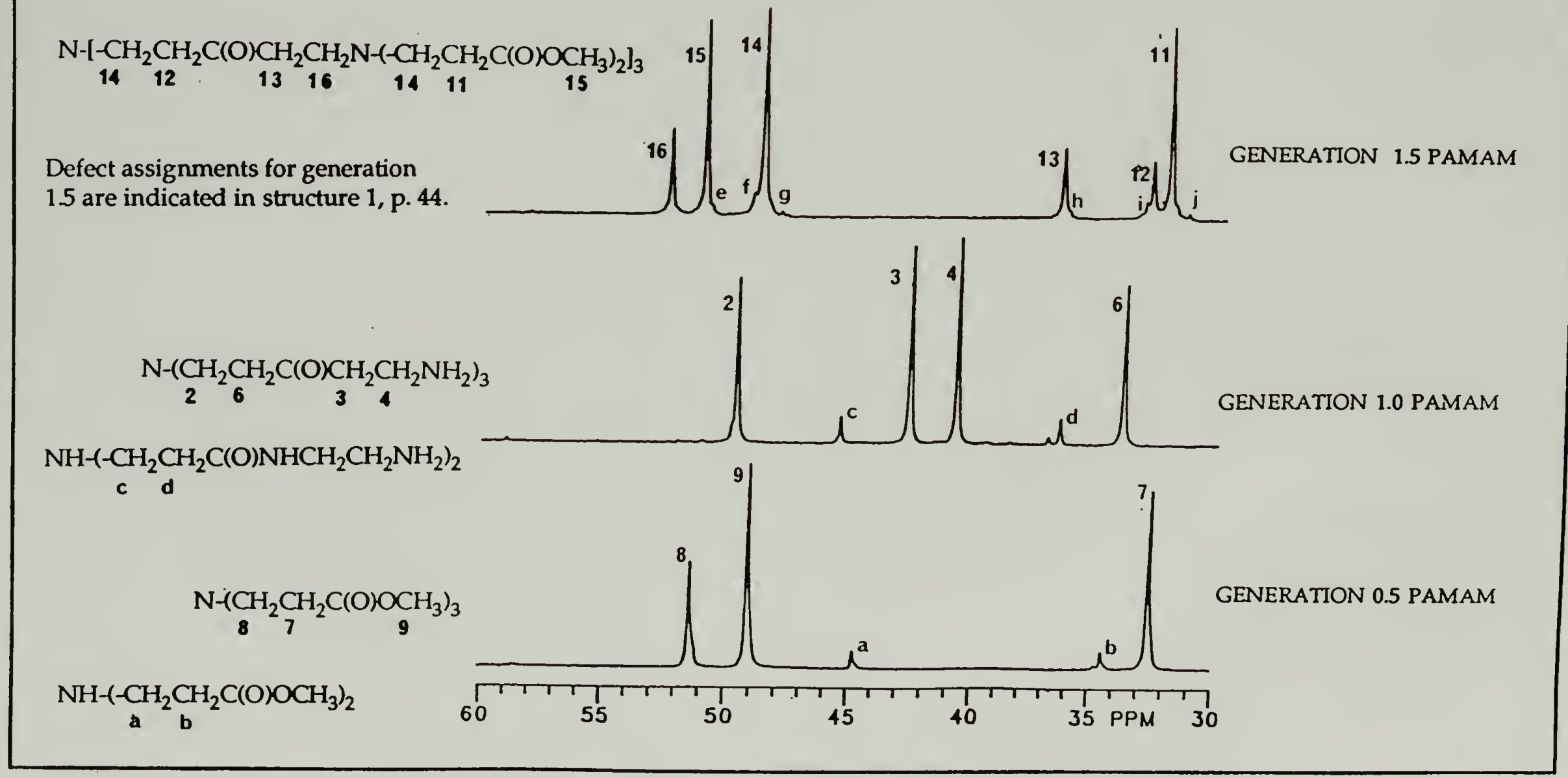

Figure 3.3. Detection of defects that may occur during the synthesis of the PAMAM dendrimers by ^{13}C NMR (50MHz); (a) generation 0.5 ($CDCl_3$); (b) generation 1.0 (D_2O); (c) genaration 1.5 ($CDCl_3$).

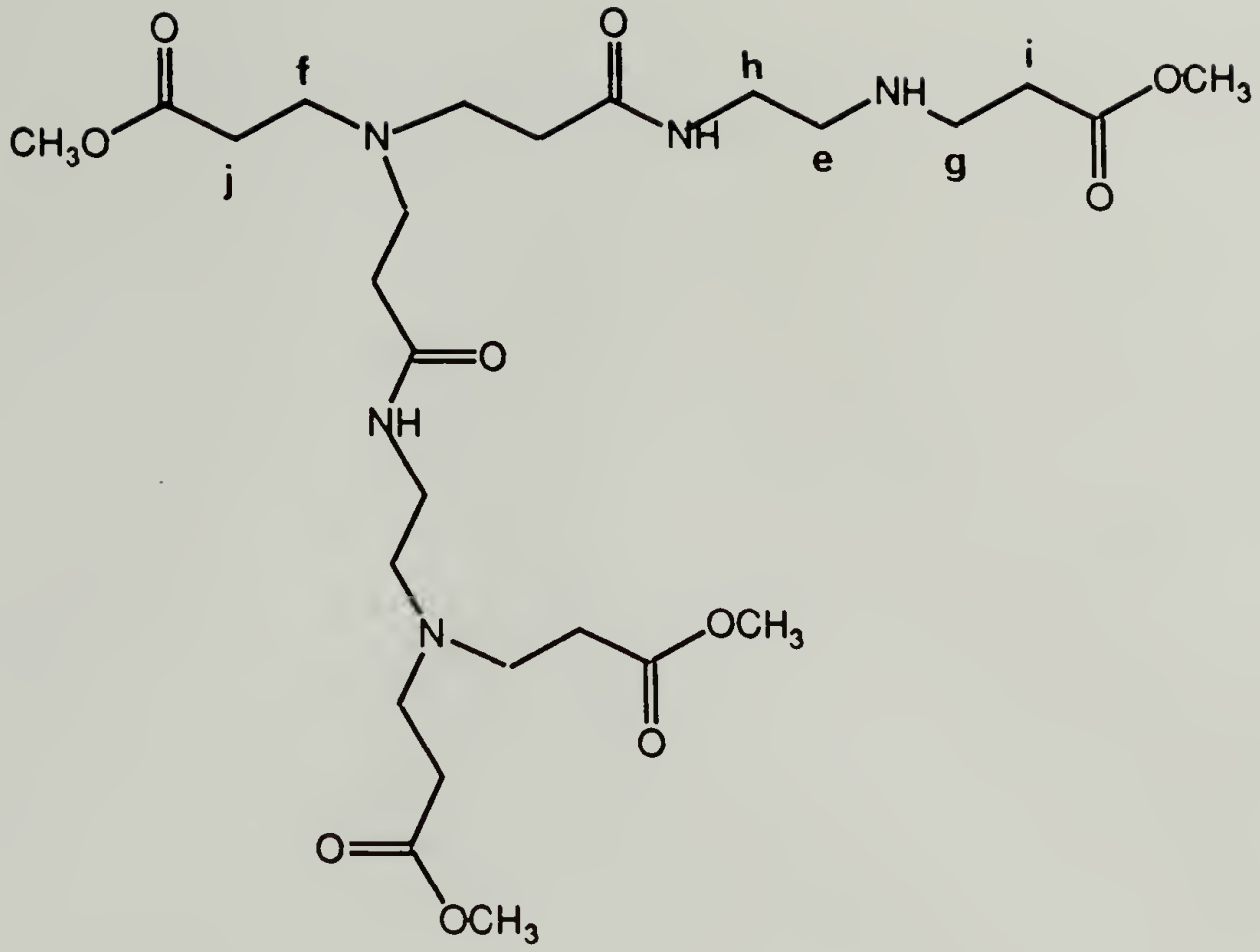

1

levels of the final polymer alone is not an accurate indication of the nature of the structure created.

Finding an appropriate technique with which to monitor the possible incomplete conversion of end groups during the alkylation process is equally important. Here once again, NMR proved to be a valuable asset. Sensitivity of the technique to incomplete alkylation was determined by acquiring ^{13}C spectra during the alkylation of a generation 4 PAMAM. Figure 3.4 demonstrates the sensitivity of the technique to the first and second alkylations of the primary amine end groups. From the decrease in the intensity of the peaks due to the terminal carbons (observed at 42.1 and 43.2 ppm) and the appearance of new resonances due to the first alkylation, at 40.3, 45.5 and 52.4 ppm (refer to Figures 3.4a and 3.4b which include the chemical shift assignments), it is apparent that significant amounts of alkylation have occurred during the first hour following the addition of the MA. After 2.5 hr,

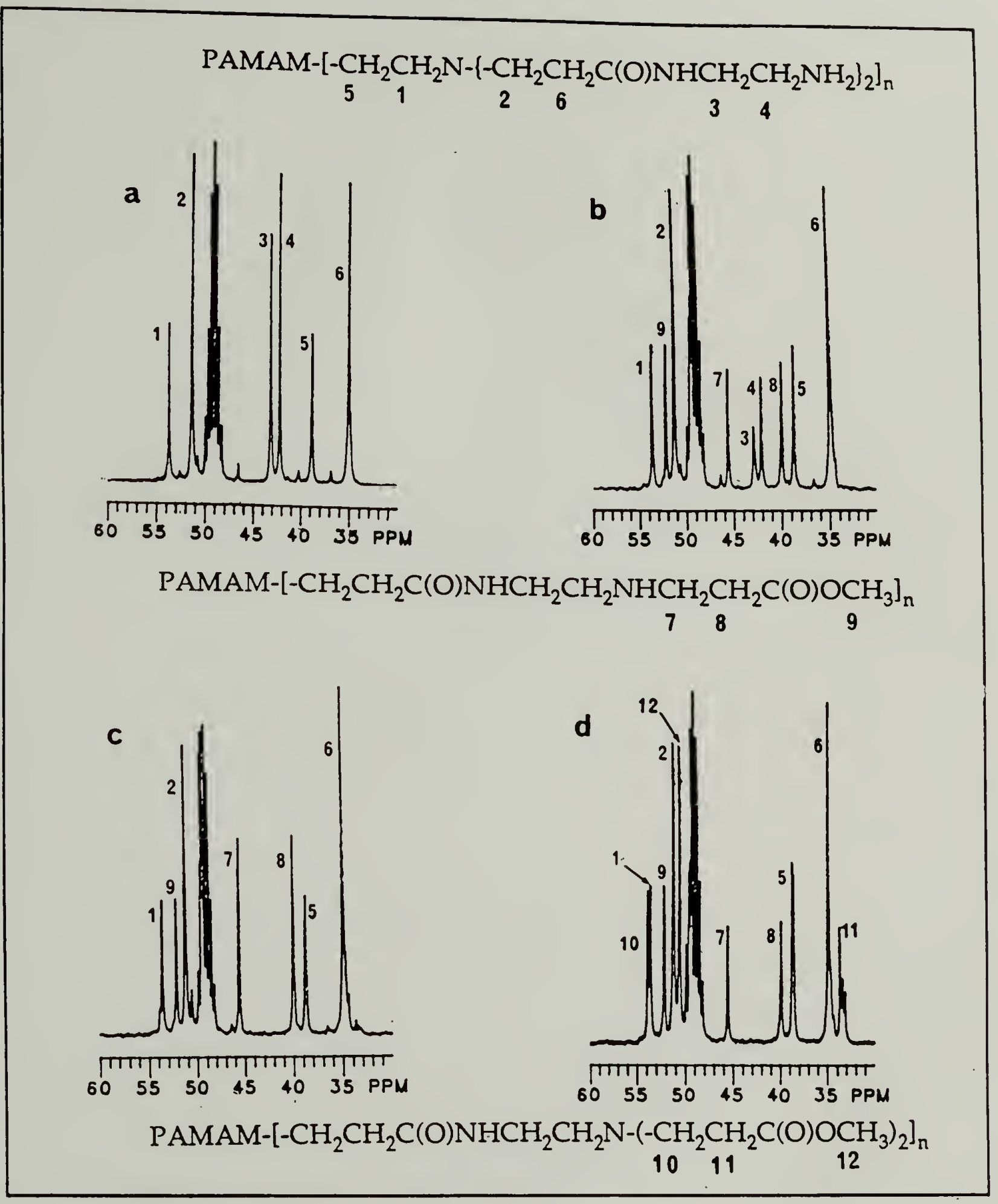

Figure 3.4. ^{13}C NMR (CD_3OD, 75 MHz, 22°C) of the alkylation of a generation 4 PAMAM; (a) before addition of MA; (b) 1.2hr. after addition of MA; (c) 2.5hr. after addition; (d) 22hr. after addition.

the peaks due to the terminal carbons of the full generation PAMAM are no longer detectable (refer to Figure 3.4c). The intensity of the peaks due to the product of the first alkylation are observed to subsequently diminish as the amines are further alkylated (refer to Figure 3.4d), eventually reaching the point where the peaks due to incomplete alkylation are no longer detectable, and peaks due to the product of the second alkylation appear at 33.8, 38.2, 50.7 and 53.7 ppm. Figure 3.5 contains the ^{13}C spectrum of the final product. It has

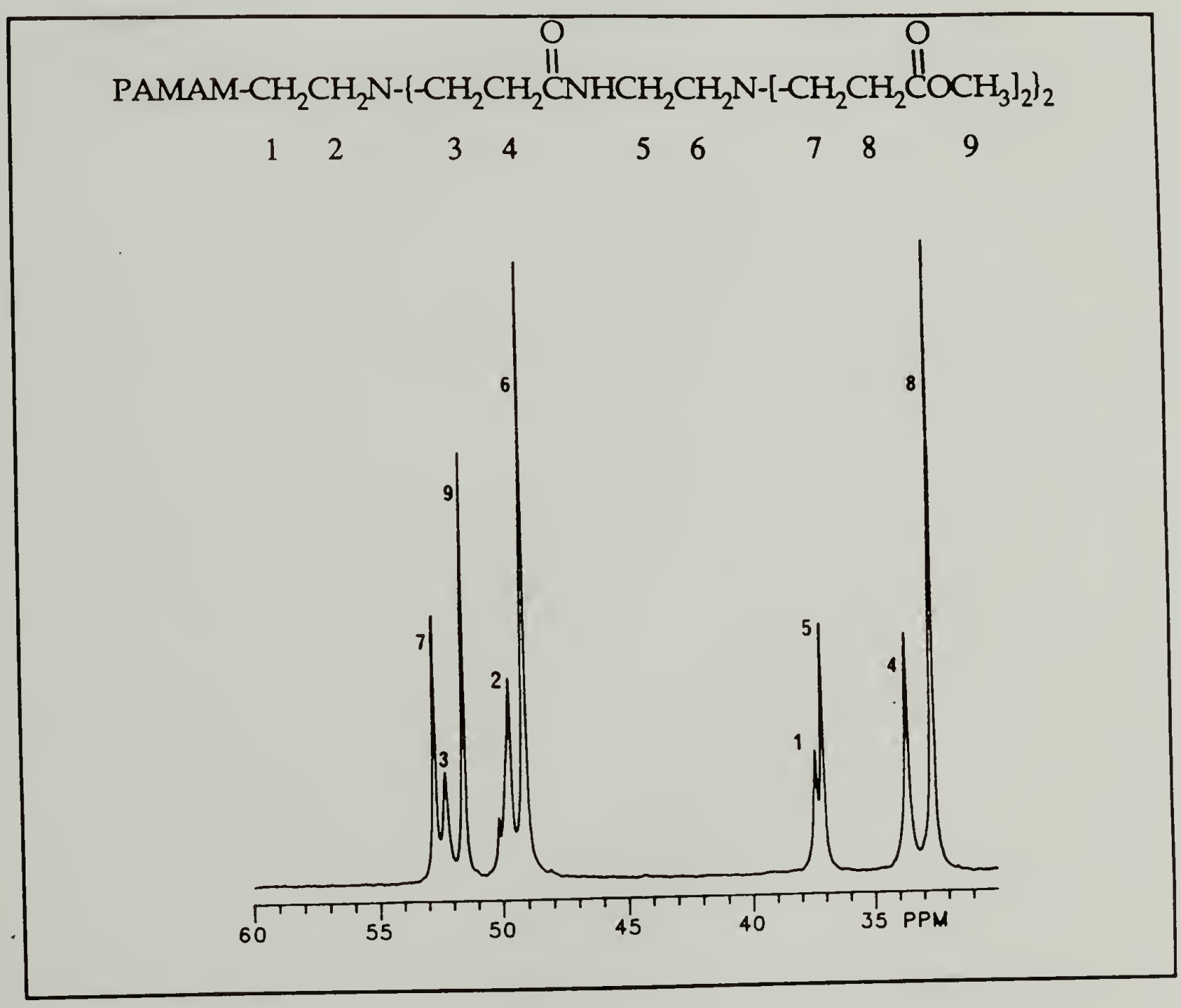

Figure 3.5. A ^{13}C NMR spectrum of a generation 4.5 PAMAM dendrimer (75 MHz, $CDCl_3$).

thus been demonstrated that the technique can be used to monitor the degree of alkylation of the end groups of the full generation PAMAM.

While complete alkylation of the amine termini with MA has proven to be possible, subsequent retro-Michael additions (RM) occur during the amidation process, prior to the removal of the excess amine, ie.: the defect levels have been shown to be independent of the method chosen for the removal of the amine (refer to Figure 3.6). Apparently, the amine acts as a base in order to catalyze the RM of ester terminated PAMAM prior to amidation. Such an occurrence is evident upon inspection of Figure 3.7, in which resonances due to the presence of incomplete alkylation, that are not observed in the ^{13}C spectrum of the generation 0.5 PAMAM, appear at 36.8 and 45.9 ppm.

The defect levels have proven to be sensitive to the temperature at which the amidation occurs, and reaction conditions have been modified in order to minimize the level of defects. Lowering the temperature of the amidation step to $0^{o}C$ from $22^{o}C$ is sufficient to reduce the number of defects due to RM to the point where the ratio of the peak due to the presence of carbons α to carbonyls in the defect (at 36.3 ppm) is ca. 1.5% of the height of the peak due to the presence of the carbon β to the carbonyl in the ^{13}C spectra. This is clearly evident upon examination of the spectra presented in Figure 8, in which the resonances due to the presence of defects are approximately 5% of the intensity of the resonance due to the presence of the carbon β to the carbonyl when the amidation was performed at room temperature. The quality of the samples was significantly improved when the amidation was performed at lower temperatures (i.e., $5^{o}C$ or $0^{o}C$) in that the level of defects was ca. 20% of that obtained for the room temperature amidations.

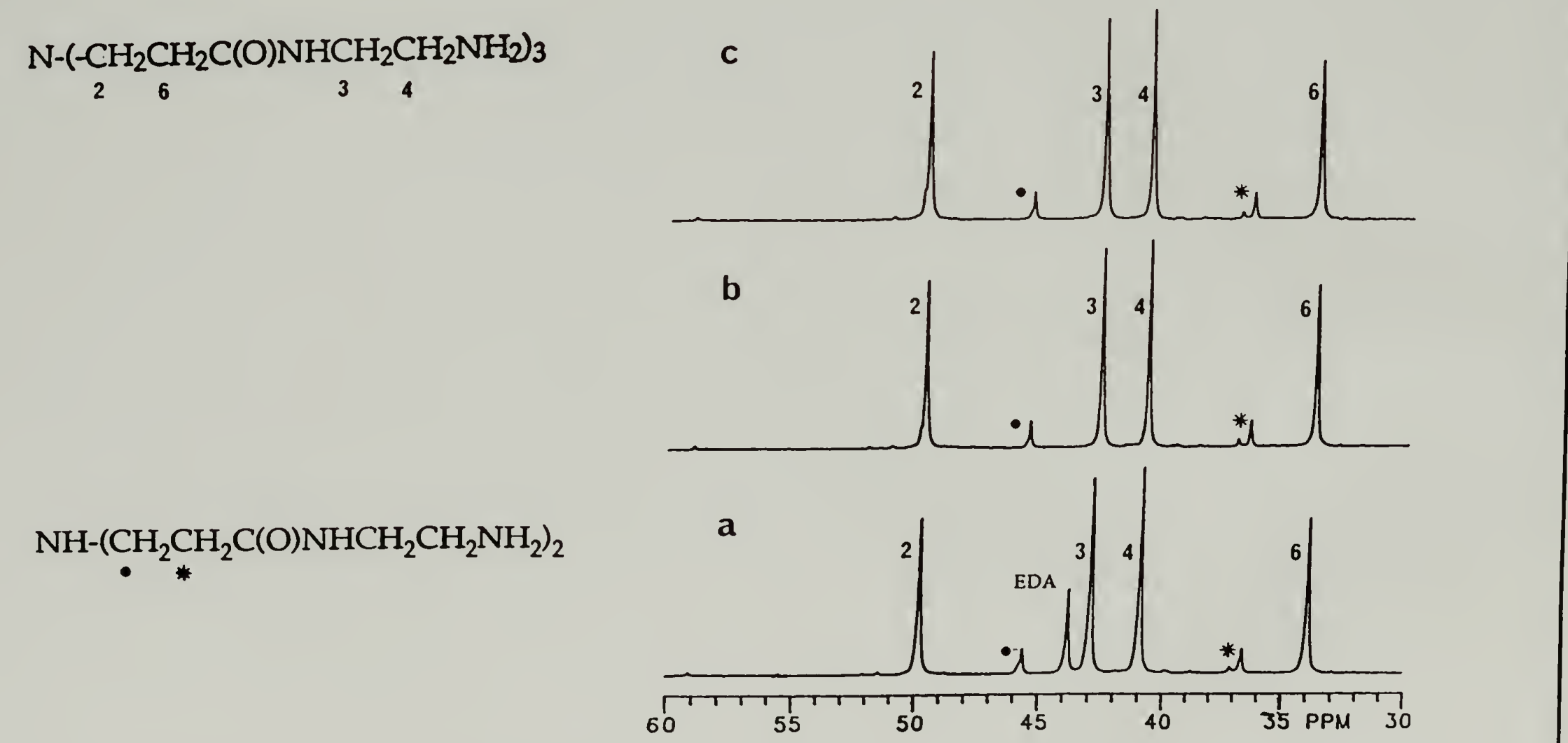

Figure 3.6. The sensitivity of retro-Michael additions of the PAMAM dendrimer to the method of EDA removal (50MHz, D_2O). (a) after removal of EDA at 35°C/20-30 Torr; (b) additional removal of EDA under vacuum at 20°C/0.5-1.0 Torr; (c) additional removal of EDA by azeotropic distillation at 35°C/20-30 Torr.

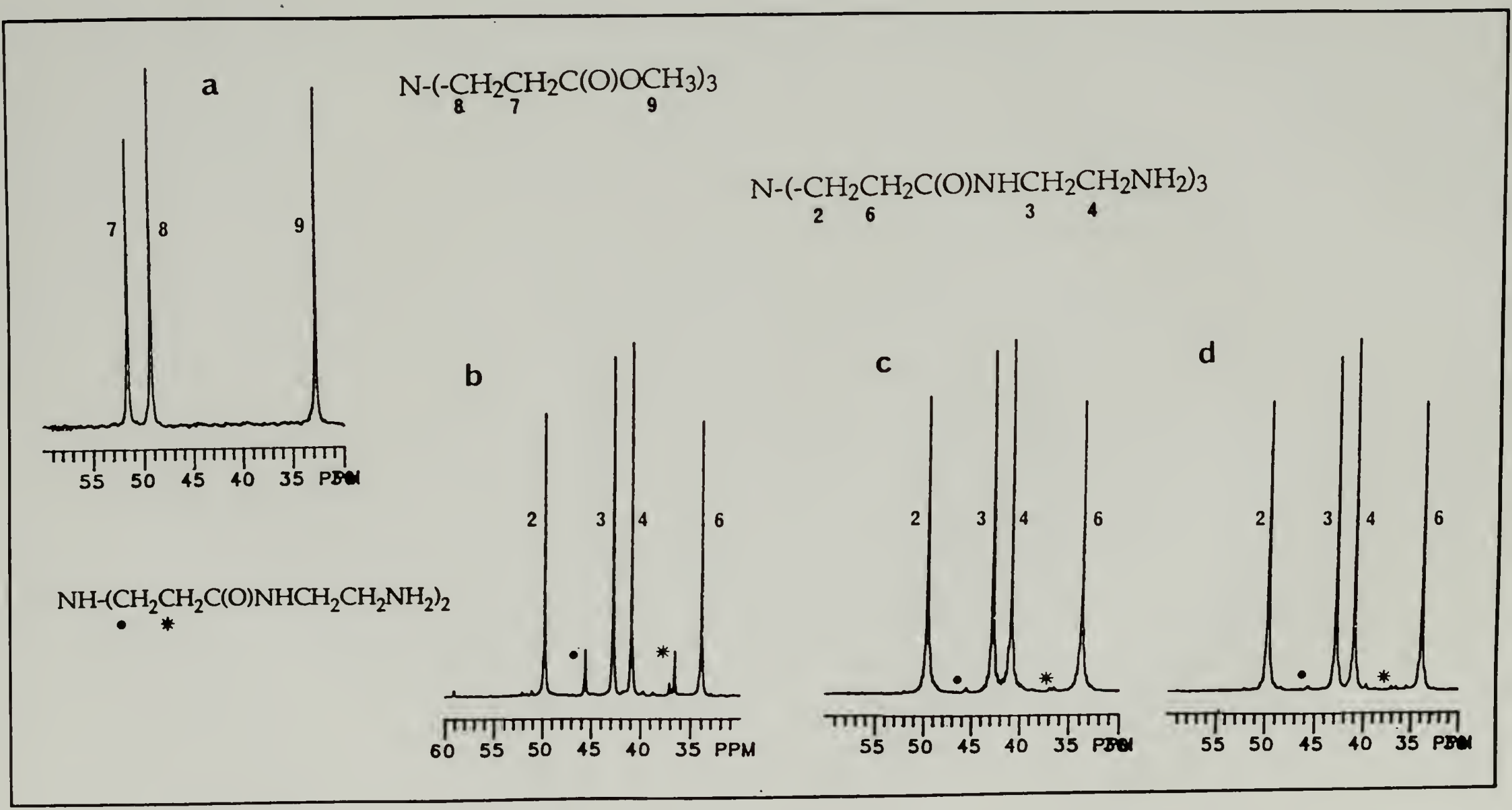

Figure 3.7. The sensitivity of retro-Michael additions of the PAMAM dendrimer to the temperature at which the amidation reaction is performed as monitorted by ^{13}C NMR (50 MHz); (a) generation 0.5 PAMAM ($CDCl_3$); (b)-(d) generation 1.0 PAMAM amidated at 22°C, 5°C and 0°C, respectively (D_2O).

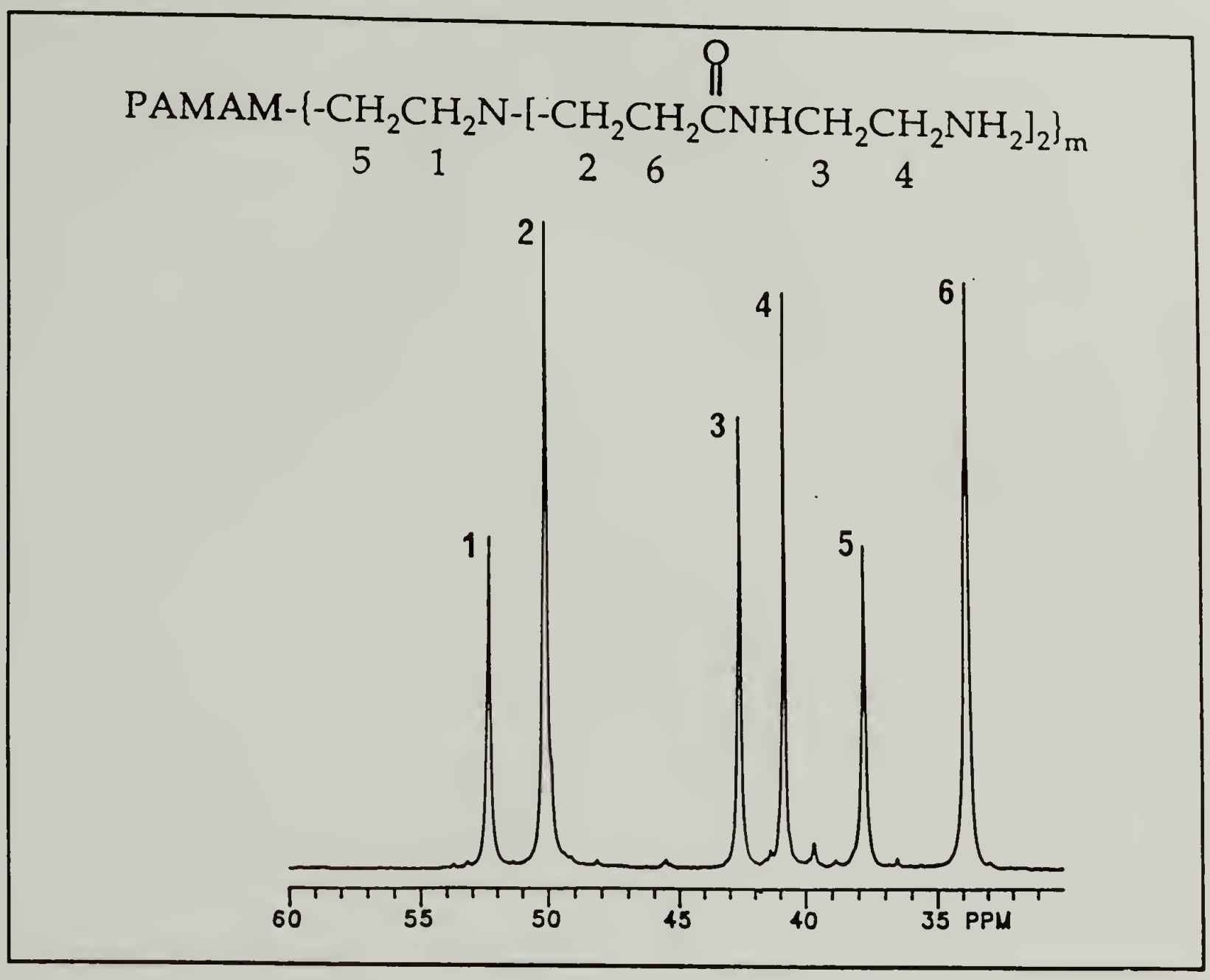

Figure 3.8. A ^{13}C NMR spectrum of a generation 6 PAMAM dendrimer terminated with NH_2 groups (75 MHz, D_2O).

3. Syntheses of Hydroxyl Terminated Poly(amidoamine).

The reaction conditions employed in this modification of the synthesis reported by Tomalia et al. (54, 56), i.e., substituting ethanolamine for ethylenediamine in the terminal step of the stepwise polymerization, permitted a decrease in the amount of nucleophile necessary in order to avoid cross-linking. The difference in nucleophilicity of alcohols and amines proved sufficient in avoiding cross-linking. A typical spectrum of an hydroxyl

terminated PAMAM is depicted in Figure 3.9. The ^{13}C NMR spectrum depicted is that of an 8 generation hydroxyl terminated PAMAM, in which only 8 different peaks are observed as the carbons of different generations are of indistinguishable chemical shifts, except for the terminal generation. The assignment of the peaks was made on the basis of the assignments reported by Tomalia (54, 56) for dendritic oligomers, and from calculations of the theoretical chemical shifts through the use of additive substituent parameters (52). The ^{13}C NMR spectra of PAMAM which have been selectively labelled

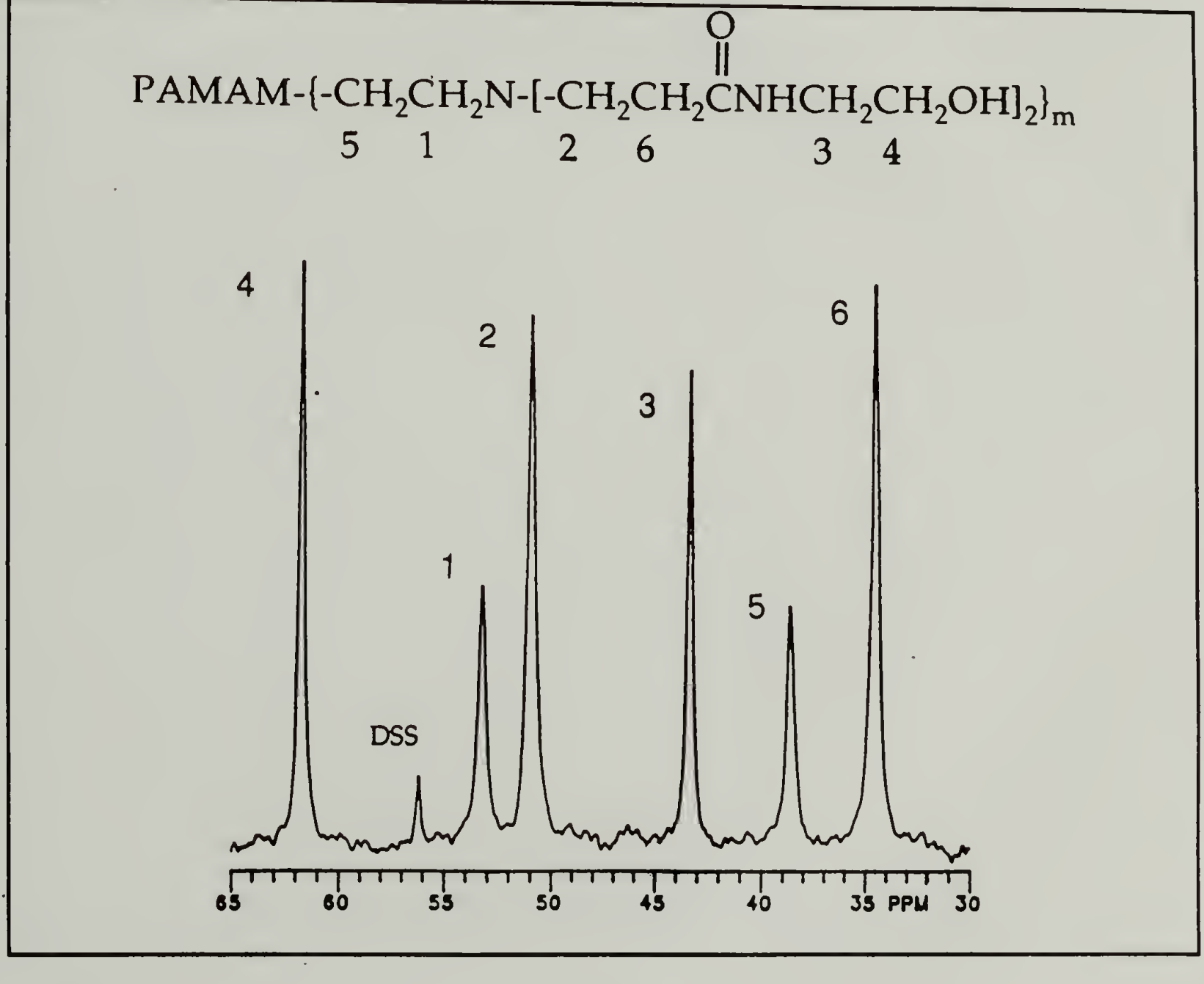

Figure 3.9. A ^{13}C NMR spectrum of a generation 8 PAMAM dendrimer terminated with OH groups (75 MHz, D_2O).

with ^2H at the position β to the carbonyl facilitated the assignment of the resonance frequency of this carbon as the intensity of this peak is significantly diminished as compared to that of the corresponding signal in the spectrum of the undeuterated analogue. The observed spin-lattice (T_1) relaxation times facilitated the distinction between the terminal and internal carbons as the end groups, whose motions are not as restricted as those of the backbone, have significantly longer relaxation times than any of the internal carbons. The peak assignments are indicated in the figure.

4. PAMAM Selectively Labelled with Deuterium.

A series of PAMAM dendrimers that is selectively labelled with deuterium has been prepared. This was accomplished by substituting d_2-MA for MA at the desired step within the stepwise polymerization, employing undeuterated MA both prior to and following the alkylation of the polymer with the d_2-MA. Otherwise, reaction conditions employed were identical to those used in the synthesis of the unlabelled, amine terminated, PAMAM discussed above. Defect levels were identical to those obtained for the unlabelled dendrimers, i.e. 1-2%. The selective substitution of d_2-MA for MA, facilitated the preparation polymers of different molecular weights, yet all labelled in the same location. In an analogous manner, polymers of similar molecular weight, each labelled at different distances from the initiator core, have also been synthesized.

C. ^{13}C NMR Relaxation Experiments.

1. Hydroxyl Terminated Poly(amidoamine) Dendrimers.

The hydroxyl terminated PAMAM series is a minor modification of the classical PAMAM structure. The base structure is that of the PAMAM, but the polymers comprising this series are terminated with primary hydroxyl groups rather than primary amines. Not only does this modification remove the problems associated with oxidation of the primary amine termini, but crosslinking of the PAMAM that can occur by transamidation, with the amine end groups acting as nucleophiles, is not a problem with the modified structure.

The relaxation measurements were obtained for a series of 11 different dendrimers of molecular weight varying from 362 to 614000, i.e., generations 1-11. Relaxation parameters were measured for the aliphatic carbons that were not obscured by the peaks due to the solvent DMSO-d_6 (the solvent obscured the resonances of carbons that are labelled 3 and 5 in Figure 3.9, appearring at 43.3 and 38.8 ppm, respectively, in D_2O). The choice of DMSO-d_6 as solvent permitted the observation of the terminal group (at 61.0 ppm) and three internal sites, i.e., carbons labelled 1, 2 and 4 in Figure 3.9 (at 52.3, 49.9, and 33.8 ppm). The reasons for not measuring the parameters of the carbonyl carbons were are two fold: 1) the relaxation times can be long (> 2 sec.), causing the data acquisition to be prohibitively long, and 2) the relaxation mechanism for the carbonyls is, in general, much more complicated than that for the protonated carbons as the relaxation process may be affected by intermolecular dipole-dipole interactions (DD), ^{14}N-^{13}C DD as well as

intramolecular ^{1}H-^{13}C DD from ^{1}H on adjacent nuclei (27). A typical inversion recovery experiment from which T_1 was calculated is illustrated in Figure 3.10. The T_1 have been calculated from the peak heights observed at the delay times indicated in the figure. The observed dependence of the ^{13}C T_1 on molecular weight is depicted in Figure 3.11. The T_1 of the carbon alpha to the carbonyl is constant above third generation (12 ends). A similar trend was observed for the other interior carbons. In fact, the relaxation rates for all of the interior carbons in the homologous series are indistinguishable. The relaxation of the interior carbons is faster than that of the terminal carbon in all cases. The low values of T_1 observed for the interior carbons are indicative of slower molecular motions in the interior of the starburst polymer. The consistency of the values observed at higher generations (ie.: above third generation) suggests that the mobility of the polymer chains may not be affected by the size of the polymer, but that the motion responsible for relaxation is dominated by segmental motion for dendritic macromolecules as it is for linear polymers (1, 18, 21, 37). This also suggests that, on average, the starburst chains do not experience a significant increase in rigidity brought on by an increase in the number of ends per unit surface area of the polymer "sphere". It is important to realize that carbons in successive generations comprising a larger polymer have identical chemical shifts and as a result the T_1 values reported for interior carbons are averages over all generations except the terminal generation.

The behavior of the T_1 values of the terminal carbon appears to be of interest. Over the range studied, the relaxation rates of this particular carbon decrease with increasing MW. The decrease in T_1 indicates a decrease in segmental mobility, and could be interpreted in terms of the model for

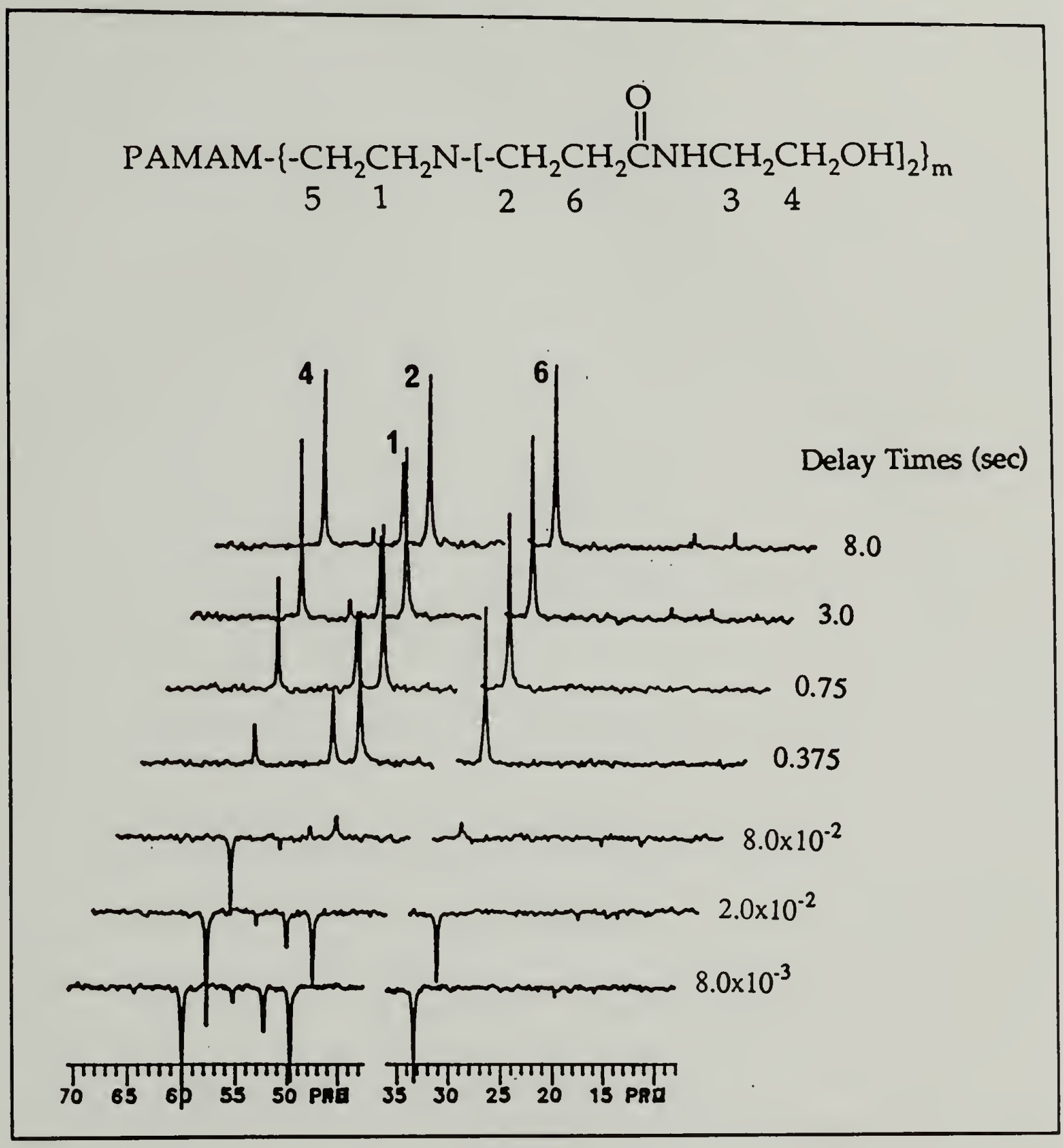

Figure 3.10. An inversion recovery experiment from which the T_1 of a generation 5 PAMAM dendrimer terminated with OH groups was calculated ($30^{o}C$, 75MHz, DMSO-d_6).

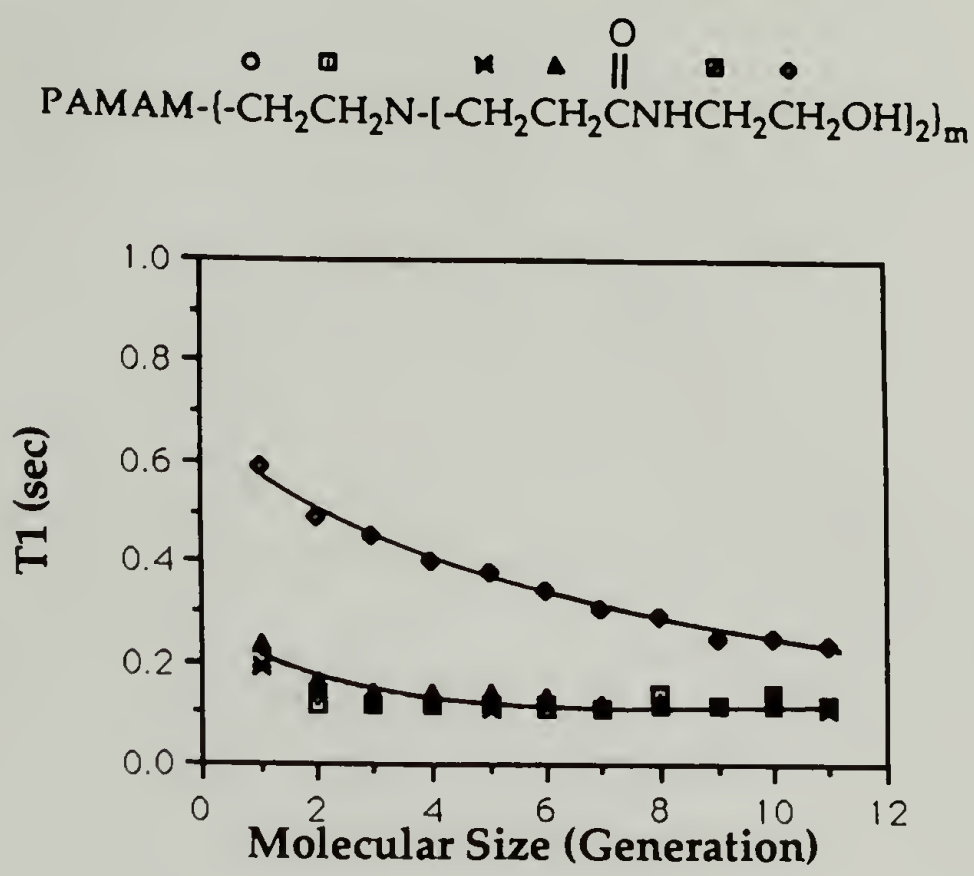

Figure 3.11. The dependence of T_1 on molecular size for OH terminated PAMAM (23^{o}C, 75 MHz, DMSO-d_6).

starburst topology as described by de Gennes (8) and Maciejewski (36). The model suggests that steric interactions induced by dense-packing of the end groups increase as the number of termini per unit surface area increases. The model further suggests that the degree of dense-packing should approach an upper limit at which continued branching in the pattern of starburst polymers is no longer possible. However, it appears that the shell that would result from such an occurrence was not created. The T_1's of the terminal carbons are dependent on MW over the entire MW range studied but are always larger than the T_1 observed for the interior carbons. The size of the polymers studied exceeded the theoretically predicted value for the "starburst limit" (generation 6.3 if one assumes 2 Kuhn steps between branch points) (8). If the anomaly of a densely packed surface, comprised of end groups, did in

fact occur, the relaxation rate of the terminal carbons should have decreased dramatically upon formation of the shell. The creation of such a shell would also affect the kinetics of the synthesis of the dendrimers, i.e., lower the rate of reaction by limiting access to the reactive sites. While no study of the effect of generation on the reaction kinetics has been reported, there is no evidence for an increase in steric hindrance of the reaction sites at higher generations, i.e., the level of defects achieved generation 8 was comparable to that achieved at generation 3.

Figure 3.12 illustrates a typical experiment from which the NOEF were determined. The NOEF were determined by comparison of the peak heights from the ^{13}C NMR spectra obtained using continuous broadband ^{1}H decoupling with those obtained with gated decoupling in which the decoupler was on only during acquisition. For all spectra obtained in NOEF measurements, the delay times between the end of acquisition and the next pulse were no less than 5 times T_1 for the peaks of interest. Figure 3.13 illustrates how the experimentally determined NOEF values of different carbons depend on MW. As was observed to be the case for T_1, the NOEF of the interior carbons becomes independent of MW at higher generations. However, unlike the MW dependence observed for the T_1's of the interior carbons, the NOEF is still dependent on MW up to generation 7. This apparent contradiction merely indicates that the data obtained are in the vicinity of the T_1 minimum, and that any analysis of the effects of the topology of chain mobility should only be discussed in terms of τ. Such a discussion is presented below, after all the trends in T_1 and NOEF are discussed.

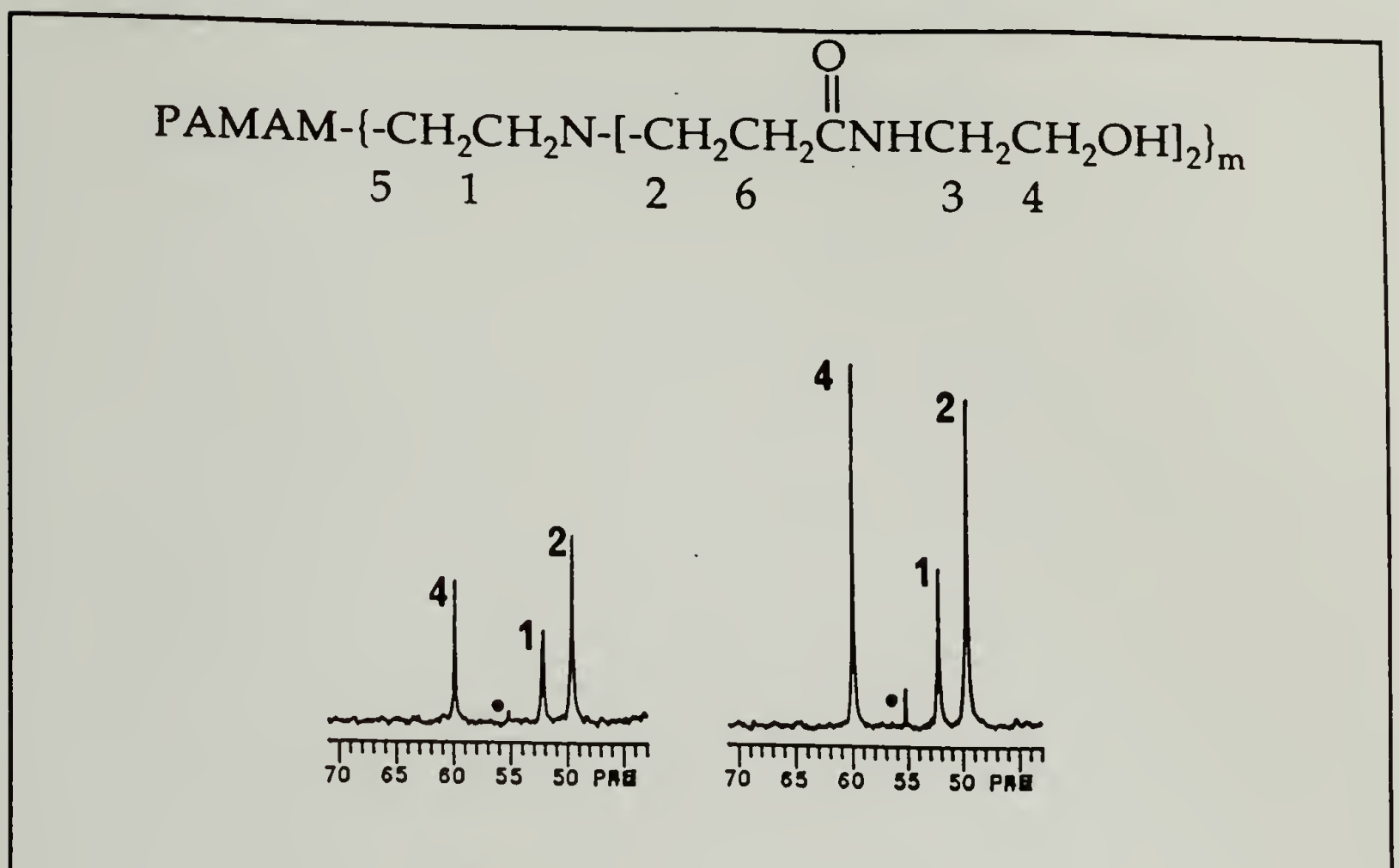

Figure 3.12. A NOEF measurement of a generation 5 PAMAM dendrimer terminated with OH groups (30°C, 75 MHz, DMSO-d_6); (a) gated decoupling; (b) full broadband decoupling.

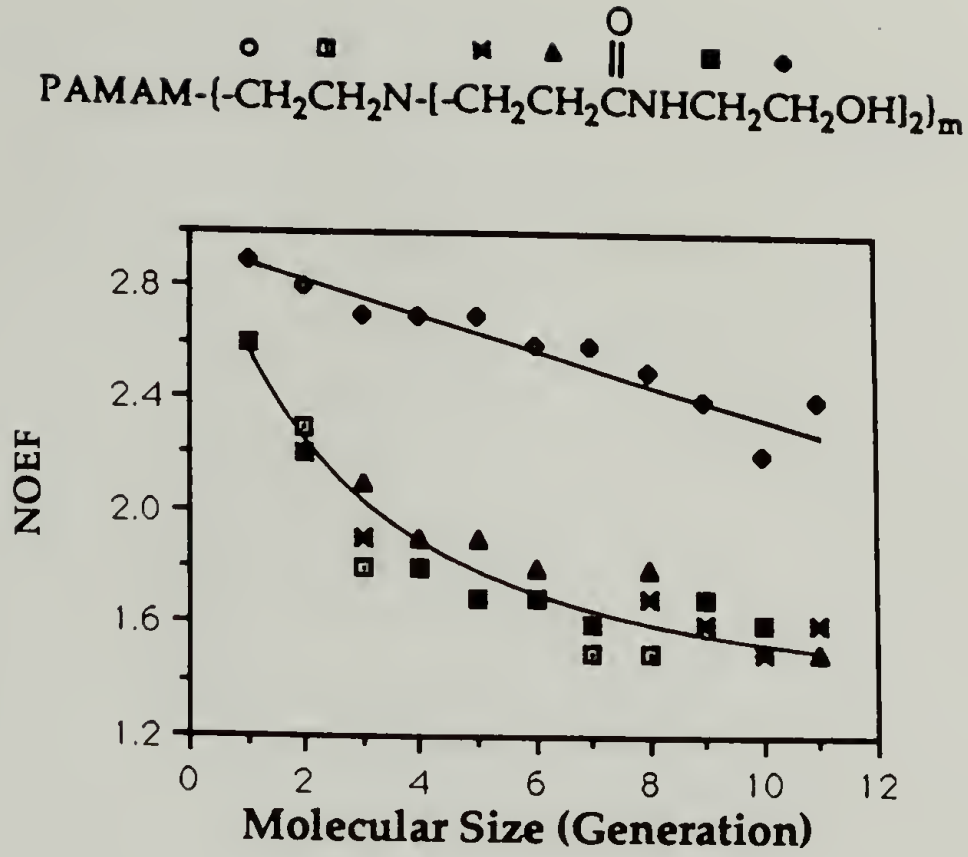

Figure 3.13. The dependence of NOEF on molecular size for OH terminated PAMAM (23^{o}C, 75 MHz, DMSO-d_6).

The observed NOEF was largest for the terminal carbon. In the case of a generation 1 dendrimer, a value of 2.9 ± 0.2 was observed. This value is close to the maximum value of 2.988 associated with relaxation that occurs entirelyby the DD mechanism in rapidly reorienting systems (25), and indicates that the application of a model to convert the relaxation data to τ based entirely on DD can be employed (2). The NOEF of the interior carbons were determined to be slightly smaller. The small values can be associated with slow rotational motions (25), and such an explanation is consistent with the small T_1 values. This notion is further corroborated by the observed small increase in the NOEF with temperature as illustrated in Figure 3.14 (the figure includes representative data; refer to the Appendix, Table A.1, for a more complete set of NOEF values as a function of temperature).

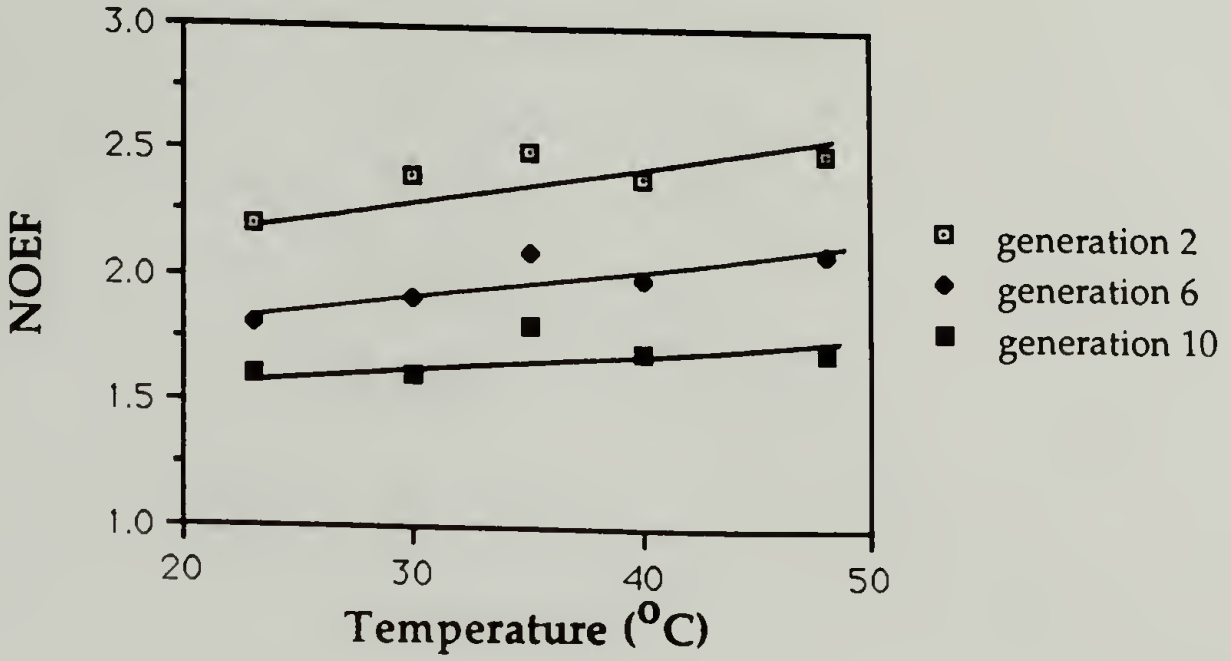

(a)

PAMAM-{-CH_2CH_2N-{-CH_2CH_2C(=O)NHCH_2CH_2OH}$_2$}$_m$

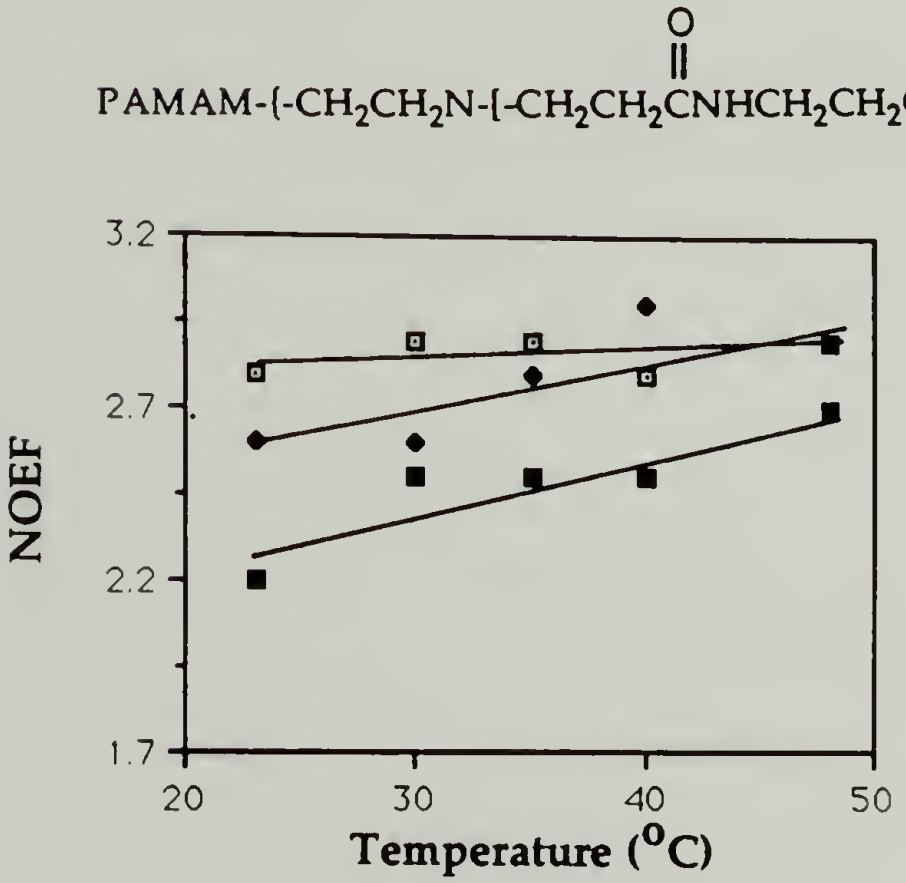

(b)

Figure 3.14. The dependence of NOEF on temperature for (a) internal sites and (b) terminal sites (75 MHz, DMSO-d_6).

The T_1 values were determined as a function of temperature as well. In all cases the observed value of the terminal carbon increased with temperature (refer to Figure 3.15 and to the Appendix, Table A.2, which contains a more complete set of T_1 values as a function of temperature), indicative of measurements being in the region where $\omega\tau < 1$ (27). The dependence of T_1 on temperature was observed to decrease with increasing MW. The T_1 values determined for the interior carbons were less temperature dependent, but in this case as well, the dependence decreased with increasing molecular weight. This suggests that some cooperative motion might exist, and therefore a broad distribution of τ exists. It also suggests that the molecular motions responsible for the relaxation of the interior ^{13}C are such that the relaxation measurements lie in the vicinity of the minimum of the T_1-τ curve. This being the case, small changes in T_1 would be indicative of relatively large changes in τ. The relaxation times of the terminal carbons, being slightly larger than those observed for the interior, would then be further away from the minimum, and as such, T_1 would be more sensitive to changes in τ.

From the data described above, it was possible to find a suitable mathematical model to convert the experimentally determined relaxation parameters to the desired τ associated with the relaxation process. The choice of model was based on the following three observations: 1) The T_1 observed at 50 MHz were higher than those observed at 75 MHz so simple models which do not display any frequency dependence would not be suitable. 2) The NOEF determined for the terminal carbon of Generation 1.0 was observed to be at the theoretical maximum value observable for relaxation occurring entirely by DD, so a model based on a DD mechanism of relaxation should be applied. 3) The T_1 of the carbons on the interior of the dendrimers were

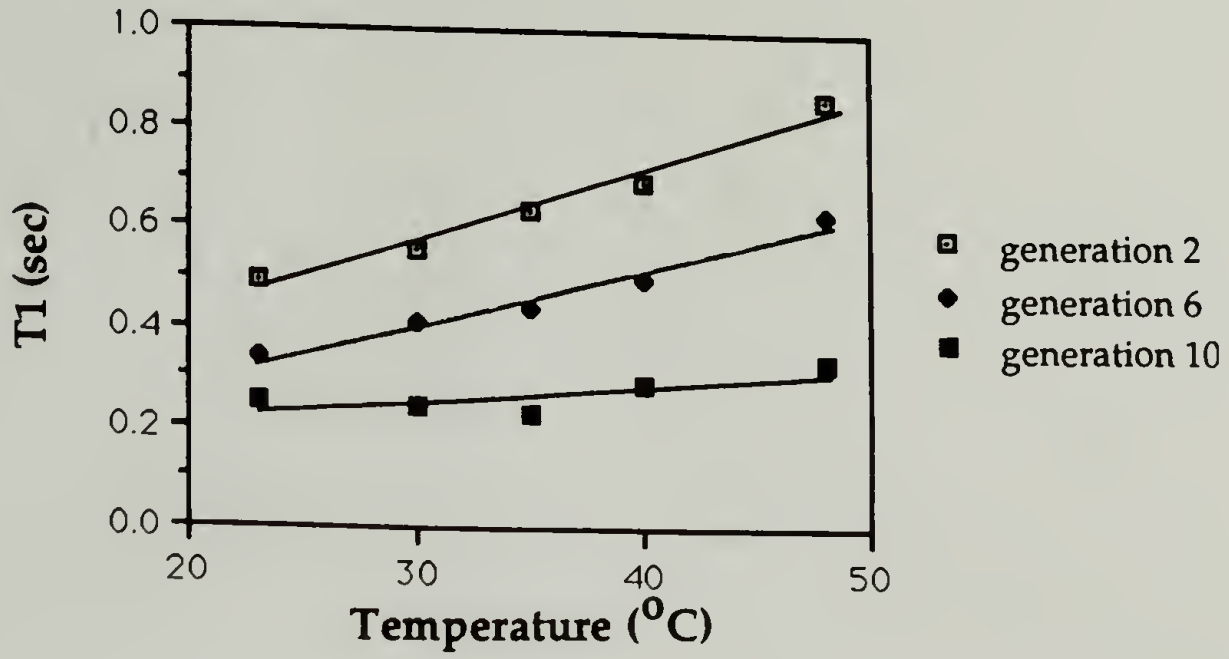

(a)

PAMAM-{-CH_2CH_2N-[-CH_2CH_2C(=O)NHCH_2CH_2OH]$_2$}$_m$

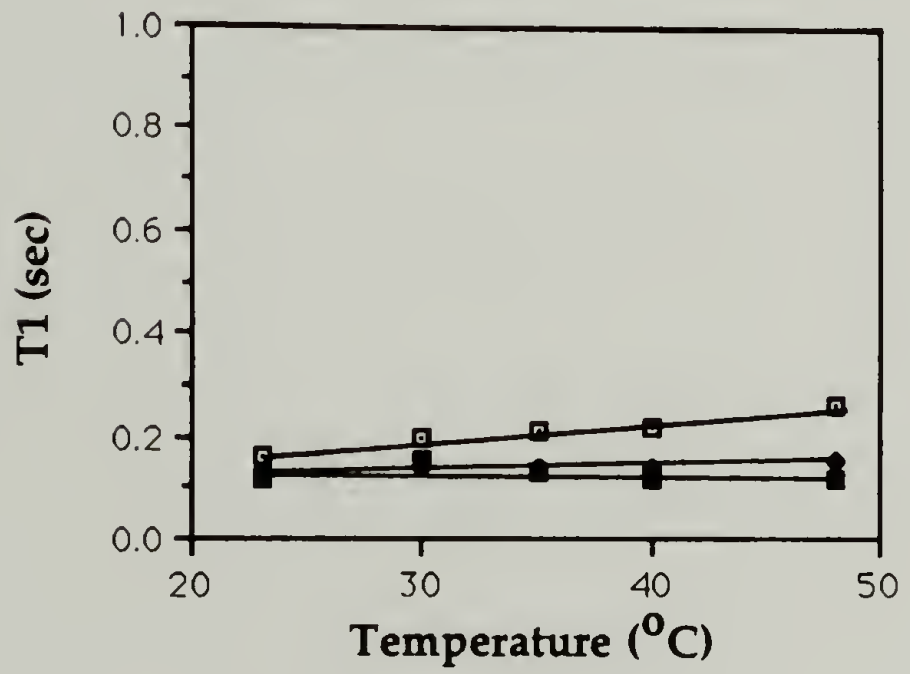

(b)

Figure 3.15. The dependence of T_1 on temperature for (a) terminal sites and (b) internal sites (75 MHz, DMSO-d_6).

found to be relatively insensitive to changes in temperature over the range studied, so a model allowing for a distribution of τ associated with the T_1 ought to be chosen. The evidence pointed to a model based on a dipole-dipole mechanism of relaxation which involved a distribution of τ's associated with the observed T_1. The model chosen was the Log(χ) distribution developed by Schaefer (50). While it has been demonstrated that molecules in solution tumble anisotropically for the most part, models based on an assumption of isotropic motion have been found to accurately reflect relaxation data of polymers (28, 51). The τ were calculated by assuming b=1000 in Equation 3, and fitting P and τ to the measured T_1 and NOEF values, making certain that the calculated values of τ and P yielded values of T_1 and NOEF that fell well within the experimental error (refer to the Appendix for the P values employed in the calculations). The τ were based on the relaxation data acquired at 75 MHz, and the data acquired at 50 MHz were used as a check of the applicability of the model. Insertion of τ determined at the higher frequency into Schaefer's equation, as applied to the lower frequency, yielded values of NOEF and T_1 which were within experimental error of the parameters measured at the second frequency (refer to Tables A.3, A.4, A.5 and A.6 in the Appendix). Hence, the model appears to reflect the processes responsible for the relaxation.

It is conceivable that alternative relaxation mechanisms, besides DD of directly bonded protons, might contribute to the relaxation process. The ^{14}N, being a quadrupolar nucleus, might be playing a role in the relaxation process of those carbons adjacent to ^{14}N via scalar coupling (SC) between the two nuclei. However, Norton has demonstrated that ^{14}N only contributes by a DD interaction to the relaxation rate of the quarternary carbons of adenosine monophosphite to which it is bound (47), i.e., no SC was observed. More

generally, no evidence for SC between protonated ^{13}C and a directly bonded quadrupolar nucleus has been observed, except in the case of ^{79}Br (29). Intermolecular ^{13}C-^{1}H DD and spin rotation mechanisms are equally unlikely. It is believed that the intermolecular DD can be ignored as the distances involved are too large as compared with the distance involved with directly bonded protons (25, 51). SR has been shown to apply only to small molecules, or to small moieties within larger molecules, which possess high degrees of symmetry., ie.: methyl groups (4). There is still, in principle, the possibility of DD between ^{14}N, ^{15}N or ^{1}H bonded to adjacent nuclei and the ^{13}C of interest. DD are extremely dependent on the distance between nuclei (ie.: the interaction decreases with distance to the -6^{th} power). As the N-C bond distance is approximately 40% longer than the H-C bond length, the contribution from the ^{14}N-^{13}C DD mechanism ought not to contribute in a significant manner to the relaxation process (25, 29). Equations 6 and 7 have been applied to a generation 1 amine terminated PAMAM. In doing so $1/T_{1,other}$ was added to both equations such that for protonated carbons:

$$\frac{1}{T_1} = (h/2\pi)^2\gamma^2_H\gamma^2_C r^{-6}N + \frac{1}{T_{1,other}} \qquad (6')$$

and for deuterated carbons :

$$\frac{1}{T_1} = \frac{8}{3}(h/2\pi)^2\gamma^2_C\gamma^2_D r^{-6}N + \frac{1}{T_{1,other}} \qquad (7')$$

Solving the equations for $T_{1,other}$ ($T_{1,CH_2} = 0.32 \pm 0.03$ sec, $T_{1,CD_2} = 3.7 \pm 0.4$ sec), shows that there is a relative contribution of 2.5% to the overall

relaxation process from mechanisms other than intramolecular DD of directly bonded ^{1}H for the ^{13}C beta to the carbonyl.

Figure 3.16 shows how the calculated τ depend on MW. The τ's of the terminal carbon exhibit a linear dependence on generation, with a small positive slope. This dependence on MW of the end group is atypical of linear polymers. While no comprehensive NMR study of the dependence of end group mobility on the MW of linear polymers has been reported in the literature, it has been demonstrated, both by fluorescence depolarisation experiments (46) and ESR work (5), that the mobility of the end group is dominated by segmental motion for polymers having a MW larger than 30,000, and as such is independent of MW. The MW dependence of the τ for those carbons on the interior of the polymer shows a strong dependence on MW. The observed dependence of the τ on MW must be due to an increase in steric hindrance as the MW of the dendrimer increases.

The trends in τ are difficult to interpret in terms of the dense-packing models in the literature (8, 36). If the density of the end groups increased to the point where the number of end groups per unit surface area was similar to that observed in ordered vesicular bilayers, as suggested by the S/E calculations discussed earlier, then there ought to be a large increase in the observed τ once the layer forms. No such increase was detected. The τ were observed to increase with increasing MW, but only slightly, and the mobility of the end groups was always observed to be greater than that of the interior carbons. On the other hand, the dependences of the τ on MW for the internal carbons was rather large. Such a dependence is also atypical of polymers. Typically, the segmental mobility of the polymer chains becomes independent of MW once a certain critical degree of polymerization is reached (1, 18, 21, 37). Once the hydrodynamic volume of the polymer coil becomes large

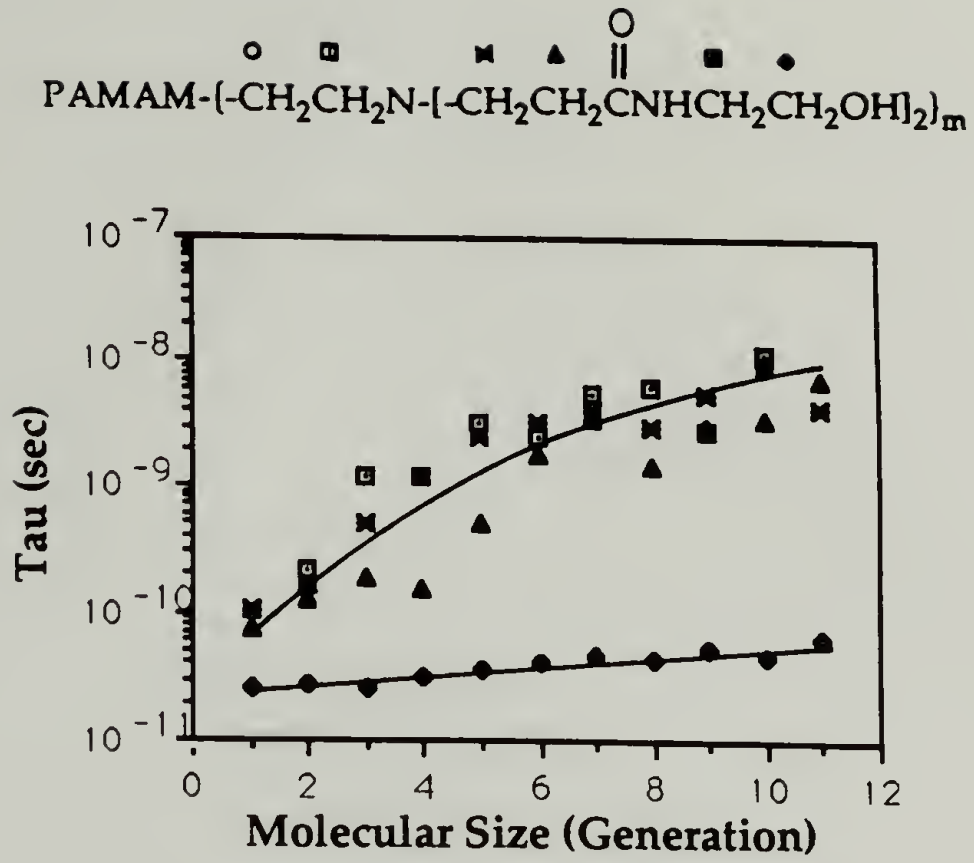

Figure 3.16. The dependence of τ on molecular size for OH terminated PAMAM (23°C, 75 MHz DMSO-d_6).

enough that the overall rate of rotation of the polymer as a whole is slow as compared to the Larmor frequency, the relaxation rate is governed by segmental motion and τ are observed to be independent of MW. The dependence on MW observed in the case of the PAMAM dendrimers indicates that the chains are becoming less and less mobile as the chain length increases. Such a phenomenon would occur if the local monomer density increased as the chains became longer, thereby reducing the segmental motion. The increase in monomer density could be accomplished if the chains were to fold back into the interior of the dendrimer rather than growing outwardly. This would necessitate the end groups not being on the surface of the spheroid, which in turn would explain the low sensitivity of the mobility of the terminal groups on MW. Working in free space, basing

the calculations on excluded volume and simulating the stepwise growth pattern of dendrimers, Lescanec and Muthukumar (26) have predicted the aforementioned trends in chain conformation. The calculations show that the end groups are not located on the surface of the polymer (below generation 8; refer to Figure 3.17). As such, the model invalidates any

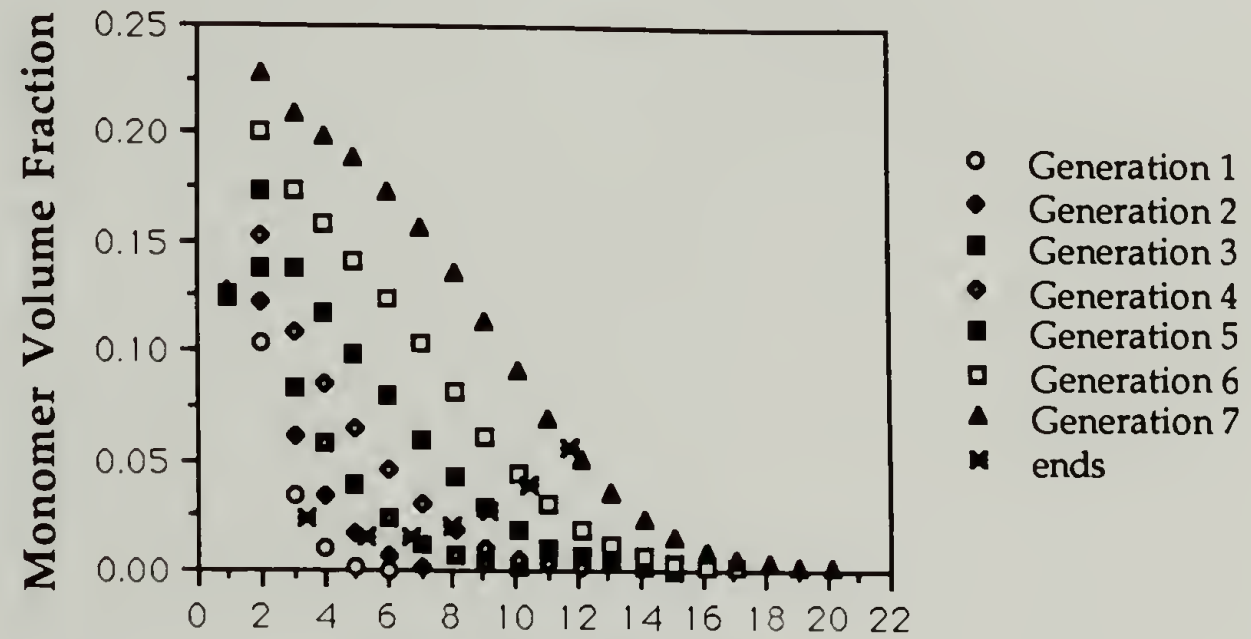

Figure 3.17. The dependence of monomer volume fraction on distance from the topological centre of a dendrimer as predicted by Lescanec and Muthukumar (26).

conclusions, for dendrimers below generation 8, that are based on the S/E calculations, as the calculations are based on the assumption that the end groups would be located on the surface of the polymer coil (58). If the end groups are not on the surface of the sphere, then the concept of an ever increasing number of end groups per unit surface area, and any conclusions drawn therefrom, i.e., the formation of a "cast shell", do not hold. These results contradict the concept of a densely packed outer generation, and the NMR relaxation study confirms these results. The model predicts that there is

a significant amount of monomer density past the average location of the end groups and that the monomer density in the vicinity of the end groups is below the level where concentration effects have been observed for linear polymers (1, 11, 19, 33, 34, 37), i.e., below 10-15 monomer mole-%. The small dependence observed for the correlation times of the terminal carbons on generation are consistent with this notion. As well, the model predicts that the density inside the polymer increases with increasing generation and does not suggest that there would be an elongation of the polymer chains, brought about in order to minimize steric interactions between end groups by increasing the amount of surface area available to the end groups. The calculated monomer density inside the dendrimer is significantly higher than that in the vicinity of the end groups. In the interior, the density is in the region where NMR relaxation data of linear polymers depend on concentration, and thus may account for the observed dependence of τ of the interior carbons on generation.

A similar set of data was accumulated for the hydroxyl terminated PAMAM in D_2O. The T_1 and NOEF dependencies on generation are presented in Figure 3.18 and 3.19, while the τ dependencies are depicted in Figure 3.20. (The suitability of Schaefer's equation was assumed to hold as the only variation from the system described above is that of solvent. Additionally, the relaxation parameters of the NH_2 terminated PAMAM in D_2O have been shown to be accurately represented by the model.) The trends observed in this solvent are identical with those observed in DMSO-d_6. For the internal ^{13}C, T_1 becomes independent of MW above third generation, the NOEF is independent of MW above sixth generation and the τ was found to be particularly sensitive to increases in MW. The terminal ^{13}C were observed

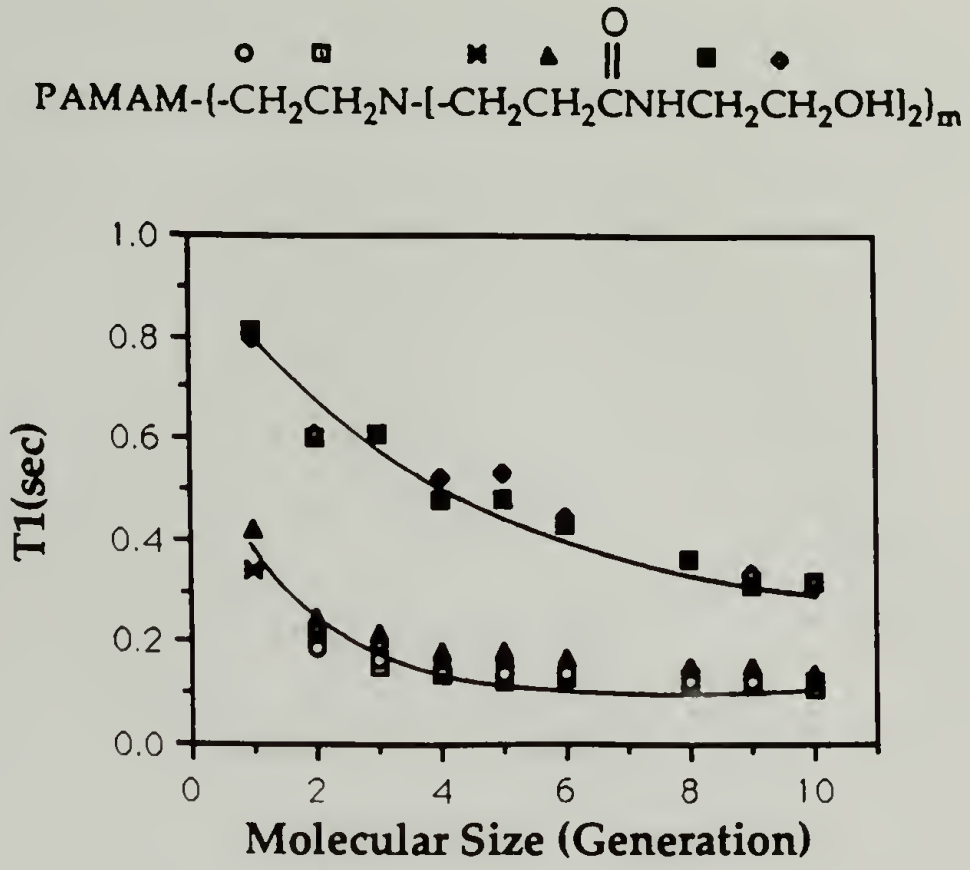

Figure 3.18. The dependence of T_1 on molecular size for OH terminated PAMAM (25°C, 75 MHz, D_2O).

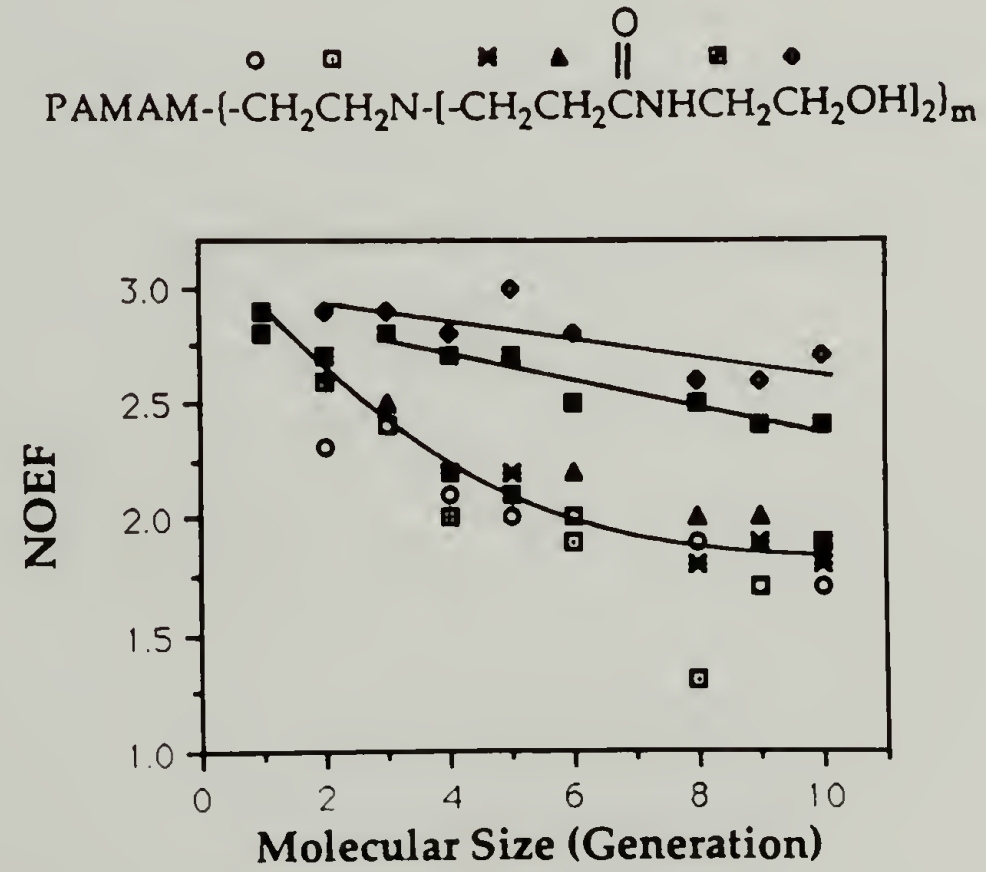

Figure 3.19. The dependence of NOEF on molecular size for OH terminated PAMAM (25°C, 75 MHz, D_2O).

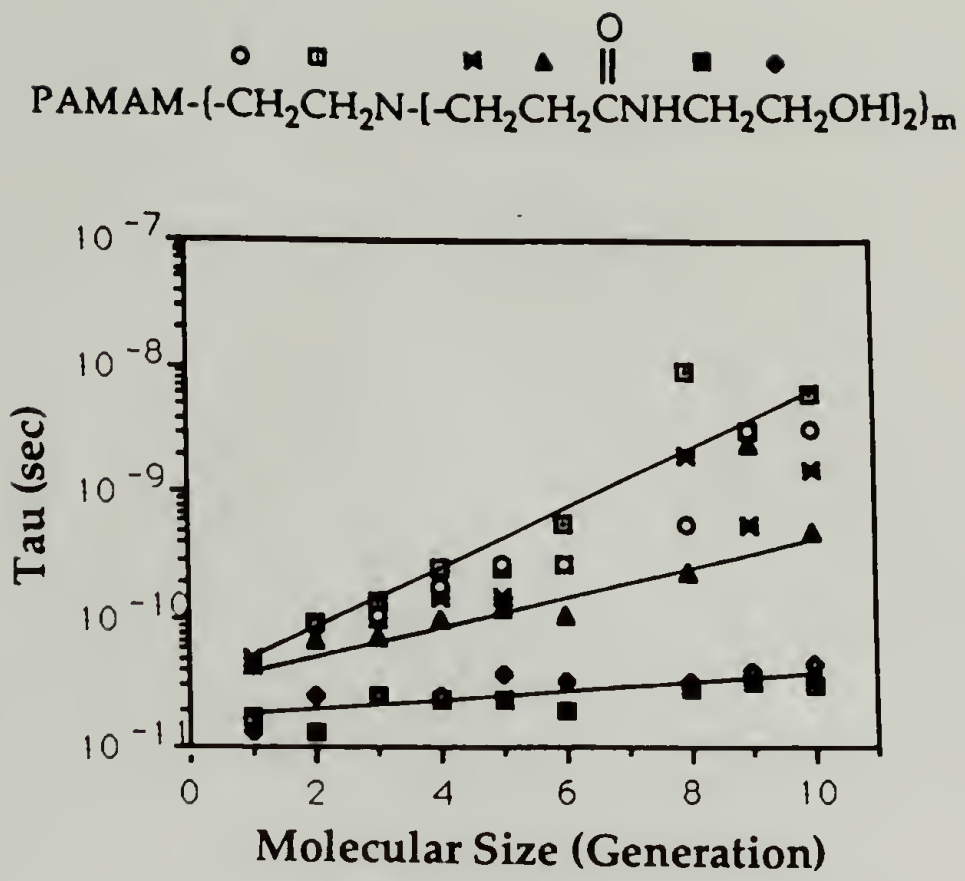

Figure 3.20. The dependence of τ on molecular size for OH terminated PAMAM (25°C, 75 MHz, D_2O).

to relax significantly more slowly, experience larger NOEF and show less sensitivity to MW (as compared to the internal ^{13}C). The only difference between the behavior in the two solvents is one of magnitude. The relaxation process occurs significantly more slowly in D_2O than in DMSO-d_6. Solvent dependence of NMR relaxation data is known (15), and there exist at least three different explanations for the phenomenon. The first possibility is that the solvents are of different viscosities so that the motions might be slower in DMSO-d_6 than in D_2O. Secondly, the degree of solvation in the two different solvents may not be the same; ie.: there could be differences in the hydrodynamic volume which would result in differences in the motional properties of the polymer chains. Lastly, there could be a strong interaction (e.g., H-bonding) between one of the solvents and the polymer. If the interaction is strong enough, the hydrodynamic volume of the moving unit

would increase, its motions would slow and the relaxation experiments would reflect this change. In order to distinguish among these three possibilities additional experiments need to be done. The necessary experiments include NMR relaxation measurements in a mixed solvent system and intrinsic viscosity measurements. Such experiments have been performed, and will be presented along with the discussion of relaxation processes in the amine terminated PAMAM.

2. Poly(amidoamine).

Changes in the mobility of the polymer chains comprising amine terminated PAMAM (generations 1-8) were monitored in a manner similar to that employed in the study of their hydroxyl terminated counterparts. Once again, the relaxation parameters were only measured for the aliphatic carbons, and only those that were not obscured by the peaks due to the solvent (DMSO-d_6). The dependencies of the relaxation parameters of the amine terminated series, as determined either in DMSO-d_6 or D_2O on MW are depicted in Figures 3.21-22. The values determined for the T_1 and NOEF showed very similar trends to those observed for the hydroxyl terminated PAMAM in either of the two solvents. Both the T_1 and NOEF of the interior carbons became independent of MW. The lack of dependence on MW occurred at values similar to those where the T_1 and NOEF of the hydroxyl terminated series did. A comparison of trends in T_1 of OH terminated PAMAM in DMSO-d_6 and D_2O (Figures 3.11 and 3.18), the NOEF of OH terminated PAMAM in DMSO-d_6 and D2O (Figures 3.13 and 3.19), with Figures 3.21-22 for the T_1 and NOEF of the NH_2 terminated PAMAM,

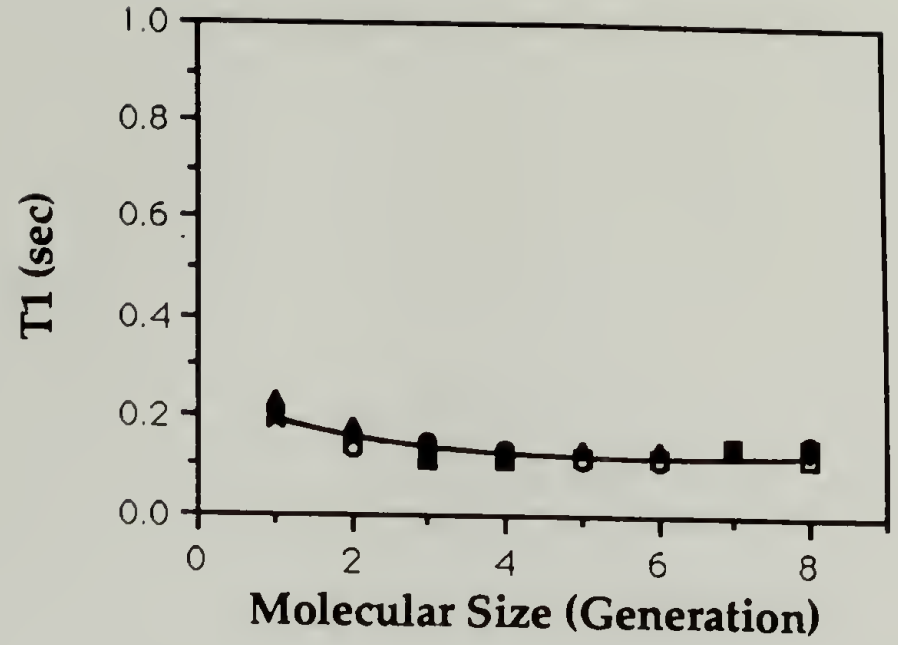

(a)

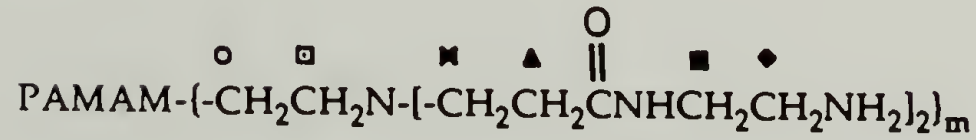

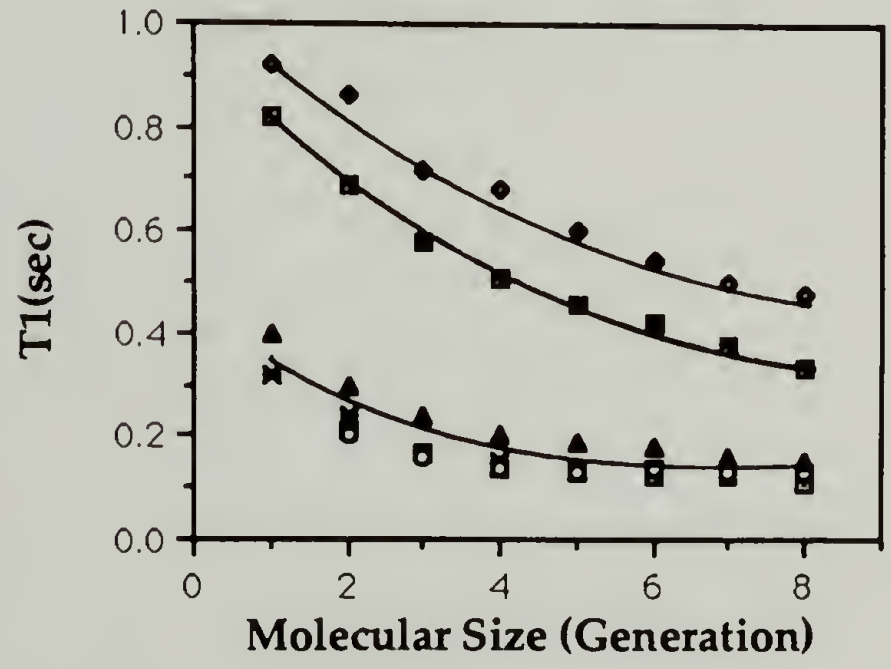

(b)

Figure 3.21. The dependence of T_1 on molecular size for NH_2 terminated PAMAM (25°C, 75 MHz); (a) DMSO-d_6; (b) D_2O.

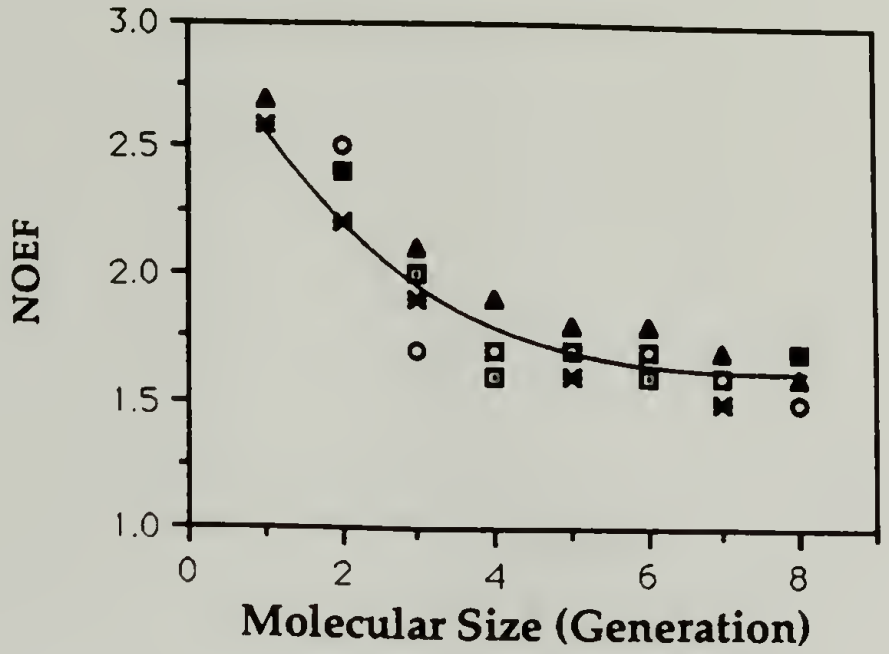

(a)

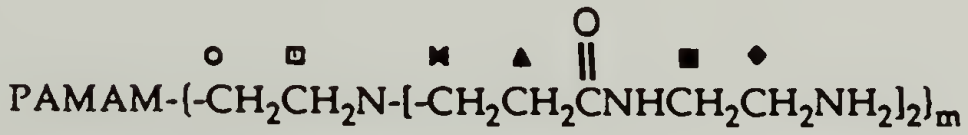

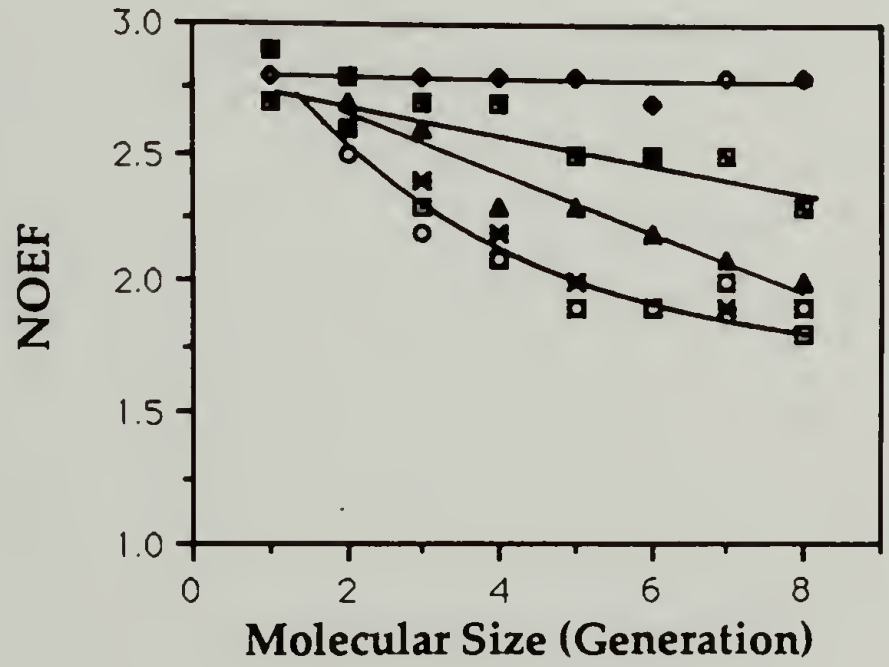

(b)

Figure 3.22. The dependence of NOEF on molecular size for NH_2 terminated PAMAM (25°C, 75 MHz); (a) DMSO-d_6; (b) D_2O.

respectivley, (also compiled in Tables A.7 and A.8 in the Appendix) clearly demonstrates that trends observed are not due to an end group effect.

The relaxation parameters were converted to τ by implementing the same model and value of b as was the case for the OH terminated PAMAM. The suitability of the model was verified in the same manner as was the suitability of the model to the OH terminated PAMAM, and here too, good agreement between the predicted and experimentally determined relaxation parameters was obtained. This indicates that the model can be used to accurately calculate the τ. The predicted and experimentally determined relaxation parameters are listed in the Appendix for comparative purposes (Tables A.9, A.10, A.11 and A.12). The dependence of τ on MW for the amine terminated dendrimers in the two solvents studied is illustrated in Figure 3.23. Once again, the plot shows a linear dependence of τ on generation for the terminal carbon, with a small positive slope. The MW dependence of τ for those carbons on the interior of the polymer show a strong dependence on MW as was the case with the hydroxyl terminated dendrimers. The relaxation parameters of the interior ^{13}C were found to be insensitive to the change in end groups, and the postulates presented in order to explain the NMR data of the hydroxyl terminated series also hold for the amine terminated series. The relaxation properties of the terminal carbon, however, did differ somewhat. The relaxation rate of the terminal carbon of the amine terminated PAMAM was slower than that observed for the hydroxyl terminated PAMAM. This indicates that the amine termini are more flexible the hydroxyl termini, but not to the extent that there is any effect on the internal carbons. The phenomenon can easily be explained if the hydrogen bonding properties of the two functional groups is such that the hydroxyl groups are more strongly

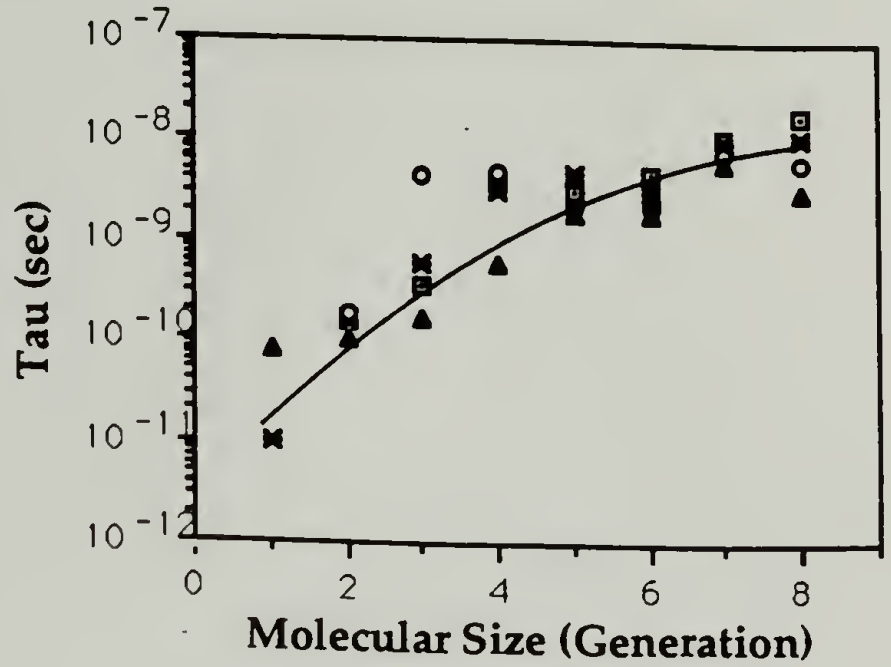

(a)

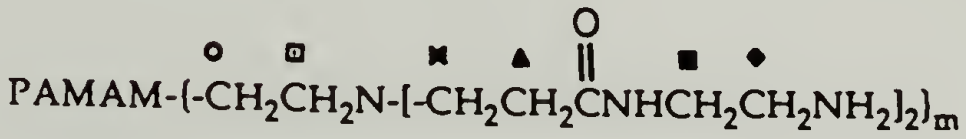

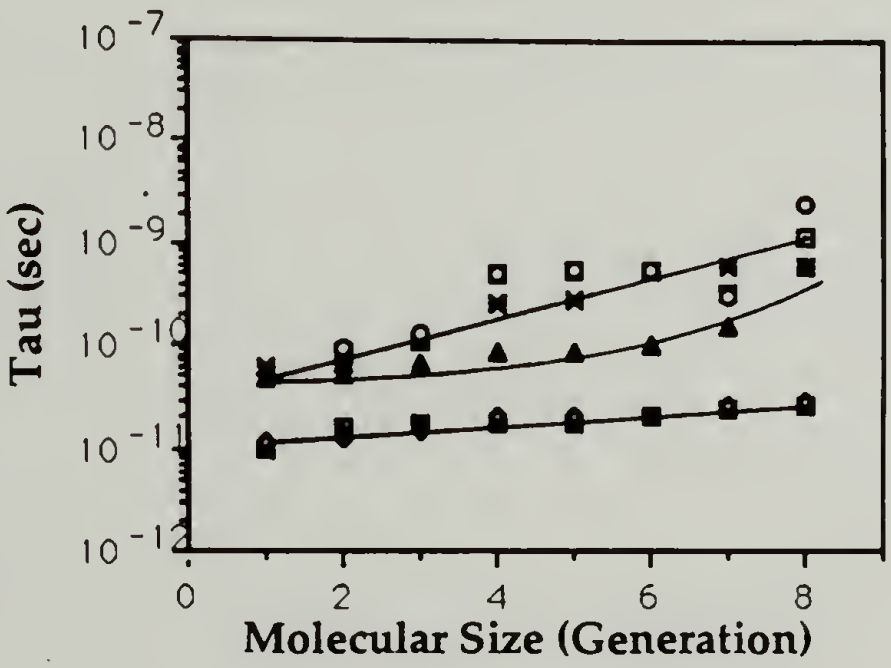

(b)

Figure 3.23. The dependence of τ on molecular size for NH_2 terminated PAMAM (25°C, 75MHz); (a) DMSO-d_6; (b) D_2O.

bound, and as a result creates a more rigid system. Joesten and Schaad have compiled as fairly extensive list of activation energies for the rupture of H-bonds by different functional groups (24). The tables of activation energies indicate that the amount of energy necessary to cleave the H-bond of OH groups is larger than that necessary for NH_2 groups. The NMR results discussed above are consistent with this observation. The OH terminated PAMAM were observed to have smaller relaxation times for the terminal ^{13}C because the H-bonds formed by the end groups are more tightly bound than those formed in the case of the NH_2 terminated PAMAM.

A series of NMR experiments was also performed on these polymers in a mixed solvent system in order to help resolve the confusion regarding the difference in the relaxation parameters observed in the two solvents. It is possible that the solvents are of different viscosities so that the motions might be slower in DMSO-d_6 than in D_2O or that the degree of solvation in the two different solvents may not be the same; ie.: there could be differences in the hydrodynamic volume which would result in differences in the motional properties of the polymer chains. As well, there could be a strong interaction (eg.: H-bonding) between one of the solvents and the polymer. If the interaction is strong enough, the hydrodynamic volume of the moving unit would increase, its motions would slow and the relaxation experiments would reflect this change. The $[\eta]$ values were determined to be comparable in the two solvents (0.04 - 0.10 dl/g, at 35.2 ^oC), thus the difference in the NMR behavior is attributed to strong H-bonding between the polymer and DMSO resulting in an increase in the hydrodynamic volume of the mobile unit (refer to Table 3.1). The dependencies of T_1, NOEF and τ, obtained in a

Table 3.1. The [η] of NH_2 terminated PAMAM as determined in H_2O and DMSO.

Molecular size (Generation)	[η] (dl/g) in H_2O	DMSO
1	0.050	0.046
2	0.045	0.044
3	0.052	0.065
4	0.068	0.069
5	0.089	0.060
6	-	0.066
7	0.10	0.081
8	-	0.058

mixed solvent system (1:1 H_2O:DMSO-d_6 weight ratio, or a 6:1 H_2O:DMSO-d_6 mole ratio), on MW are presented in Figures 3.24, 3.25 and 3.26. The data obtained are identical to those obtained in DMSO-d_6 itself (in order to facilitate the comparison the data are also listed in Tables A.1, A.2 and A.13 of the Appendix). This suggests that there is a strong interaction between the DMSO and the polymer so that the hydrodynamic volume of the mobile species is larger in the presence of DMSO and, as a result, the chain moves more slowly. The selective solvation of the PAMAM by DMSO is not particularly surprising as DMSO is known to be a strong H-bond acceptor (9), thus enabling strong interactions with the amine and amide functional groups comprising the polymer to form.

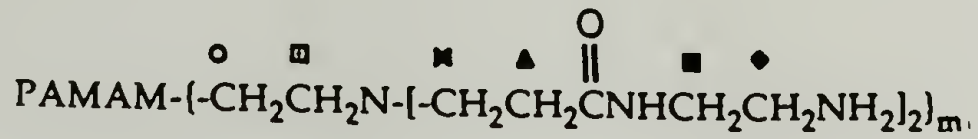

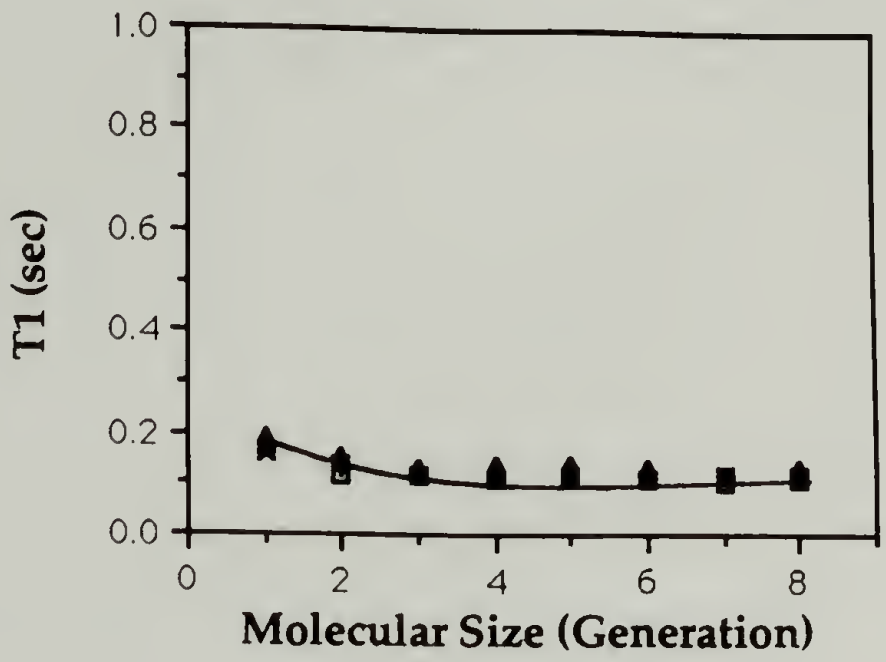

Figure 3.24. The dependence of T_1 on molecular size obtained in a mixed solvent system (1:1 H_2O:DMSO-d_6 weight ratio, or a 6:1 H_2O:DMSO-d_6 mole ratio) for NH_2 terminated PAMAM (25°C, 75 MHz).

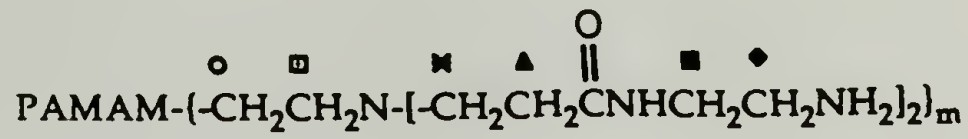

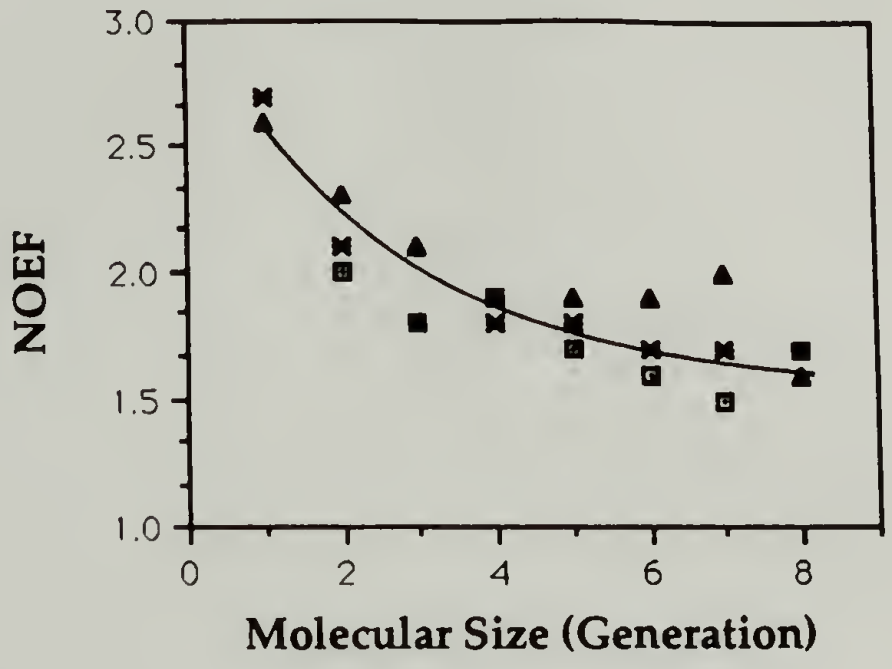

Figure 3.25. The dependence of NOEF on molecular size obtained in a mixed solvent system (1:1 H_2O:DMSO-d_6 weight ratio, or a 6:1 H_2O:DMSO-d_6 mole ratio) for NH_2 terminated PAMAM (25°C, 75 MHz).

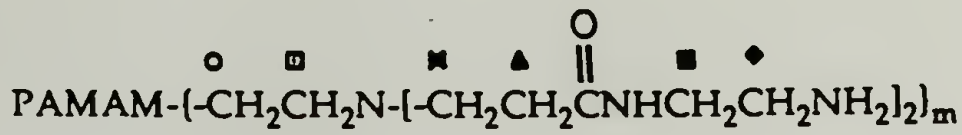

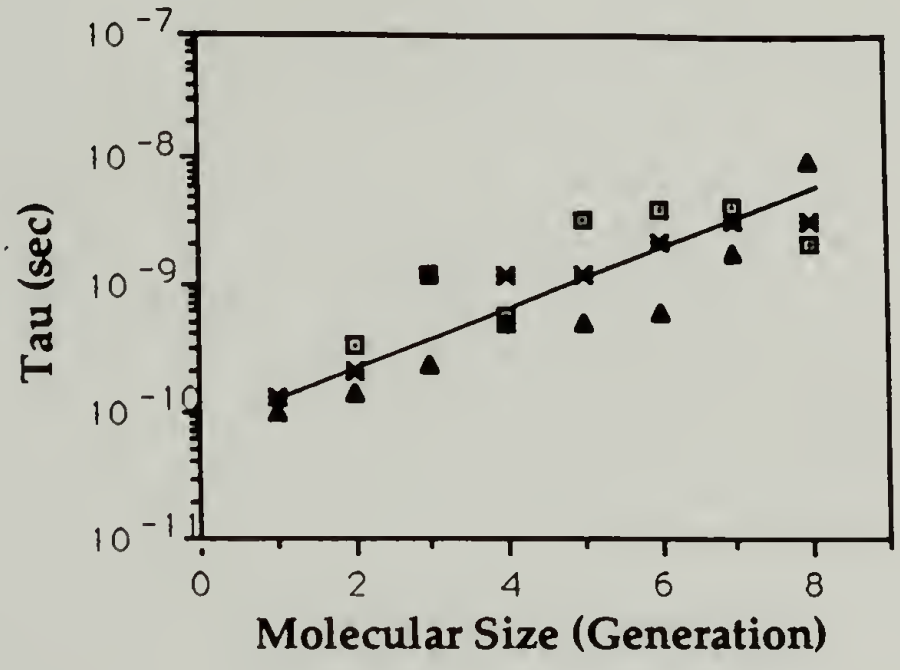

Figure 3.26. The dependence of τ on molecular size obtained in a mixed solvent system (1:1 H_2O:DMSO-d_6 weight ratio, or a 6:1 H_2O:DMSO-d_6 mole ratio) for NH_2 terminated PAMAM (25°C, 75 MHz).

D. ^{2}H NMR Relaxation Experiments.

In order to obtain some understanding of the effects of the topology on a more localized level, the PAMAM had to be selectively labelled. Deuterium was chosen as the nucleus with which to label the dendrimers. The selection was based on the low natural abundance of the isotope (0.01%), the fact that only minimal changes in the nature of the polymer occur upon the incorporation of the isotope, and the insensitivity of the relaxation process for the quadrupolar nucleus to interatomic distances. It was most feasible to incorporate the deuterium into the polymer by preparing labelled MA. MA was selected for deuteration rather than EDA as the alkylation requires only small excesses of the MA, whereas the amidation requires large excesses of the EDA. By substituting the d_2-MA for MA at the desired point in the stepwise polymerization, polymers of different MW, yet all labelled in the same location, could be prepared. In an analogous manner, polymers of similar MW, each labelled at different distances from the core, could also be synthesized (refer to Figure 3.27). A notation has been developed in order to facilitate discussion of the labelled dendrimers, and is as follows: G_nD_m, where n and m are integers, is applied such that the number following 'G' indicates the generation of the polymer and the number following 'D' indicates the generation which is deuterated, (eg.: G_7D_3 is used to describe a generation 7 PAMAM which is selectively deuterated at generation 3). The resulting polymers would allow a ^{2}H NMR study of the effect of the topology on the mobility of the polymer chains as a function of MW and location. Unlike the natural abundance ^{13}C study, the ^{2}H study would not yield a statistical average over the different generations comprising a polymer but

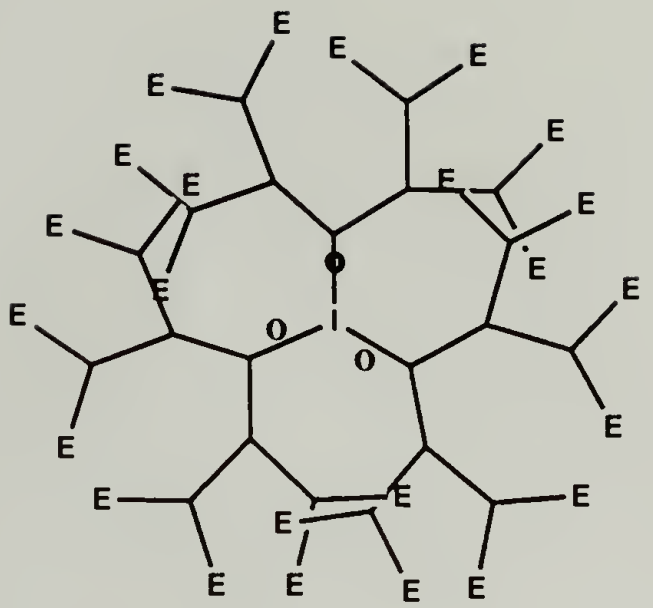

(a)

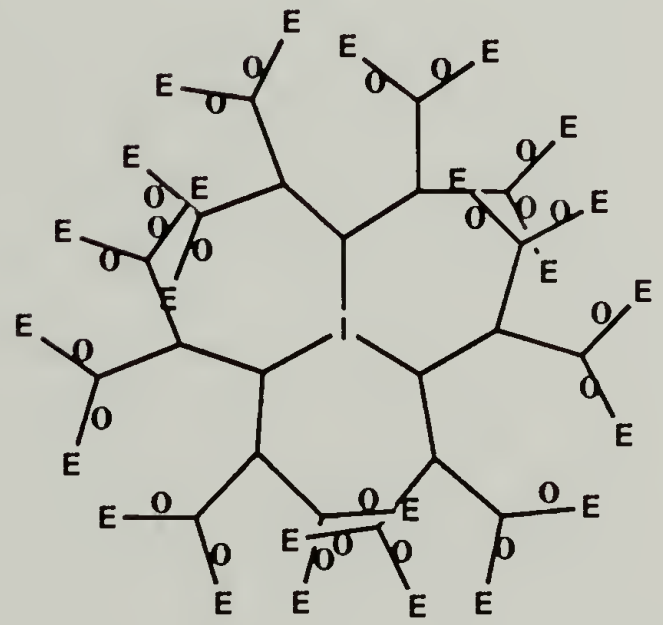

(b)

Figure 3.27. An illustration of PAMAM dendrimers selectively labelled along the chains. 'E' denotes the chain ends; 'I' denotes the initiator core; 'o' is used to indicate the location of the labels. (a) A generation 4 dendrimer labelled at generation 1. (b) A generation 4 dendrimer labelled at generation 4.

would be specific to a particular site. This enables the ^2H study to address the concept of radial gradients that have been postulated to exist in the dendrimer (8, 36). The gradients are said to form because of the very nature of the starburst topology, i.e., the number of branch points increasing exponentially with increasing chain length would cause the steric hindrance at larger generations to grow progressively as one proceeds outward from the topological centre. Should such a phenomenon occur, there would be an accompanying decrease in the mobility of the dendrimer chains with increasing distance from the initiator core. The range of generations over which a ^2H labeling study would be valid is somewhat limited by natural abundance ^2H present in the dendrimer. The ratio of the ^2H present due to natural abundance to that present due to selective labelling depends on the generation of the polymer under investigation and the generation at which the polymer has been labelled. The calculated ratios of the natural abundance ^2H present in the different polymers prepared to the amount of ^2H present in the dendrimers due to the labelling with d_2-MA are contained in Table 3.2. Inspection of the table indicates that the natural abundance is a significant fraction of the total ^2H present in the dendrimer once the ^2H is buried 6 generations down into the bulk of the polymer. At this level of deuteration, the amount of ^2H in the polymer due to the natural abundance of the isotope is comparable in size to the experimental error and, therefore could introduce additional errors in the relaxation measurements, i.e., typically, NMR experiments are accurate to within approximately 10%, and once the ^2H is buried 6 generations down into the bulk of the polymer the amount of ^2H in the polymer due to the natural abundance of the isotope is 6%.

Both the T_1 and the spin-spin relaxation times (T_2) of the deuterated PAMAM were measured. A typical experiment from which both relaxation

Table 3.2. The ratios calculated for the amount of ^2H in the selectively labelled dendrimers due to the labelling with d_2-MA to that present due to the 0.01% natural abundance of the isotope.

Molecular size (generations)	Labelled Generation							
	1	2	3	4	5	6	7	8
1	2900							
2	800	1700						
3	330	680	1500					
4	150	300	630	1300				
5	72	150	390	610	1300			
6	35	71	140	290	600	1300		
7	17	35	70	140	290	900	1300	
8	9	17	35	70	140	290	590	1300

parameters were calculated is shown in Figure 3.28. The T_1 were determined from the peak heights observed at the delay times indicated, while the T_2 were determined from the width of the peaks at half height (W) according to the equation (10):

$$T_2 = 1/2\pi W. \qquad (13)$$

The relaxation times are presented as a function of generation in Figure 3.29. Three patterns in the dependence of the relaxation rates on generation are immediately obvious: 1) the T_1 of the ^2H located in the terminal generation decreases with increasing molecular weight; 2) the T_1 observed for PAMAM

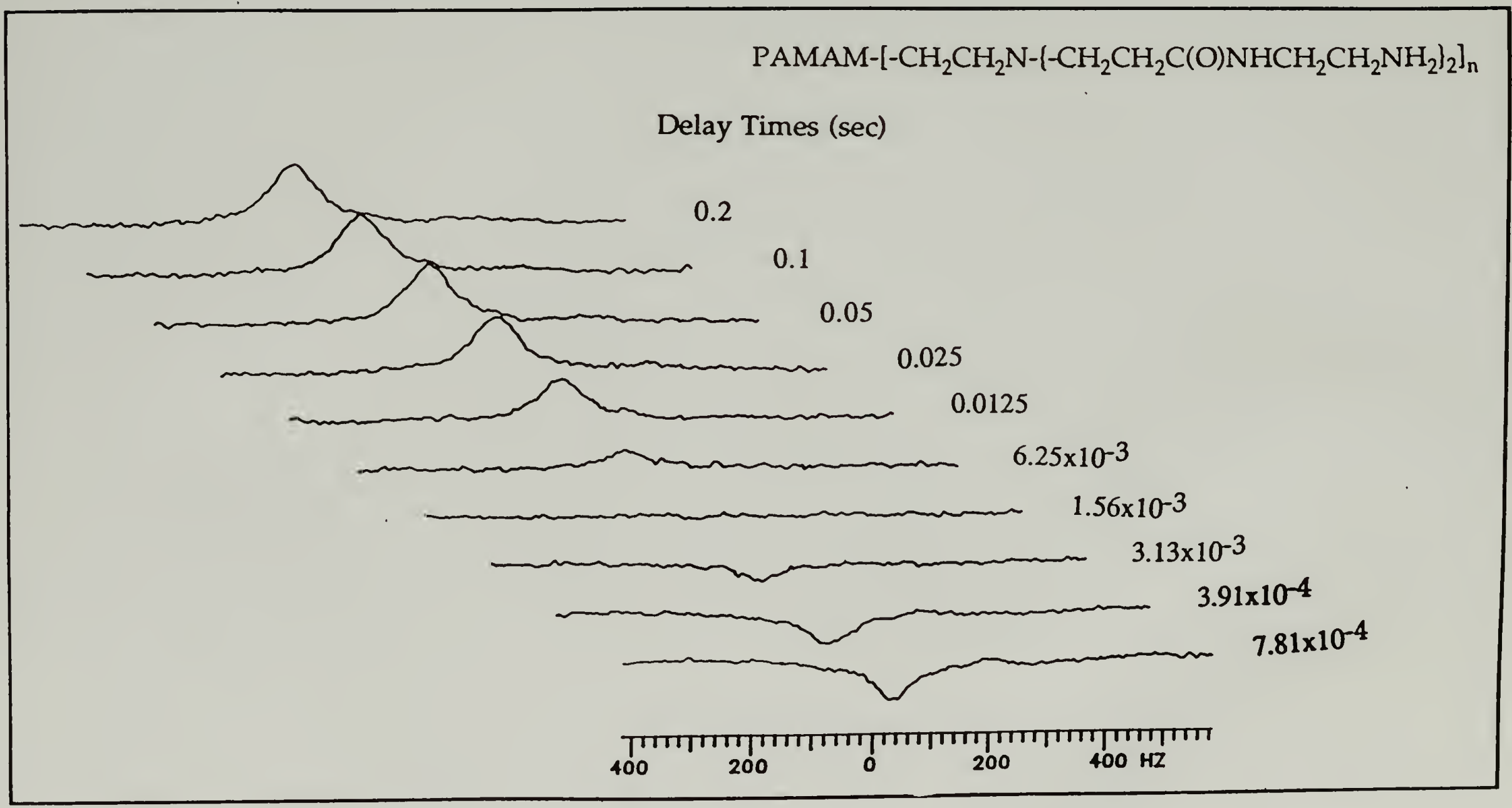

Figure 3.28. An inversion recovery experiment from which the ^2H T_1 was calculated for a G_3D_1 PAMAM dendrimer terminated with NH_2 groups (25°C, 46MHz, H_2O).

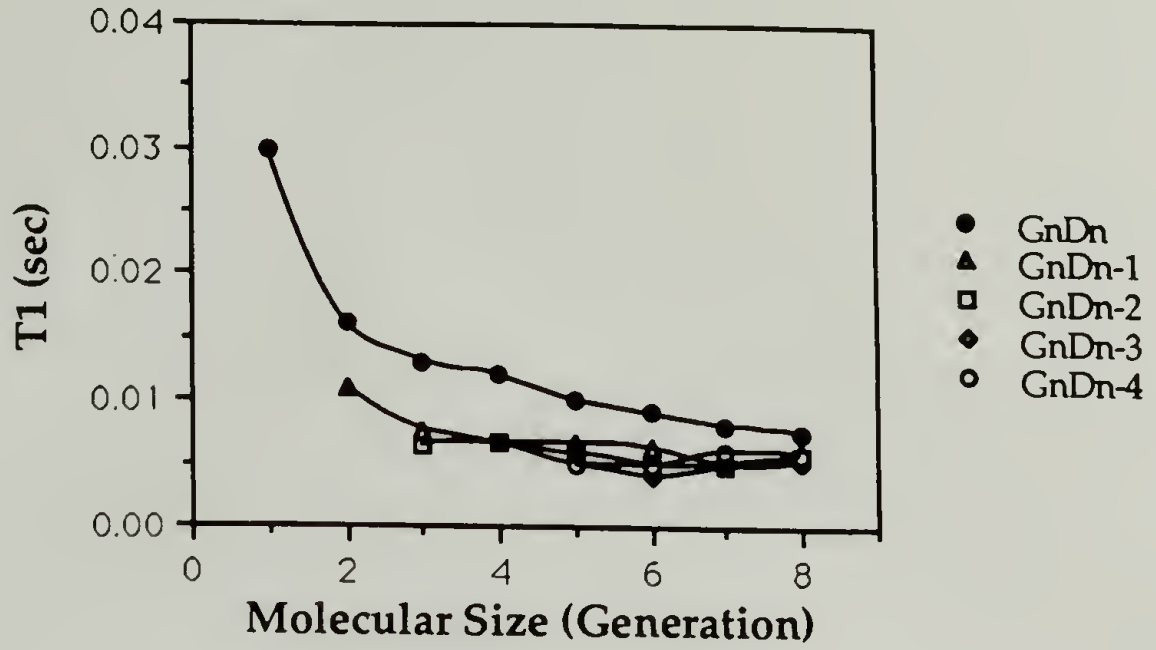

(a)

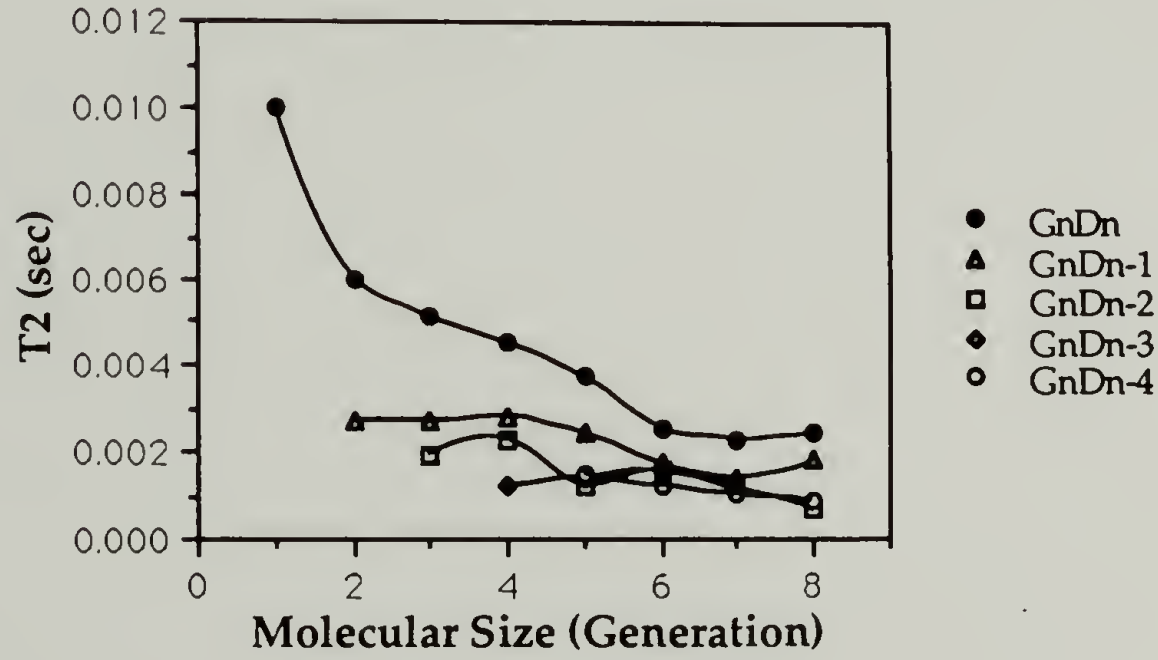

(b)

Figure 3.29. The dependencies of (a) ^2H T_1 and (b) ^2H T_2 on molecular size for NH_2 terminated PAMAM (25°C, 46 MHz, D_2O).

labelled in the last generation is larger than that observed when the deuterium is located further away from the ends of the chain; 3) once the labelled sites are not located in the terminal generation, there is no dependence of the relaxation rates on the location of the labelling. These first two trends are in good agreement with the ^{13}C relaxation study previously discussed. The data indicate the terminal groups are more mobile than interior sites, and that the mobility of the terminal groups decreases with increasing MW. Interpretation of the last of the three patterns mentioned above is fairly simple as well. The data indicate that no significant radial gradients are detectable. For example, the relaxation rates of a series of generation 7 PAMAM, each labelled at different sites within the dendrimer, are identical, within the experimental error. As such, there are no significant differences in the mobility of the ^{2}H probe irrespective of its location, so long as it is located in the interior of the polymer and not in the terminal generation.

The relaxation data were converted to correlation times as was the case with the ^{13}C data. Once again Schaefer's Log(χ) distribution was employed. The quadrupolar coupling constant necessary for the implementation of Schaefer's equation was determined from the ratio of equations 1 and 8 such that:

$$\frac{1/T_{1,CH_2}}{1/T_{1,^2H}} = \frac{20h^4 \gamma^2_H \gamma^2_C r^{-6} N}{3\pi^2 (e^2 qQ)^2} \qquad (14)$$

By substituting the values of T_{1,CH_2} and $T_{1,^2H}$ determined for a generation 1 PAMAM (the latter of which has been determined for a G_1D_1 dendrimer)

into the equations, a value of 170 KHz was obtained. The τ were based on the relaxation data acquired at 46.0 MHz, and the data acquired at 30.7 MHz were used as a check of the applicability of the model. Insertion of τ determined at the higher frequency into Schaefer's equation, as applied to the lower frequency, yielded theoretical values of T_2 and T_1 which were consistent with the experimental parameters determined at the second frequency (refer to Tables A.14 and A.15 in the Appendix). Hence, the model accurately reflects the processes responsible for the relaxation. In addition, the correlation times calculated from the ^2H relaxation data are in good agreement with the correlation times calculated from the ^{13}C relaxation data. Not only does this further insure the applicability of Schaefer's model to the PAMAM system, but it indicates that the quadrupolar coupling constant employed is an appropriate one and eliminates the possibility of the calculated τ being a frequency dependent phenomenon. The correlation times have been plotted in Figure 3.30 as a function of the overall generation of the PAMAM and of the labelled generation. As was the case when the relaxation times were plotted in a similar manner, no dependence on the site of deuteration was observed within any series of PAMAM of a given MW, so long as one does not consider the terminal generation. This indicates that there are no radial gradients created within the PAMAM starburst polymers. The lack of any detectable radial gradients reinforces the interpretation of the ^{13}C relaxation data in terms of Muthukumar's model. The model does not predict the existence of the radial gradients as suggested elsewhere (8, 36, 55). Instead the model suggests that there is an increase in the local monomer density as the MW of the system increases. As was the case with the ^{13}C data, this was observed for the ^2H data in that the correlation times were observed to increase with increasing generation. The monomer density was calculated to

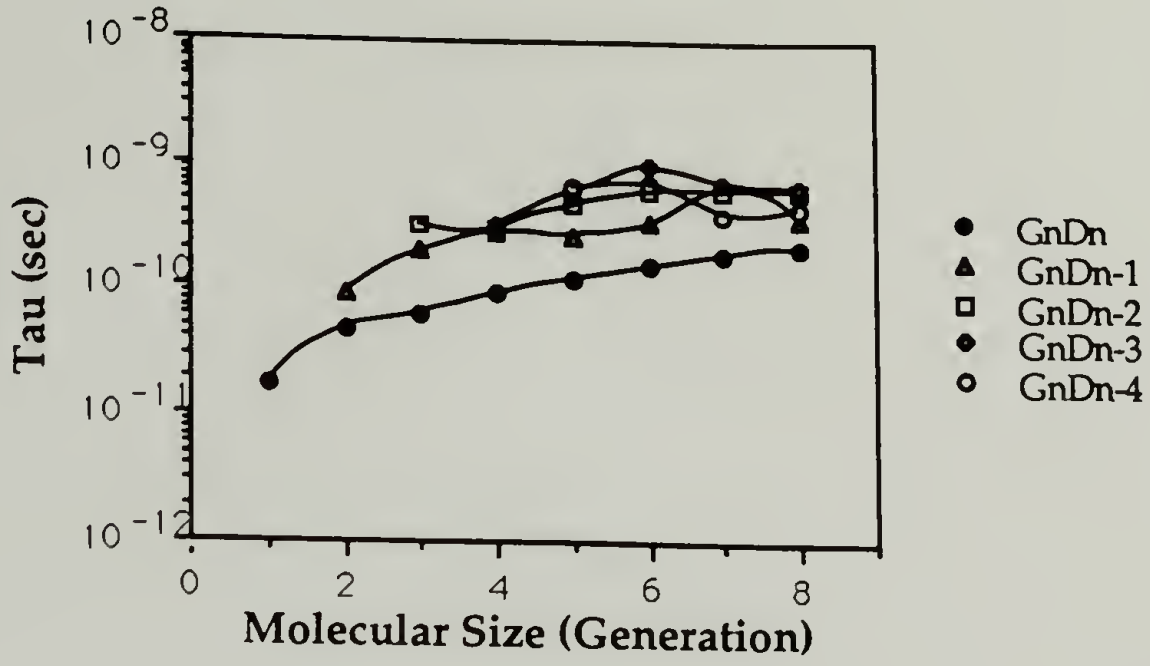

Figure 3.30. The dependence of τ on molecular size for NH_2 terminated PAMAM (25°C, 46.0 MHz, D2O).

lie in the region where NMR relaxation data of linear polymers was observed to depend on concentration (1, 11, 19, 33, 34, 37, 52), and as such, the observed dependence of τ on MW can be explained by the increasing monomer density within the dendrimer.

There is once again observed to be a greater mobility in the terminal generation than that observed for the bulk of the polymer. This behavior is precisely what would be predicted from the ^{13}C relaxation study, and is interpreted in an identical manner to the ^{13}C relaxation study discussed above. The calculations performed by Muthukumar show that the end groups are not located on the surface of the polymer. The model predicts that there is a significant amount of monomer density past the average location of the end groups but it also predicts that the monomer density in the vicinity of the end groups is below the level where concentration effects have been observed for with the ^{13}C correlation times presented in Figure 3.19, suggests that the behavior of the terminal unit may be somewhat different in the two studies.

However, one must recall that the site of deuteration is not identical to that of the terminal carbons of the ^{13}C study. The deuteration is present on the carbon immediately after the branch point, and as such, is five bond lengths further away from the end of the chain than is a terminal carbon as illustrated in structure 2. The intermediate behavior of the ^{2}H correlation times for the terminally labelled PAMAM, as compared to the internal ^{2}H and terminal ^{13}C correlation times is believed to be due to this difference in location alone. The location of the ^{2}H being intermediate between the two extremes allows its motional properties to be intermediate between the two as well.

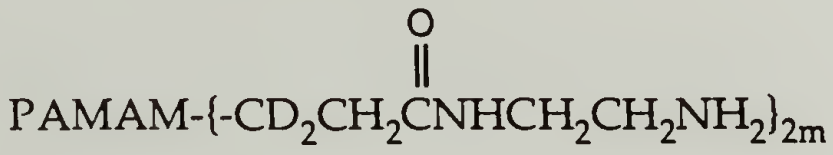

2

CHAPTER 4

CONCLUSIONS

The ^{2}H and ^{13}C dynamic NMR experiments are in good agreement. No evidence of dense-packing of the end groups was detected by ^{13}C NMR, and selective labelling of the amine terminated PAMAM showed no evidence for the formation of radial gradients of the segmental mobility within the polymer. There does, however, appear to be an decrease in the mobility of the chains with increasing MW. The evidence is consistent with the model presented by Muthukumar in which a folding back of the chains into the interior of the polymer is postulated. Such a phenomenon would prevent the ends of the chains from lying on the surface of the polymer "sphere" so that there would not be an ever increasing number of chain ends per unit surface area as postulated within the dense-packing theory. The folding back of the chains also prevents the formation of radial gradients within the polymer coil by filling in the postulated unoccupied volume between chains. As a result, the local monomer density increases as folding back into the interior becomes more facile, and the mobility of the chains in the interior is reduced with increasing MW.

APPENDIX

RELAXATION PARAMETER TABLES

Table A.1. The temperature dependence of NOEF for OH terminated PAMAM starburst polymers (75 MHz in DMSO-d_6).

Molecular size-Temperature (Generation-^{o}C)	NOEF of Carbon[a] 6	2	1	4
1-23	2.6	2.6		2.9
1-30	2.8	2.7		2.9
1-35	2.7	2.7		2.9
1-40	2.8	2.7		2.9
1-48	2.8	2.8		2.9
2-23	2.2	2.2	2.3	2.8
2-30	2.4	2.4	2.5	2.9
2-35	2.5	2.5	2.3	2.9
2-40	2.4	2.5	2.5	2.8
2-48	2.5	2.6	2.7	2.9
3-23	2.1	1.9	1.8	2.7
3-30	2.1	2.0	2.0	2.8
3-35	2.2	2.1	2.0	2.8
3-40	2.3	2.2	2.1	2.9
3-48	2.4	2.3	2.3	2.9
4-23	1.9	1.8	1.8	2.7
4-30	2.0	1.9	1.9	2.7
4-35	2.1	2.0	1.9	2.8
4-40	2.1	2.0	2.0	2.8
4-48	2.2	2.1	2.1	2.8
5-23	1.9	1.7	1.7	2.7
5-30	2.0	1.8	1.8	2.7
5-35	2.0	1.9	1.8	2.8
5-40	2.1	1.9	1.9	2.8
5-48	2.1	2.0	1.9	2.8

[a] The experimental error is approximately 10%.

Continued on next page.

Table A.1 continued

Molecular size-Temperature (Generation-^{o}C)	NOEF of Carbon 6	2	1	4
6-23	1.8	1.7	1.7	2.6
6-30	1.9	1.8	1.5	2.6
6-35	2.1	1.8	2.0	2.8
6-40	2.0	2.0	1.8	3.0
6-48	2.1	1.9	2.1	2.9
7-23	1.6	1.6	1.5	2.6
7-30	1.7	1.6	1.7	2.5
7-35	1.8	17	1.6	2.6
7-40	1.8	1.7	1.9	2.7
7-48	1.9	1.9	1.8	2.7
8-23	1.8	1.7	1.8	2.5
8-30	1.8	1.7	1.8	2.6
8-35	1.8	1.7	1.9	2.6
8-40		1.8	1.8	2.6
8-48	1.9	1.9	2.1	2.7
9-23	1.7	1.6	1.7	2.4
9-30	2.0	1.8	1.7	2.9
9-35	1.9	1.8	1.7	2.4
9-40	1.8	1.6	1.9	2.7
9-48	2.2	2.0	1.7	2.9
10-23	1.6	1.5	1.6	2.2
10-30	1.6	1.6	1.4	2.5
10-35	1.8	1.6	1.6	2.5
10-40	1.7	1.6		2.5
10-48	1.7	1.6	1.7	2.7
11-23	1.5	1.6		2.4
11-30	1.8	2.0	1.8	2.4
11-35	1.7	1.7	2.0	2.5
11-40	1.8	1.6	1.7	2.3
11-48	1.8	2.1	2.0	2.8

Table A.2. The temperature dependence of T_1 for OH terminated PAMAM (75 MHz, DMSO-d_6).

Molecular size-Temperature (Generation-^{o}C)	T_1 of Carbon[a] 6	2	1	4
1-23	0.23	0.19		0.59
1-30	0.27	0.22		0.68
1-35	0.30	0.25		0.78
1-40	0.33	0.27		0.88
1-48	0.38	0.31		1.0
2-23	0.16	0.14	0.12	0.49
2-30	0.20	0.15	0.15	0.56
2-35	0.21	0.17	0.15	0.64
2-40	0.22	0.18	0.17	0.70
2-48	0.26	0.22	0.19	0.87
3-23	0.14	0.12	0.12	0.45
3-30	0.16	0.14	0.13	0.52
3-35	0.17	0.14	0.13	0.58
3-40	0.19	0.15	0.15	0.65
3-48	0.21	0.18	0.16	0.78
4-23	0.14	0.12	0.12	0.40
4-30	0.15	0.13	0.12	0.47
4-35	0.16	0.13	0.13	0.53
4-40	0.17	0.14	0.13	0.60
4-48	0.19	0.16	0.14	0.71
5-23	0.14	0.12	0.11	0.40
5-30	0.14	0.12	0.11	0.42
5-35	0.14	0.12	0.12	0.48
5-40	0.15	0.13	0.12	0.52
5-48	0.17	0.14	0.14	0.63

[a] reported in sec ± 10%.

Continued on next page.

Table A.2 continued

Molecular size-Temperature (Generation-^{o}C)	T_1 of Carbon 6	2	1	4
6-23	0.13	0.12	0.11	0.34
6-30	0.14	0.12	0.13	0.41
6-35	0.14	0.12	0.12	0.44
6-40	0.14	0.13	0.13	0.50
6-48	0.15	0.15	0.12	0.63
7-23	0.12	0.11	0.11	0.31
7-30	0.12	0.12	0.10	0.31
7-35	0.13	0.12	0.11	0.34
7-40	0.13	0.12	0.10	0.38
7-48	0.14	0.12	0.12	0.46
8-23	0.12	0.12	0.14	0.29
8-30	0.12	0.12	0.11	0.32
8-35	0.14	0.12	0.13	0.36
8-40	0.14	0.12	0.12	0.42
8-48	0.15	0.13	0.12	0.50
9-23	0.12	0.12	0.12	0.25
9-30	0.13	0.13	0.13	0.33
9-35	0.13	0.12	0.12	0.34
9-40	0.13	0.13	0.14	0.38
9-48	0.14	0.11	0.12	0.44
10-23	0.12	0.13	0.14	0.25
10-30	0.15	0.12	0.12	0.24
10-35	0.13	0.12	0.11	0.23
10-40	0.12	0.12	0.10	0.29
10-48	0.12	0.12	0.11	0.33
11-23	0.12	0.11	0.12	0.23
11-30	0.14	0.10	0.10	0.31
11-35	0.14	0.12	0.10	0.29
11-40	0.14	0.11		0.36
11-48	0.16	0.09	0.13	0.33

Table A.3. The experimentally determined NOEF for OH terminated PAMAM starburst polymers (50 MHz, 23°C, DMSO-d_6).

Molecular size (Generation)	ends	NOEF of Carbon[a] 6	2	1	4
1	3	2.7	2.7		2.9
2	6	2.5	2.4	2.7	2.8
3	12	2.2	2.1	2.1	2.9
4	24	2.1	1.9	1.9	2.7
5	48	1.9	1.8	1.8	2.8
6	96	1.9	1.8	1.8	2.6
7	192	1.9	1.8	1.5	2.5
8	384	1.9	1.8	1.7	2.7
9	768	1.7	1.7	1.6	2.5
10	1536	1.6	1.6		2.4

[a] The experimental error in the NOEF is estimated to be 10%.

Table A.4. The calculated NOEF determined for OH terminated PAMAM starburst polymers (50 MHz, 23°C, DMSO-d_6).

Molecular size (Generation)	ends	NOEF of Carbon[a] 6	2	1	4
1	3	2.7	2.7		2.9
2	6	2.5	2.4	2.7	2.8
3	12	2.2	2.1	2.1	2.9
4	24	2.1	1.9	1.9	2.7
5	48	1.9	1.8	1.8	2.8
6	96	1.9	1.8	1.8	2.6
7	192	1.9	1.8	1.5	2.5
8	384	1.9	1.8	1.7	2.7
9	768	1.7	1.7	1.6	2.5
10	1536	1.6	1.6	1.5	2.2

[a] The predicted values were calculated by implimenting Schaefer's Log(χ) distribution, employing the values of P and τ determined from the relaxation data obtained at 75 MHz.

Table A.5. The experimentally determined T_1's for OH terminated PAMAM starburst polymers (50 MHz, 23°C, DMSO-d_6).

Molecular size (Generation)	ends	T_1 of Carbon[a]			
		6	2	1	4
1	3	0.19	0.16		0.54
2	6	0.14	0.13	0.12	0.43
3	12	0.11	0.09	0.08	0.38
4	24	0.10	0.08	0.09	0.34
5	48	0.08	0.08	0.08	0.33
6	96	0.06	0.06	0.07	0.23
7	192	0.09	0.09	0.08	0.20
8	384	0.10	0.10	0.06	0.24
9	768	0.06	0.06	0.08	0.18
10	1536	0.09	0.09		0.19

[a] T_1 is reported in sec ± 10%.

Table A.6. The calculated T_1's determined for OH terminated PAMAM starburst polymers (50 MHz, 23°C, DMSO-d_6).

Molecular size (Generation)	ends	T_1 of Carbon[a]			
		6	2	1	4
1	3	0.19	0.16		0.54
2	6	0.14	0.13	0.12	0.43
3	12	0.11	0.09	0.08	0.38
4	24	0.10	0.08	0.09	0.34
5	48	0.08	0.08	0.08	0.33
6	96	0.06	0.06	0.07	0.23
7	192	0.09	0.09	0.08	0.20
8	384	0.10	0.10	0.06	0.24
9	768	0.06	0.06	0.08	0.18
10	1536	0.09	0.09		0.19

[a] The calculated values were calculated by implementing Schaefer's Log(χ) distribution, employing the values of P and τ determined from the relaxation data obtained at 75 MHz.

Table A.7. The ^{13}C T_1 and NOEF of the -NH_2 and -OH terminated PAMAM observed in D_2O and DMSO-d_6 (75 MHz, 23°C[a]).

	-NH_2 Terminated				-OH Terminated			
	D_2O		DMSO-d_6		DMSO-d_6		D_2O	
	T_1[b]	NOE[b]	T_1[b]	NOE[b]	T_1[b]	NOE[b]	T_1[b]	NOE[b]
1-1[c]								
1-2	0.32	2.9	0.19	2.6	0.19	2.6	0.34	2.8
1-3	0.82	2.7					0.81	2.9
1-4	0.92	2.8			0.59	2.9	0.80	2.8
1-5								
1-6	0.19	2.9	0.23	2.7	0.23	2.6	0.42	2.9
2-1	0.21	2.6	0.14	2.4	0.12	2.3	0.20	2.6
2-2	0.24	2.6	0.15	2.2	0.14	2.2	0.21	2.7
2-3	0.69	2.8					0.60	2.6
2-4	0.86	2.8			0.49	2.8	0.61	2.9
2-5	0.20	2.5	0.13	2.5			0.19	2.3
2-6	0.30	2.7	0.18	2.4	0.16	2.2	0.25	2.7
3-1	0.17	2.3	0.11	2.0	0.12	1.8	0.15	2.4
3-2	0.17	2.4	0.12	1.9	0.12	1.9	0.18	2.4
3-3	0.58	2.7					0.61	2.8
3-4	0.72	2.8			0.45	2.7	0.61	2.9
3-5	0.16	2.2	0.15	1.8			0.17	2.4
3-6	0.24	2.6	0.15	2.1	0.14	2.1	0.22	2.5
4-1	0.13	1.9	0.11	1.6	0.12	1.8	0.14	2.0
4-2	0.14	2.0	0.12	1.7	0.12	1.8	0.15	2.2
4-3	0.46	2.5					0.48	2.7
4-4	0.60	2.8			0.40	2.7	0.52	2.8
4-5	0.13	1.9	0.13	1.7			0.14	2.1
4-6	0.19	2.3	0.13	1.9	0.14	1.9	0.18	2.2

[a] 25°C for the NH_2 terminated PAMAM.

[b] The experimental errors are estimated at 10%. T_1 is reported in sec.

[c] The first number indicates the molecular size of the dendrimers in terms of generation, and the second number indicates the carbon of interest.

Continued on next page.

Table A.7 continued

	-NH_2 Terminated				-OH Terminated			
	D_2O		DMSO-d_6		DMSO-d_6		D_2O	
	T_1	NOE	T_1	NOE	T_1	NOE	T_1	NOE
5-1	0.13	1.9	0.12	1.7	0.12	1.7	0.12	2.1
5-2	0.14	2.0	0.12	1.6	0.11	1.7	0.15	2.2
5-3	0.46	2.5					0.48	2.7
5-4	0.60	2.8			0.38	2.7	0.53	3.0
5-5	0.13	1.9	0.11	1.7			0.14	2.0
5-6	0.19	2.3	0.13	1.8	0.14	1.9	0.18	2.1
6-1	0.12	1.9	0.12	1.6	0.11	1.7	0.13	1.9
6-2	0.14	1.9	0.12	1.7	0.12	1.7	0.14	2.0
6-3	0.42	2.5					0.43	2.5
6-4	0.54	2.7			0.34	2.6	0.44	2.8
6-5	0.14	1.9	0.11	1.7			0.14	2.0
6-6	0.18	2.2	0.13	1.8	0.13	1.8	0.17	2.2
7-1	0.12	2.0	0.14	1.6	0.11	1.5		
7-2	0.13	1.9	0.13	1.5	0.11	1.6		
7-3	0.38	2.5						
7-4	0.50	2.8			0.31	2.6		
7-5	0.13	2.0	0.13	1.6				
7-6	0.16	2.1	0.14	1.7	0.12	1.6		
8-1	0.11	1.8	0.12	1.7	0.14	1.5	0.12	1.3
8-2	0.13	1.9	0.14	1.7	0.12	1.7	0.13	1.8
8-3	0.33	2.3					0.36	2.5
8-4	0.48	2.8			0.29	2.5	0.36	2.6
8-5	0.13	1.9	0.15	1.4			0.12	1.9
8-6	0.15	2.0	0.14	1.6	0.12	1.8	0.15	2.0
9-1					0.12	1.7	0.12	1.7
9-2					0.12	1.6	0.12	1.9
9-3							0.31	2.4
9-4					0.25	2.4	0.33	2.6
9-5							0.12	1.7
9-6					0.12	1.7	0.15	2.0

Continued next page.

Table A.7 continued

	-NH_2 Terminated				-OH Terminated			
	D_2O		DMSO-d_6		DMSO-d_6		D_2O	
	T_1	NOE	T_1	NOE	T_1	NOE	T_1	NOE
10-1					0.14	1.6	0.11	1.9
10-2					0.13	1.5	0.12	1.8
10-3							0.32	2.4
10-4					0.25	2.2	0.32	2.7
10-5							0.12	1.7
10-6					0.12	1.6	0.14	1.9
11-1					0.12			
11-2					0.11	1.6		
11-3								
11-4					0.23	2.4		
11-5								
11-6					0.12	1.5		

Table A.8. The ^{13}C P and τ of the -NH_2 and -OH terminated PAMAM observed in D_2O and DMSO-d_6 (75 MHz, 23°C[a]) calculated from Schaefer's Log(χ) distribution.

	-NH_2 Terminated				-OH Terminated			
	D_2O		DMSO-d_6		DMSO-d_6		D_2O	
	P	τ[b]	P	τ[b]	P	τ[b]	P	τ[b]
1-1[c]								
1-2	120	6.3	50	1.0	44	10	52	4.9
1-3	21	1.0					44	1.7
1-4	28	1.1			52	2.6	28	1.3
1-5								
1-6	85	4.6	54	8.1	37	7.4	77	4.3
2-1	42	8.7	42	17	44	22	44	9.4
2-2	36	6.9	18	15	22	17	60	9.3
2-3	29	1.6					18	1.3
2-4	27	1.2			40	2.8	56	2.6
2-5	32	9.0	68	19			17	8.9
2-6	38	5.1	25	10	16	13	48	7.0
3-1	20	11	18	37	7	1.8	35	14
3-2	29	11	9	57	10	1.9	26	10
3-3	24	1.7					56	2.6
3-4	29	1.5			28	2.7	56	2.6
3-5	17	13	3	450			28	11
3-6	34	6.8	12	17	15	2.1	28	7.4
4-1	8	49	9	400	7	120	10	25
4-2	10	25	7	320	7	120	17	15
4-3	16	1.8					27	2.4
4-4	32	2.0			28	3.2	35	2.5
4-5	8	49	5	500			14	19
4-6	18	8.9	7	58	16	15	13	10

[a] 25°C for the NH_2 terminated PAMAM.
[b] reported in sec x 10^{11}.
[c] The first number indicates the molecular size of the dendrimers in terms of generation, and the second number indicates the carbon of interest.

Continued next page.

Table A.8 continued

	-NH_2 Terminated				-OH Terminated			
	D_2O		DMSO-d_6		DMSO-d_6		D_2O	
	P	τ	P	τ	P	τ	P	τ
5-1	7	56	6	320	6	340	21	26
5-2	9	27	7	480	9	250	18	15
5-3	15	1.7					27	2.4
5-4	32	2.0			31	3.5	160	3.8
5-5	7	56	9	220			9	27
5-6	18	8.9	5	200	6	50	8	12
6-1	9	56	7	480	9	250	7	57
6-2	6	55	6	320	6	340	9	28
6-3	16	2.1					16	2.0
6-4	26	2.0			25	4.0	41	3.3
6-5	6	55	6	220			8	28
6-6	13	10	5	200	5	180	14	11
7-1	14	32	5	1100	11	550		
7-2	7	59	8	1000	6	400		
7-3	18	2.5						
7-4	38	2.7			30	4.5		
7-5	11	30	6	830				
7-6	11	15	4	630	6	350		
8-1	9	120	6	320	4	650	22	900
8-2	7	57	4	630	6	320	5	200
8-3							18	2.8
8-4					21	4.3	24	3.3
8-5	7	57					9	58
8-6	8	240	5	1100	6	150	8	240
9-1					6	300	6	320
9-2					7	550	9	56
9-3							14	3.2
9-4					18	5.3	26	3.9
9-5							6	320
9-6					6	320	8	240

Continued next page.

Table A.8 continued

	-NH_2 Terminated				-OH Terminated			
	D_2O		DMSO-d_6		DMSO-d_6		D_2O	
	P	τ	P	τ	P	τ	P	τ
10-1					5	1200	12	60
10-2					8	1000	6	150
10-3							14	3.0
10-4					9	4.5	36	4.6
10-5							6	320
10-6					6	350	6	50
11-1							12	60
11-2					9	420	6	150
11-3							14	3.0
11-4					20	6.3	36	4.6
11-5							6	320
11-6					9	750	6	50

Table A.9. The experimental NOEF determined for NH_2 terminated PAMAM starburst polymers (50 MHz, 25°C, D_2O).

Molecular size (Generation)	ends	NOEF of Carbon[a] 1	2	3	4	5	6
1	3		3.0	2.8	2.6		2.8
2	6	3.0	2.8	2.9	2.9	2.4	2.7
3	12	2.3	2.5	2.7	2.9	2.3	2.5
4	24	2.2	2.4	2.5	2.9	2.4	2.6
5	48	2.1	2.1	2.6	2.8	2.0	2.3

[a] The experimental errors are estimted at 10%

Table A.10. The calculated NOEF determined for NH_2 terminated PAMAM starburst polymers (50 MHz, 25°C, D_2O).

Molecular size (Generation)	ends	NOEF of Carbon[a] 1	2	3	4	5	6
1	3		2.9	2.8	2.9		2.9
2	6	2.7	2.7	2.8	2.8	2.6	2.8
3	12	2.4	2.5	2.8	2.8	2.3	2.7
4	24	2.2	2.3	2.8	2.8	2.2	2.4
5	48	1.9	2.0	2.5	2.8	1.9	2.4

[a] The calculated values were calculated by implementing Schaefer's Log(χ) distribution, employing the values of P and τ determined from the relaxation data obtained at 75 MHz.

Table A.11. The experimentally determined T_1's for NH_2 terminated PAMAM starburst polymers (50 MHz, 25°C, D_2O).

Molecular size (Generation)	ends	T_1 of Carbon[a]					
		1	2	3	4	5	6
1	3		0.28	0.73	0.78		0.37
2	6	0.16	0.17	0.52	0.71	0.16	0.21
3	12	0.14	0.13	0.48	0.65	0.12	0.18
4	24	0.12	0.11	0.44	0.65	0.11	0.16
5	48	0.10	0.11	0.39	0.54	0.11	0.14

[a] The T_1 are reported in sec ± 10%.

Table A.12. The calculated T_1's determined for NH_2 terminated PAMAM starburst polymers (50 MHz, 25°C, D_2O).

Molecular size (Generation)	ends	T_1 of Carbon[a]					
		1	2	3	4	5	6
1	3		0.31	0.76	0.88		0.39
2	6	0.19	0.22	0.65	0.81	0.17	0.28
3	12	0.14	0.15	0.53	0.68	0.13	0.21
4	24	0.11	0.12	0.47	0.64	0.11	0.16
5	48	0.10	0.10	0.40	0.50	0.10	0.16

[a] The calculated values were calculated by implimenting Schaefer's Log(χ) distribution, employing the values of P and τ determined from the relaxation data obtained at 75 MHz.

Table A.13. The T_1, NOEF and τ for NH_2 terminated PAMAM (75 MHz, 1:1 DMSO-d_6:H_2O, 25°C).

	T_1 (sec)[a]	NOE[a]	τ (sec x 10^{-11})
1-1[b]			
1-2	0.16	2.7	13
1-6	0.19	2.6	10
2-1	0.12	2.0	32
2-2	0.14	2.1	21
2-6	0.15	2.3	14
3-1	0.12	1.8	120
3-2	0.12	1.8	120
3-6	0.13	2.1	23
4-1	0.11	1.9	56
4-2	0.11	1.8	120
4-6	0.14	1.9	50
5-1	0.12	1.7	320
5-2	0.11	1.8	120
5-6	0.14	1.9	50
6-1	0.11	1.6	400
6-2	0.11	1.7	220
6-6	0.13	1.9	59
7-1	0.10	1.5	420
7-2	0.12	1.7	320
7-6	0.12	2.0	180
8-1	0.11	1.7	220
8-2	0.12	1.7	320
8-6	0.13	1.6	1000

[a] The experimental errors are estimated at 10%.
[b] The first number indicates the molecular size of the dendrimers in terms of generation, and the second number indicates the carbon of interest.

Table A.14. The T_1 and T_2 data obtained for PAMAM selectively labelled with ^2H, and the calculated τ values as determined from Schaefer's Log(χ) distribution (46.0 MHz, H_2O, 25°C).

polymer	T_1[a]	T_2[a]	P	τ[b]
G_1D_1	300	100	12	1.7
G_2D_2	160	60	13	4.7
G_2D_1	110	27	12	9.0
G_3D_3	130	38	12	6.2
G_3D_2	76	27	15	20
G_3D_1	64	19	1	32
G_4D_4	120	43	14	9.0
G_4D_3	67	28	17	28
G_4D_2	68	15	14	30
G_4D_1	66	12	14	32
G_5D_5	100	42	16	12
G_5D_4	67	24	16	27
G_5D3	58	12	15	46
G_5D_2	50	14	17	60
G_5D_1	49	15	18	64
G_6D_6	91	25	14	15
G_6D_5	64	17	15	33
G_6D_4	50	16	18	60
G_6D_3	40	16	25	97
G_6D_2	49	12	17	70
G_7D_7	81	23	14	19
G_7D_6	49	14	18	65
G_7D_5	51	12	16	61
G_7D_4	48	11	16	70
G_7D_3	61	10	14	40
G_8D_8	76	24	15	22
G_8D_7	60	18	16	37
G_8D_6	58	8.0	14	60
G_8D_5	51	8.7	15	66
G_8D_4	58	8.7	13	45

[a] Reported in sec x 10^{-5} ± 10%.

[b] Reported in sec x 10^{-11}.

Table A.15. The observed and predicted[a] values of the T_1, for the PAMAM selectively labelled with ^2H (30.7 MHz, H_2O, 25°C).

polymer	predicted values	observed values
G_2D_1	92	93
G_3D_1	51	63
G_4D_1	52	51
G_5D_4	55	49
G_5D_2	39	48
G_6D_5	50	57
G_7D_5	39	42

[a] The predicted values were calculated by implementing Schaefer's Log(χ) distribution, employing the values of p and τ determined from the relaxation data obtained at 46.0 MHz. The experimental errors are estimated at 10%.

BIBLIOGRAPHY

1) Allerhand, A. and Hailstone, R.K.; "Carbon-13 Fourier Transform Nuclear Magnetic Resonance. X. Effect of Molecular Weight on ^{13}C Spin-Lattice Relaxation times of Polystyrene in Solution"; J. Chem. Phys.; **56**, 3718-20 (1972).

2) Blum, F.D.; Durairaj, B. and Padmanabhan, A.S.; "Backbone Dynamics of Poly(isopropyl acrylate) in Chloroform. A Deuterium NMR Study"; Macromolecules, **17**, 2837-46 (1984).

3) Breitmaier, E.; Spohn, K.H. and Berger, S.; "^{13}C Spin-Lattice Relaxation Times and the Mobility of Organic Molecules in Solution"; A.C.I.E.E., **14**, 144-159 (1975).

4) Boere, R.T.and Kidd, R.G.; "Rotational Correlational Times in Nuclear Magnetic Relaxation"; Annual Reports on NMR Spectroscopy, vol. 13, pp. 320-385; Webb, G.A. ed.; Academic Press, New York, 1982.

5) Bullock, A.T.; Cameron, G.G. and Krajewski, V.; "Electron Spin Resonance Studies of Spin-Labeled Polymers. 11. Segmental and End-Group Mobility of Some Acrylic Ester Polymers"; J. Phys. Chem., **80**, 1792-1797 (1976).

6) Cutnell, J.D. and Glasel, J.A.; "^{1}H Spin-Lattice Relaxation and Reduced Values for ^{13}C Nuclear Ovewrhauser Enhancement"; J. Am. Chem. Soc., **99**, (1977).

7) Cutnell, J.D.; Glasel, J.A. and Hruby, V.J.; "An Investigation of Contributions to Carbon-13 Spin-Lattice Relaxation in Amino Acids and Peptide Hormones"; Org. Mag. Res., **7**, 256 (1975).

8) de Gennes, P.G. and Hervet, H.; "Statistics of "Starburst" Polymers; J. Physique-Lettres, **44**, 351-360 (1983).

9) Engberts, J.B.F.N.; "Mixed Aqueous Solvent Effects on Kinetics and Mechanisms of Organic Reactions"; Water; A Comprehensive Treatise, Vol 6, pp. 211-217; Franks, F. ed.; Plenum Press, New York, 1979.

10) Farrar, T.C. and Becker, E.D.; "Pulse and Fourier Trabsform NMR; Introduction to Theory and Methods; Academic Press, New York, 1971.

11) Ghesquiere, D.; Ban, B.; Chochaty, C.; "Proton and Carbon-13 Spin-Lattice Relaxation Studies of the Conformation and Dynamic Behavior of Poly(4-vinylpyridine) in Methanol Solutions"; Macromolecules, **10**, 743-52 (1977).

12) Gronski, W.; Murayama, N.; "^{13}C-Relaxationsuntersuchungen zum Einfluss des Losungsmittels auf die Kettenbewegung von Polystyrol"; Makromol. Chem., **179**, 1509-19 (1978).

13) Hall, H.K. Jr. and Polis, D.W.; ""Starburst" Polyarylamines and their Semiconducting Complexes as Potential Electroactive Materials"; Polymer Bulletin, **17**, 409-416 (1987).

14) Hamill, W.D.Jr.; Horton, W.J. and Grant D.M.; "Nuclear Magnetic Resonance Relaxation Studies of Carbon-13 Labelled Uracil in Transfer Ribonucleic Acid"; J. Am. Chem. Soc., **102**, 5454 (1980).

15) Heatley, F.; "Nuclear Magnetic Relaxation of Synthetic Polymers in Dilute Solution"; Prog. NMR Spect., **13**, 47-85 (1979).

16) Heatley, F. and Wood, B.; "A Proton Magnetic Relaxation Study of the Mechanism and Solvent Dependence of the Molecular Motion of Polystyrene in Dilute Solution"; Polymer, **19**, 1405-13 (1978).

17) Heatley, F. and Begum, A.; "Molecular Motion of Poly(methyl methacrylate), Polystyrene and Poly(propoylene oxide) in solution Studied by ^{13}C nmr. Spin-Lattice Relaxation Measurements ; Effects due to Distribution of Correlation Times"; Polymer, **17**, 399-408 (1976).

18) Heatley, F. and Watson, I.; "Contributions to the Proton Relaxation of Poly(ethylene oxide) in Benzene Solution"; Polymer, **17**, 1019-20 (1976).

19) Heatley, F.; "Molecular Motions in Polyisobutylene and Poly(propylene oxide) Studied by 13C Nuclear Magnetic Resonance"; Polymer, **16**, 493-496 (1973).

20) Inoue, Y. and Konno, T.; "A Carbon-13 NMR study of Molecular Motion of Polystyrene in Solution"; Polym. J., **8**, 457-65 (1976).

21) Inoue, Y.; Nishioka, A. and Chujo, R.; "Carbon-13 Spin-Lattice Relaxation Study of Linear Polymers in Solution"; J. Poly. Chem. Phys. Ed., **11**, 2237-52 (1973).

22) Israelachvili, J.B.; Intermolecular and Surface Forces; with Applications to Colloidal and Biological Systems; p.251; Academic Press, New York, 1985.

23) Jackman, L.M.; Greenberg, E.S.; Szeverenyi, N.M. and Schnorr, G.K.; "Determination of Deuterium Quadrupole Coupling Constant in the Liquid State"; J.C.S. Chem. Comm., 141-142 (1974).

24) Joesten, M.D. and Schaad, L.J.; H-Bonds, pp. 293-379; Marcel Decker inc., New York, 1974.

25) Kuhlmann, K.F.; Grant, D.M. and Harris R.K.; "Nuclear Overhauser Effects and ^{13}C Relaxation Times in ^{13}C-{H} Double Resonance Spectra"; J. Chem. Phys., **52**, 3439-48 (1970).

26) Lescanec, R. and Muthukumar, M.; submitted to Macromolecules.

27) Levy, G.C.; Topics in Carbon-13 NMR Spectroscopy; Vol. 1, John Wiley and Sons inc., New York, 1974.

28) Levy, G.C.; Axelson, D.E.; Schwartz, R. and Hochmann. J.; " Interpretation of Complex Motions in Solutoin. A Variable Frequency Carbon-13 Relaxation Study of Chain Segment Motions in Poly(n-alkyl methacrylates)"; J. Am. Chem. Soc., **100**, 410-23 (1978)

29) Levy, G.C., Cargioli, J.D. and Anet, F.A.; "Carbon-13 Spin-Lattice Relaxation in Benzene and Substituted Aromatic Compounds"; J. Am. Chem. Soc., **95**, 1527 (1973).

30) Lickfield, G.C.; Savitsky, G.B. ; Beyerlein, A.L. and Spencer, H.G.; "A Method for Studying the ^{13}C NMR Relaxation Times as a Function of Position along the Polymeric Chain"; Macromolecules, **16**, 396-8 (1983).

31) Lin, T.L.; Chen, S.H.; Gabriel, N.E. and Roberts, M.F.; "Use of Small-Angle Neutron Scattering To Determine the Structure and Interaction of Dihexanoylphosphatidylcholine"; J. Am. Chem. Soc., **108**, 3499-507 (1986).

32) Liu, K.J. and Anderson; "Solvent Effects on the proton Magnetic Relaxation of Polystyrene in Solution"; Macromolecules, **3**, 163 (1970).

33) Liu, K.J. and Ullmann, R.; "Proton Magnetic Relaxation in Polyethylene Oxide Solutions"; J. Chem. Phys., **48**, 1158-68 (1968).

34) Liu, K.J. and Ullmann, R; "Nuclear Magnetic Resonance of Polydimethylsiloxanes in Solution"; Macromolecules, **2**, 525-28 (1969).

35) Lyerla, J.R.; Horikawa, T.T. and Johnson, D.E.; "Carbon-13 Relaxation Study of Stereoregular Poly(methyl methacrylate) in Solution"; J. Am. Chem. Soc., **99**, 2463-67 (1977).

36) Maciejewski, M.; "Concepts of Trapping Topologically by Shell Molecules"; J. Macromol. Sci.-Chem., **A17(4)**, 689-703 (1982).

37) Matsuo, K.; Kuhlmann, K.H.; Yang, W.H.; Geny, F.; Stockmayer, W.H. and Jones, A.A.; "Fluorine Magnetic Resonance in Poly(p-fluorostyrene) and Poly(m-fluorostyrene)"; J. Poly. Chem. Phys. Ed., **15**, 1347-62 (1977).

38) McLachlan, L.A.; Natusch, D.F.S. and Newman, R.H.; "Spin-Lattice Relaxation in Ordered Systems"; J. Mag. Res., **4**, 358-65 (1971).

39) Mitchell, D.J. and Ninham, B.W.; "Micelles, Vesicles and Microemulsions"; J. Chem. Soc. Faraday Trans II, **77**, 601-629 (1981).

40) Naylor, A.M. and Goddard, W.A. III; "Simulations of Starburst Dendrimer Polymers"; Polymer Preprints, **29**, 215 (1988).

41) Naylor, A.M.; Goddard, W.A. III; Keifer, G.E. and Tomalia, D.A.; "Starburst Dendrimers. 5. Molecular Shape Control"; J. Am. Chem. Soc., **111**, 2339-2341 (1989).

42) Naylor, A.M.; "Insights on Enzyme and Polymers from Molecular Dynamics Simulations: Applications to Dihydrofolate Reductase Complexes and Starburst Dendrimers"; Ph.D. Thesis.

43) Newkome, G.R.; Yoa, Z. Baker, G.R. and Gupta, V.K.; "Cascade Macromolecules: A New Approach to Micelles. A [27] Arborol"; J. Org. Chem., **50(11)**, 2003-4 (1986).

44) Newkome, G.R.;Yao, Z.; Baker, G.R.; Gupta, V.K.; Russo, P.S. and Saunders, M.J.; Miller, J.E. and Bouillion, K.; "Two-directional Cascade Molecules: Synthesis and Characterization of [9]-n-[9] Arborols"; J. Chem. Soc., 752-3 (1986);

45) Newkome, G.R.; Yoa, Z. Baker, G.R.; Gupta, V.K.; Russo, P.S. and Saunders, M.J.;Cascade Molecules: "Synthesis and Characterization of a Benzene[9]-Arborol"; J. Am. Chem. Soc., **108**, 849-50 (1985).

46) North, A.M. and Soutar, I.; "Fluorescence Depolarization Measurements of Polymer Segmental Mobility"; J.C.S. Faraday Transactions I, **68**, 1101-1116 (1972).

47) Norton, R.S. and Allerhand, A.; "Effect of ^{13}C-^{14}N Dipolar Interactions on Spin-Lattice Relaxation Times and Intensiteis of Nonprotonated Carbon Resonances"; J. Am. Chem. Soc., **98**, 1007-1014 (1976).

48) Nugent, W.A. and McKinney, R.J.; "Linear Dimerization of Acrylates by Palladium and Rhodium Catalysis: Effect of Lewis and Protic Acic Additives"; J. Molec. Cryst., **29**, 65-76 (1985).

49) Saito, H.; Mantsch, H.H. and Smith, I.C.P.; "Correlation between Deuterium and Carbon-13 Relaxation Times. A Convenient Means to Determine the Mechanism of ^{13}C Relaxation and ^{2}H Quadrupole Coupling Constants"; J. Am. Chem. Soc., **95**, 8453-55 (1973).

50) Schaefer, J.; "Distribution of Correlation Times and the Carbon-13 Nuclear Magnetic Resonance Spectra of Polymers"; Macromolecules, **6**, 882-888 (1973).

51) Schaefer, J. and Natusch, F.S.; "Carbon-13 Overhauser Effect in Polymer Solutions"; Macromolecules, **5**, 416-427 (1972).

52) Silverstein, R.M.; Bassler, G.C. and Morrill, T.C.; Spectrometric Identification of Organic Compounds; Fourth Edition; p. 261; John Wiley and Sons, New York, 1981.

53) Slichter, W.P. and Davis, D.D.; "Nuclear Magnetic Resonance Study of Polyisobutylene Solutions"; Macromolecules, **1**, 47-53 (1968).

54) Smith, P.B.; Martin, S.J.; Hall, M.J. and Tomalia, D.A.; "A Characterization of the Structure and Synthetic Reactions of Polyamidoamine "Starburst" Polymers"; Applied Polymer Analysis and Characterization; Ed. J. Mitchell, Jr.; Hanser Publishers, New York (1987), p357-385.

55) Tomalia, D.A.; Baker, H.; Dewald, J.; Hall, M.; Kallos, G.; Martin, S. Roeck, J.; Ryder, J. and Smith, P.; "Dendritic Macromolecules: Synthesis of Starburst Dendrimers"; Macromolecules, **19**, 2466-68 (1986).

56) Tomalia, D.A.; Baker, H.; Dewald, J.; Hall, M.; Kallos, G.; Martin, S. Roeck, J.; Ryder, J. and Smith, P.; "A New Class of Polymers: Starburst-Dendritic Macromolecules"; Polym. J. (Tokyo), **17(1)**, 117-32 (1985).

57) Tomalia, D.A.; Berry, V.; Hall, M. and Henstrand, D.M.; "Starburst Dendrimers. 4. Covalently Fixed Unimolecular Assemblages Reminiscent of Spheroidal Micelles"; Macromolecules, **20**, 1164-7, (1987).

58) Tomalia, D.A.; Hall, M. and Henstrand, D.M.; "Starburst Dendrimers. 3. The Importance of Branch Junction Symmetry in the Development of Topological Shell Molecules"; J. Am. Chem. Soc., **109**, 1601-3 (1987).

59) Tomalia, D.A.; Hedstrand, D.M. and Wilson, L.R.; "Dendritic Macromolecules: Starburst Dendrimers as Mcro-Networks Leading to Infinite Network Systems"; submitted to Kirk-Othmer Encyclopedia of Polymer Science and Engineering.

60) Tomalia, D.A.; Hedstrand, D.M.,; Wilson, L.R. and Downing, D.M.; "Starburst Dendrimers. Size, Shape and Surface Control of Macromolecules;" submitted for publication.

61) Tomalia, D.A.; McConnell, J.R.; Padias, A.B. and Hall, H.K. Jr.; "Starburst Polyether Dendrimers"; J. Org. Chem., **52**, 5305-12 (1987).